US010241887B2

(12) United States Patent
Poghosyan et al.

(10) **Patent No.: US 10,241,887 B2**

(45) **Date of Patent: Mar. 26, 2019**

(54) **DATA-AGNOSTIC ANOMALY DETECTION**

(71) Applicant: **VMware, Inc.**, Palo Alto, CA (US)

(72) Inventors: **Arnak Poghosyan**, Yerevan (AM); **Ashot Nshan Harutyunyan**, Yerevan (AM); **Naira Movses Grigoryan**, Yerevan (AM); **Mazda A. Marvasti**, Irvine, CA (US)

(73) Assignee: **VMware, Inc.**, Palo Alto, CA (US)

(*) Notice: Subject to any disclaimer, the term of this patent is extended or adjusted under 35 U.S.C. 154(b) by 419 days.

(21) Appl. No.: **13/853,321**

(22) Filed: **Mar. 29, 2013**

(65) **Prior Publication Data**

US 2014/0298098 A1 Oct. 2, 2014

(51) **Int. Cl.**

G06F 11/00	(2006.01)
G06F 11/34	(2006.01)
G06F 17/18	(2006.01)
G06F 11/07	(2006.01)
G05B 23/02	(2006.01)
G06K 9/00	(2006.01)
G06K 9/62	(2006.01)

(52) **U.S. Cl.**

CPC ***G06F 11/3452*** (2013.01); ***G05B 23/0235*** (2013.01); ***G06F 11/0706*** (2013.01); ***G06F 11/0751*** (2013.01); ***G06F 17/18*** (2013.01); ***G06K 9/00536*** (2013.01); ***G06K 9/6284*** (2013.01)

(58) **Field of Classification Search**

CPC . G06F 15/78; G06F 13/22; G06F 7/22; G06F 11/0793; G06F 11/1032; G06F 11/104; G06F 11/3452; G06F 12/04; G06F 13/12; G06F 17/30595; G06F 2003/0691; G06F 3/0601; G06F 7/24; G06F 9/4812; G06F 11/0751; G06F 11/076

USPC 714/26, 37, 47.2, 47.3

See application file for complete search history.

(56) **References Cited**

U.S. PATENT DOCUMENTS

6,216,066	B1 *	4/2001	Goebel	G05B 23/0232 340/438
7,076,695	B2 *	7/2006	McGee	G06F 11/0709 702/179
7,467,067	B2	12/2008	Marvasti	
7,707,285	B2 *	4/2010	Marvasti	709/224
7,801,703	B2	9/2010	Marvasti	
7,934,126	B1 *	4/2011	Bennett	G06F 11/079 714/26
8,060,342	B2	11/2011	Marvasti	
8,078,913	B2 *	12/2011	Goldszmidt et al.	714/26
8,171,033	B2	5/2012	Marvasti	
8,457,928	B2 *	6/2013	Dang et al.	702/186

(Continued)

Primary Examiner — Elmira Mehrmanesh

(57) **ABSTRACT**

This disclosure presents computational systems and methods for detecting anomalies in data output from any type of monitoring tool. The data is aggregated and sent to an alerting system for abnormality detection via comparison with normalcy bounds. The anomaly detection methods are performed by construction of normalcy bounds of the data based on the past behavior of the data output from the monitoring tool. The methods use data quality assurance and data categorization processes that allow choosing a correct procedure for determination of the normalcy bounds. The methods are completely data agnostic, and as a result, can also be used to detect abnormalities in time series data associated with any complex system.

36 Claims, 50 Drawing Sheets

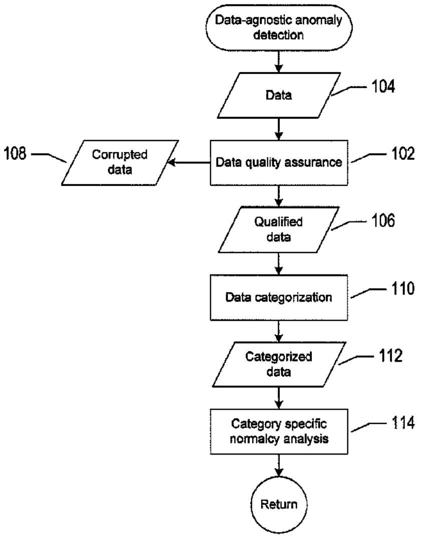

(56) **References Cited**

U.S. PATENT DOCUMENTS

2005/0283680	A1*	12/2005	Kobayashi	G06F 11/3636 714/39
2008/0077687	A1*	3/2008	Marvasti	709/224
2008/0103855	A1*	5/2008	Hernandez	G06Q 30/02 705/7.33
2008/0270071	A1*	10/2008	Marvasti et al.	702/179
2010/0223499	A1*	9/2010	Panigrahy et al.	714/19
2012/0041575	A1*	2/2012	Maeda	G05B 23/024 700/80
2013/0158917	A1*	6/2013	Uchida	G01R 31/3658 702/63
2013/0218909	A1*	8/2013	Chu et al.	707/752
2014/0058705	A1*	2/2014	Brill	G06Q 10/063 702/183

* cited by examiner

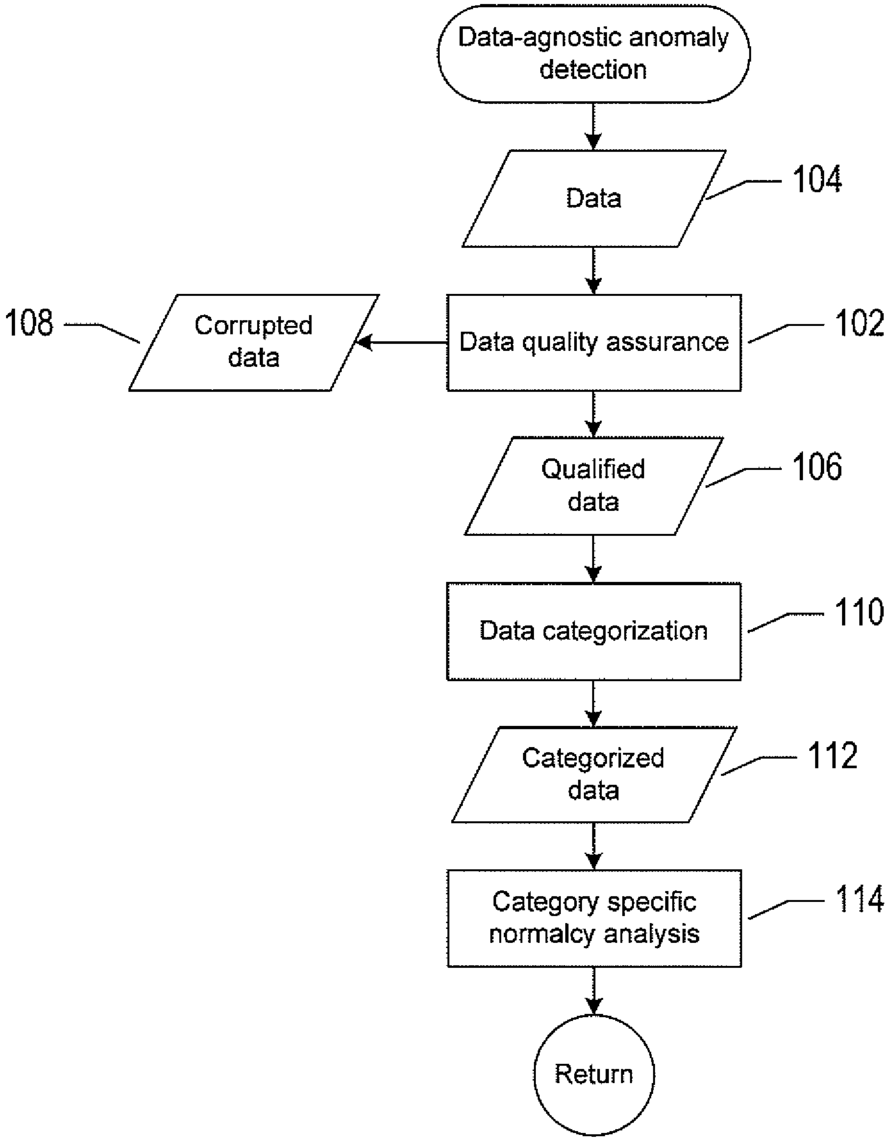
Data-agnostic anomaly detection
Data
104
Data quality assurance
102
Corrupted data
108
Qualified data
106
Data categorization
110
Categorized data
112
Category specific normalcy analysis
114
Return

FIG. 1

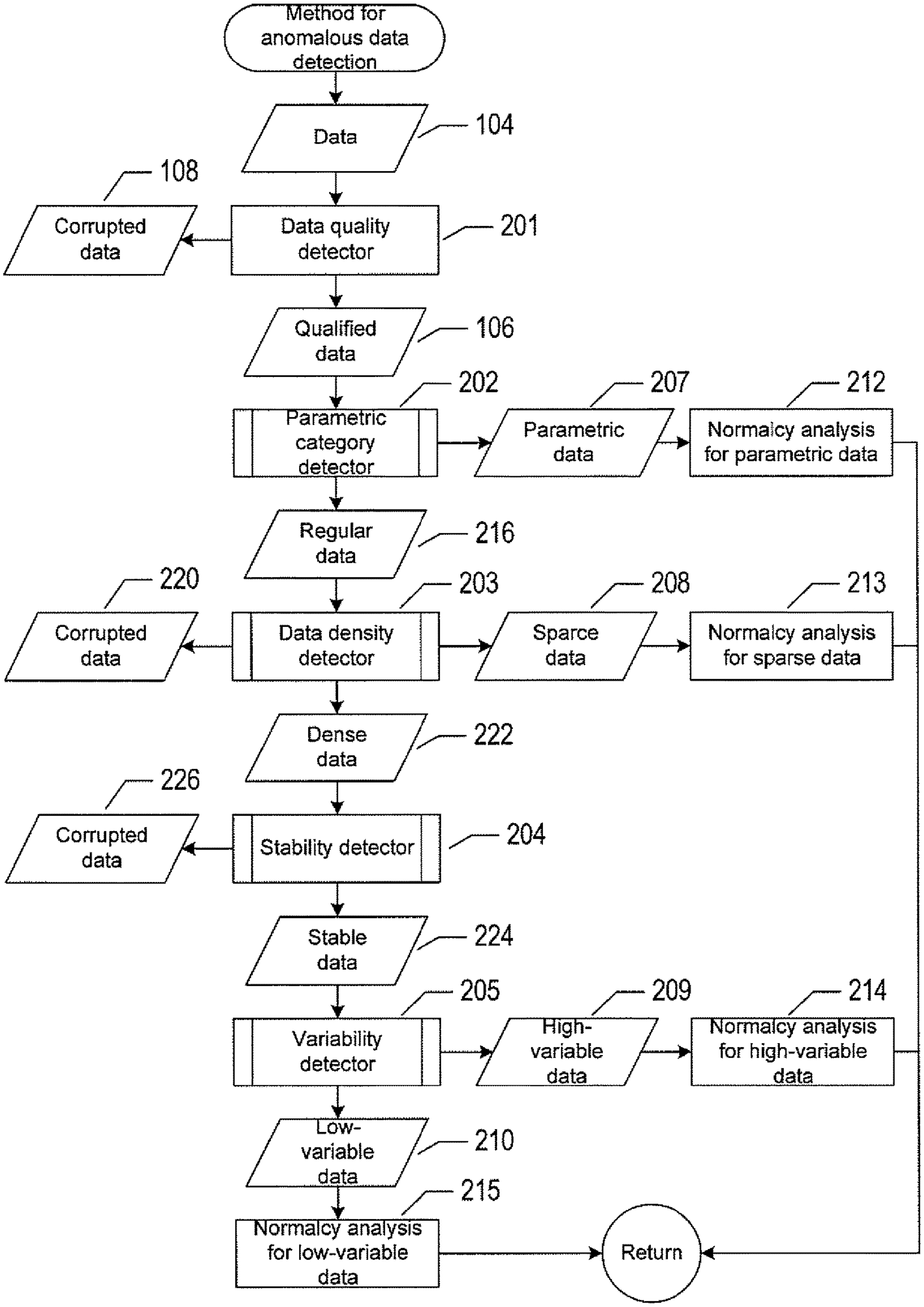
Method for anomalous data detection
Data
104
108
Corrupted data
Data quality detector
201
Qualified data
106
202
207
212
Parametric category detector
Parametric data
Normalcy analysis for parametric data
Regular data
216
220
203
208
213
Corrupted data
Data density detector
Sparce data
Normalcy analysis for sparse data
Dense data
222
226
Corrupted data
Stability detector
204
Stable data
224
205
209
214
Variability detector
High-variable data
Normalcy analysis for high-variable data
Low-variable data
210
215
Normalcy analysis for low-variable data
Return

FIG. 2

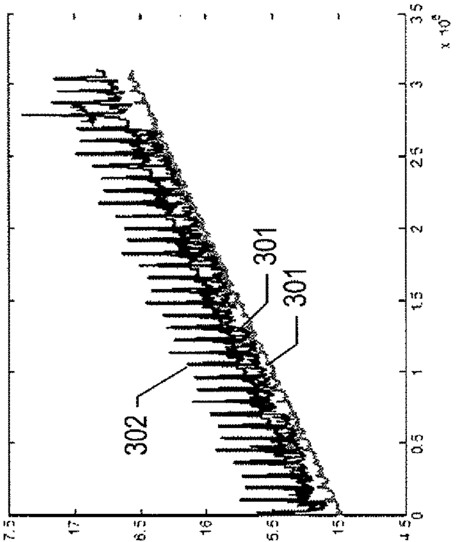

FIG. 3A

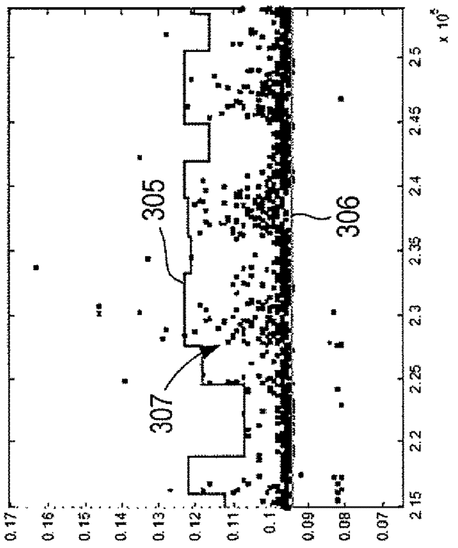

FIG. 3B

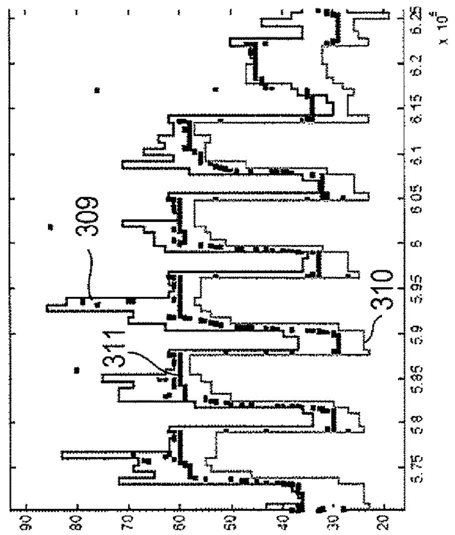

FIG. 3C

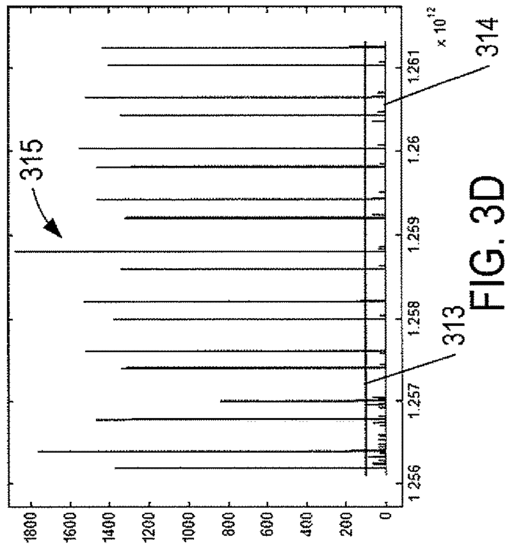

FIG. 3D

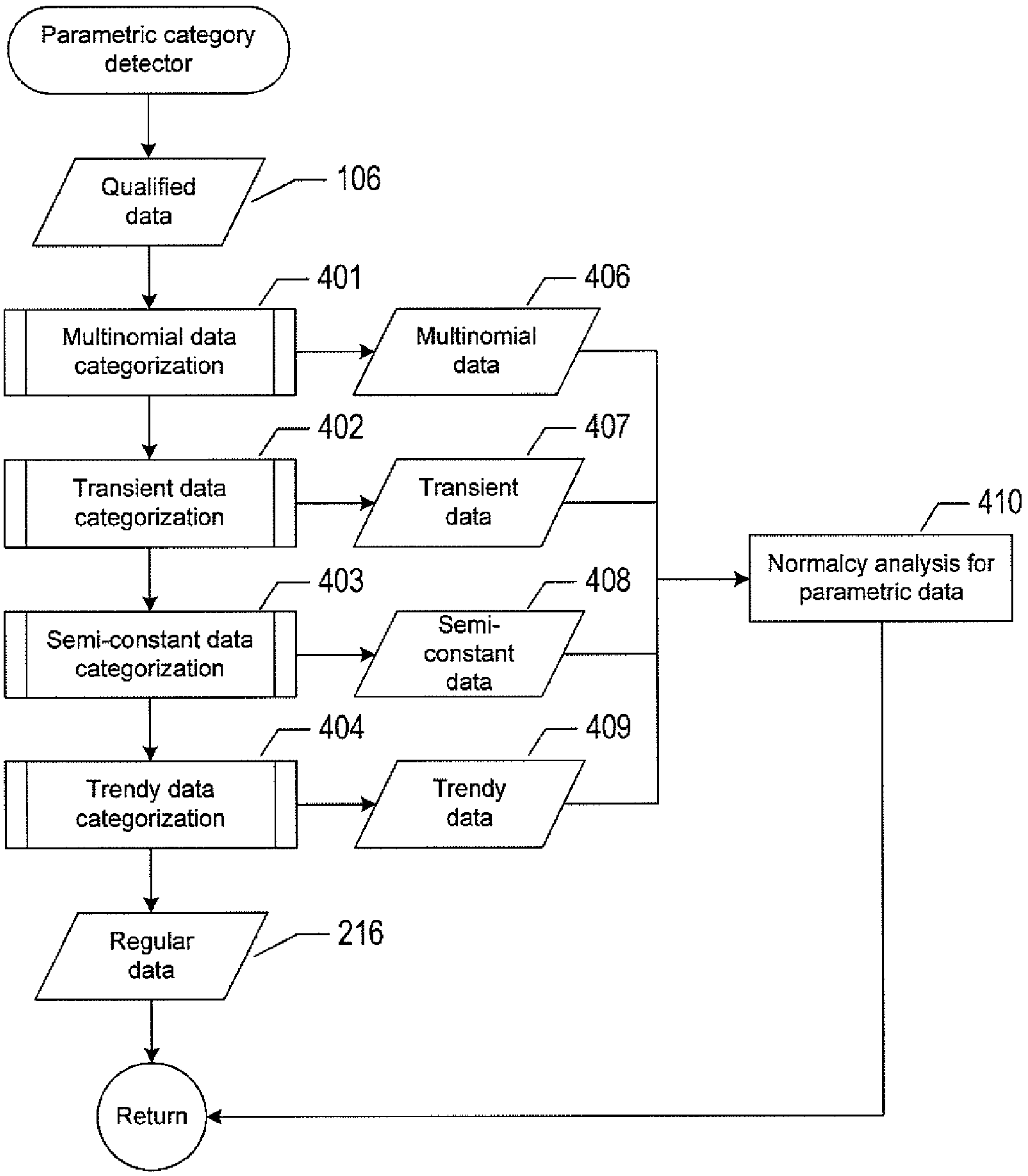
Parametric category detector
Qualified data
106
Multinomial data categorization
401
Multinomial data
406
Transient data categorization
402
Transient data
407
Semi-constant data categorization
403
Semi-constant data
408
Trendy data categorization
404
Trendy data
409
Normalcy analysis for parametric data
410
Regular data
216
Return

FIG. 4

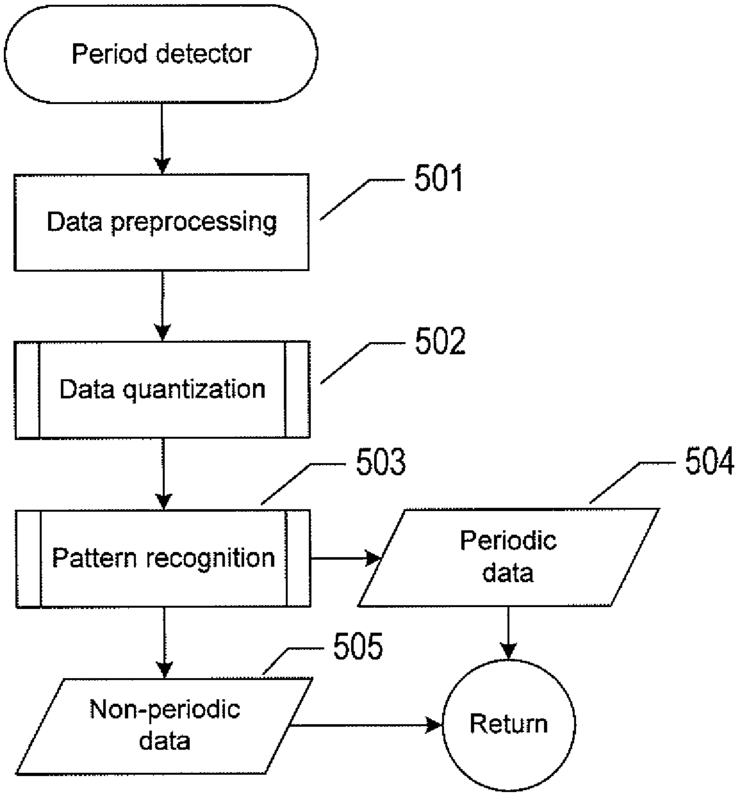
Period detector
Data preprocessing
501
Data quantization
502
503
504
Pattern recognition
Periodic data
505
Non-periodic data
Return

FIG. 5

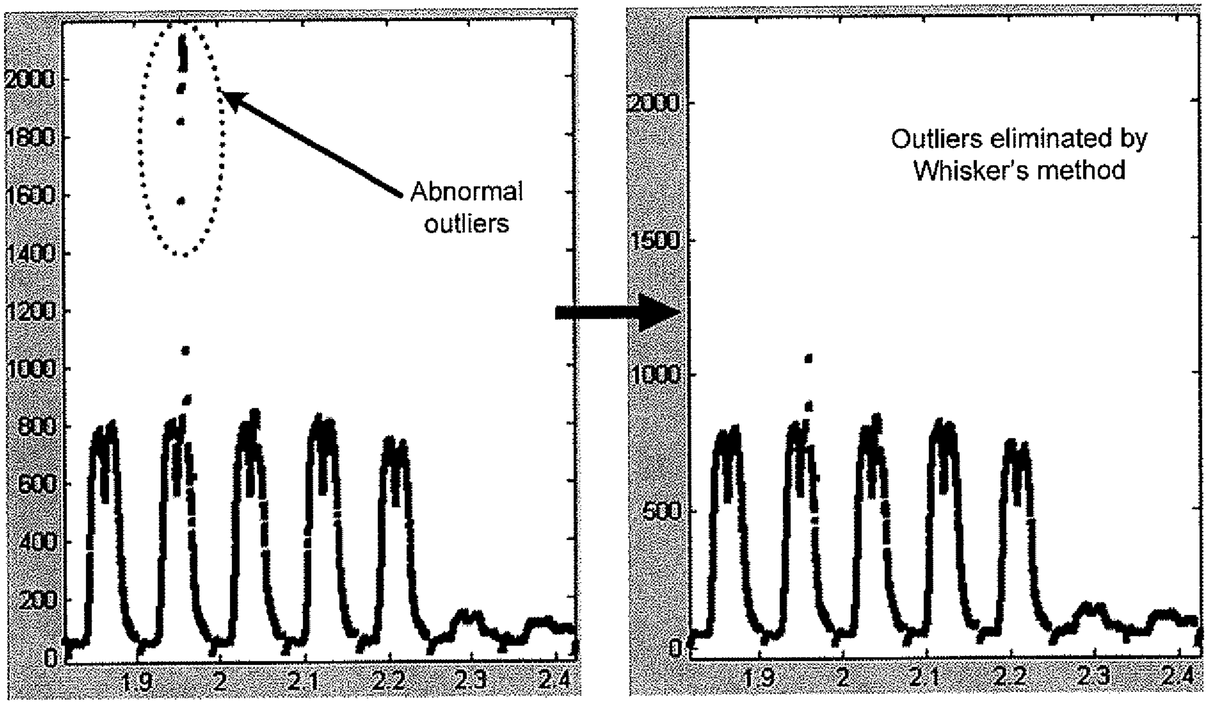
2000
1800
1600
1400
1200
1000
800
600
400
200
0
1.9
2
2.1
2.2
2.3
2.4
Abnormal outliers
2000
1500
1000
500
0
1.9
2
2.1
2.2
2.3
2.4
Outliers eliminated by Whisker's method

FIG. 6

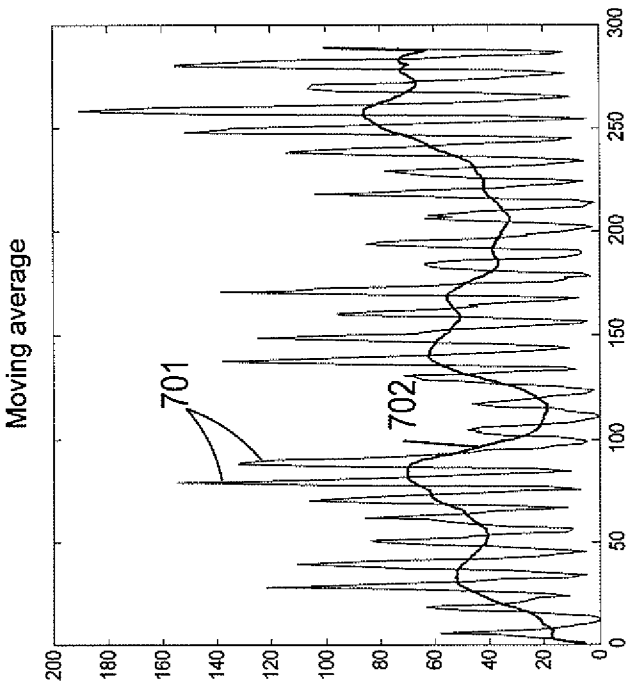
Moving average
701
702
200
180
160
140
120
100
80
60
40
20
0
0
50
100
150
200
250
300

FIG. 7A

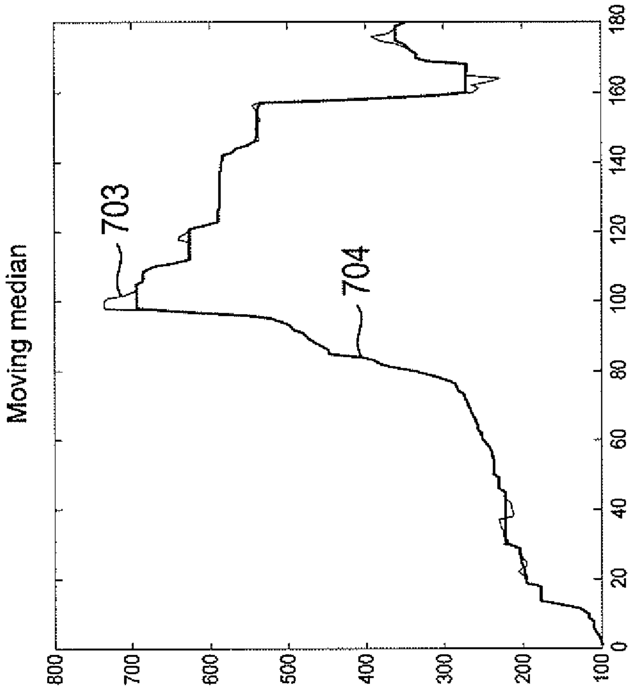
Moving median
703
704
800
700
600
500
400
300
200
100
0
20
40
60
80
100
120
140
160
180

FIG. 7B

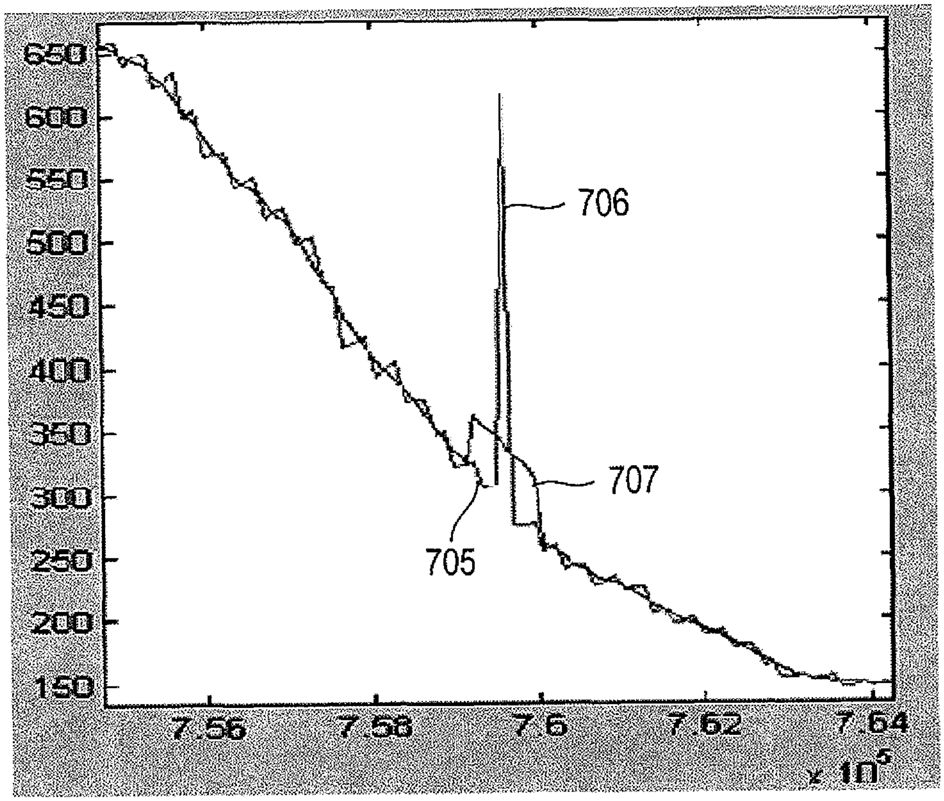
650
600
550
500
450
400
350
300
250
200
150
7.56
7.58
7.6
7.62
7.64
x 10^5
706
707
705

FIG. 7C

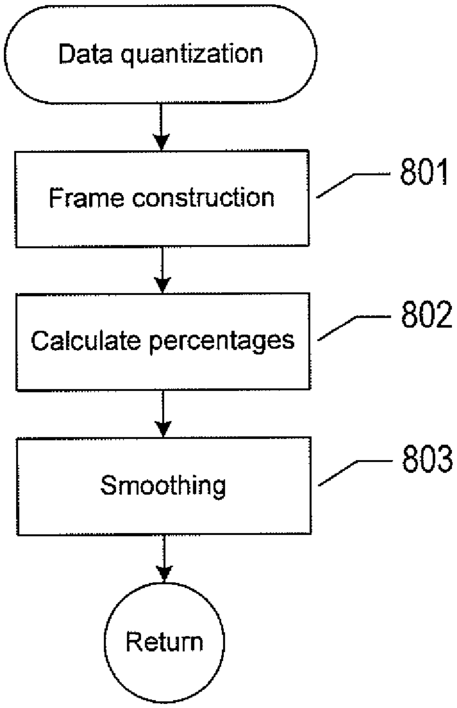
Data quantization
Frame construction
801
Calculate percentages
802
Smoothing
803
Return

FIG. 8

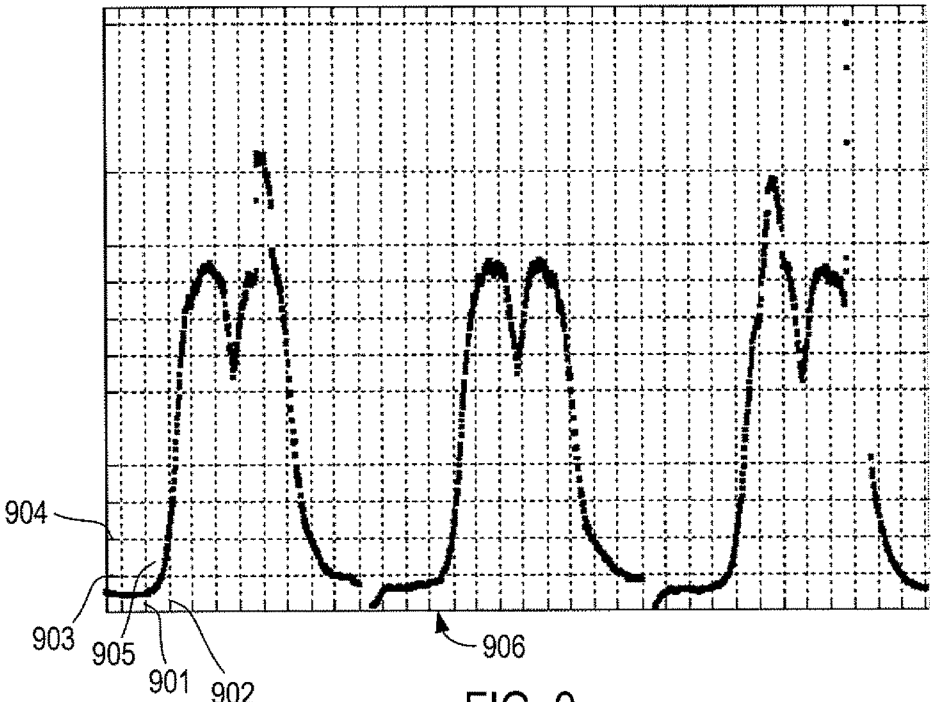
904
903
905
901
902
906

FIG. 9

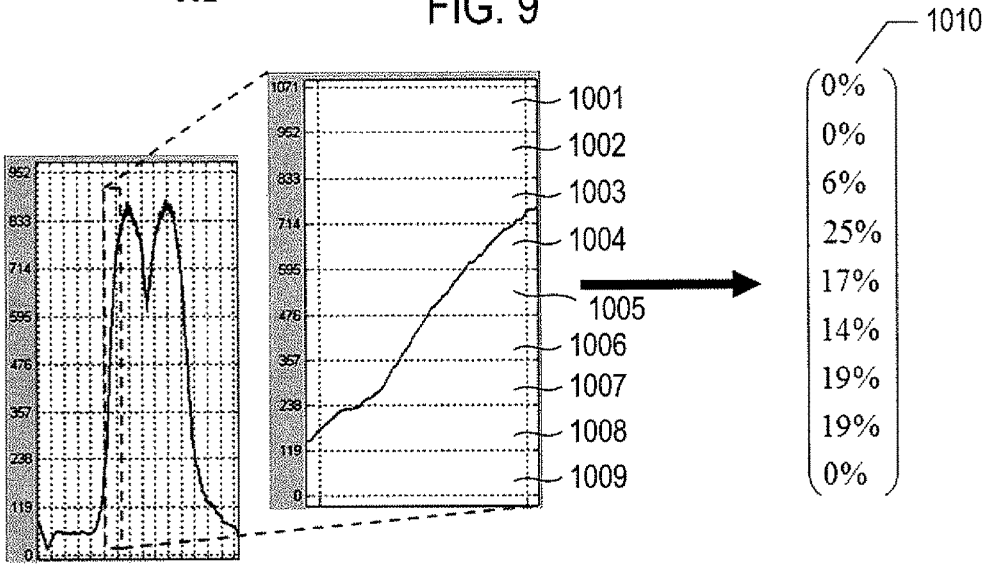
1010
952
833
714
595
476
357
238
119
0
1071
952
833
714
595
476
357
238
119
0
1001
1002
1003
1004
1005
1006
1007
1008
1009
0%
0%
6%
25%
17%
14%
19%
19%
0%

FIG. 10

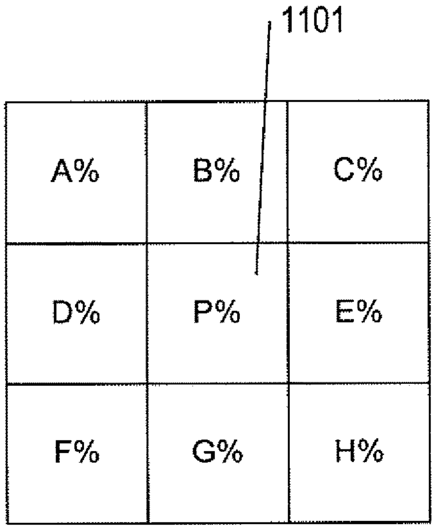

A%	B%	C%
D%	P%	E%
F%	G%	H%

FIG. 11A

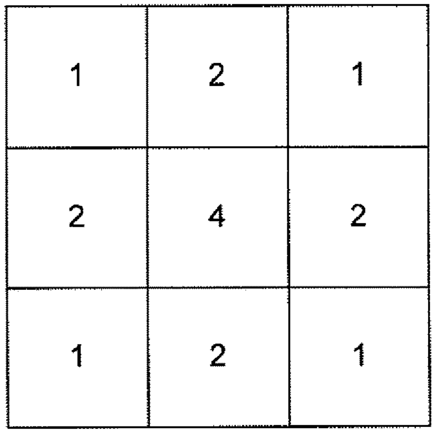

1	2	1
2	4	2
1	2	1

FIG. 11B

$$\overset{1202}{\begin{pmatrix} a \\ b \\ c \\ d \\ e \\ f \\ g \end{pmatrix}} \to \overset{1204}{\begin{pmatrix} a \\ a+b \\ a+b+c \\ a+b+c+d \\ a+b+c+d+e \\ a+b+c+d+e+f \\ a+b+c+d+e+f+g \end{pmatrix}}$$

FIG. 12

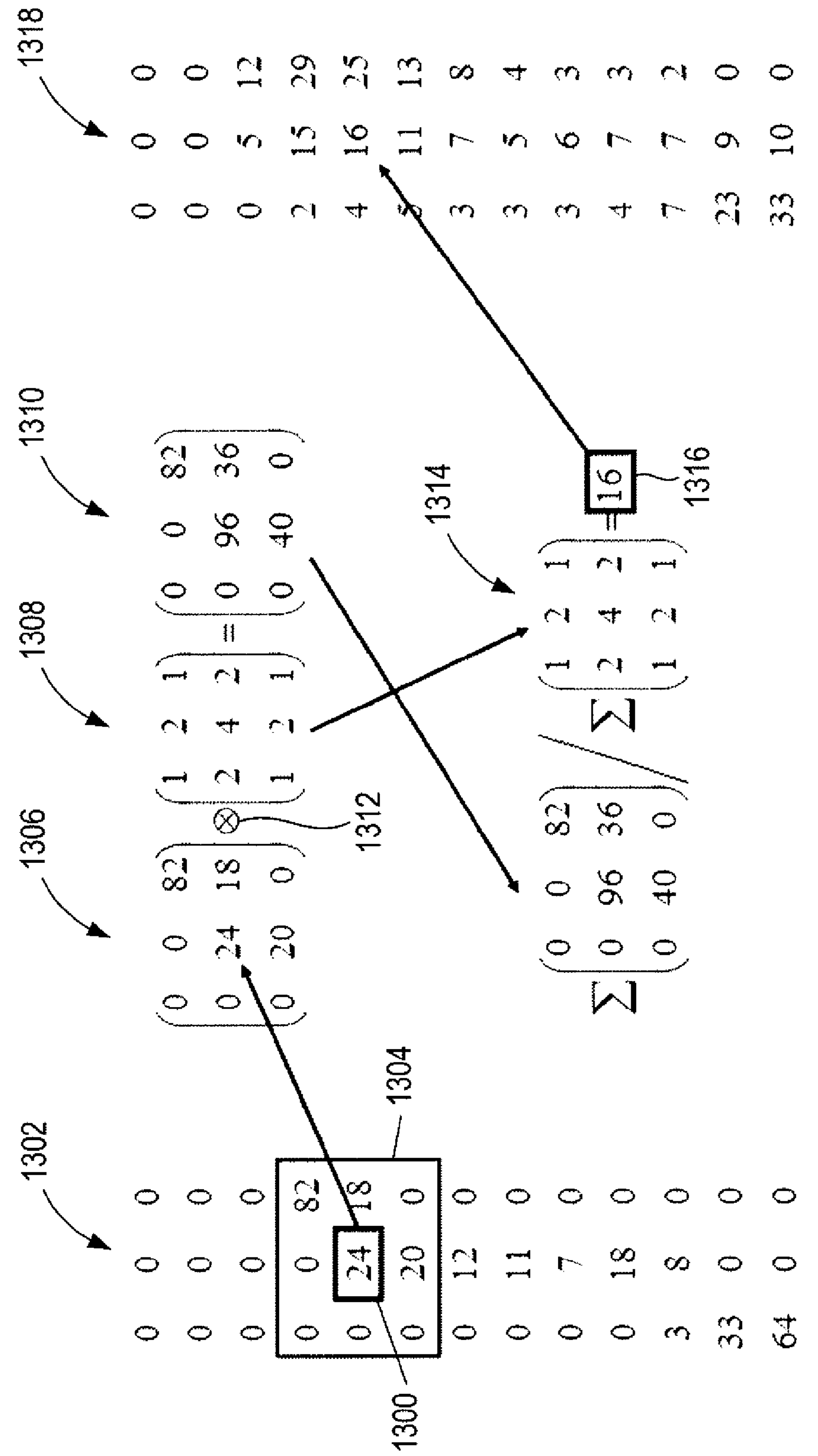
1302
1304
1300
0 0 0
0 0 0
0 0 0
0 0 82
0 24 18
0 20 0
0 12 0
0 11 0
0 7 0
0 18 0
3 8 0
33 0 0
64 0 0
1306
1308
1310
1312
0 0 82
0 24 18
0 20 0
⊗
1 2 1
2 4 2
1 2 1
=
0 0 82
0 96 36
0 40 0
1314
Σ
0 0 82
0 96 36
0 40 0
/ Σ
1 2 1
2 4 2
1 2 1
= 16
1316
1318
0 0 0
0 0 0
0 5 12
2 15 29
4 16 25
5 11 13
3 7 8
3 5 4
3 6 3
4 7 3
7 7 2
23 9 0
33 10 0

FIG. 13

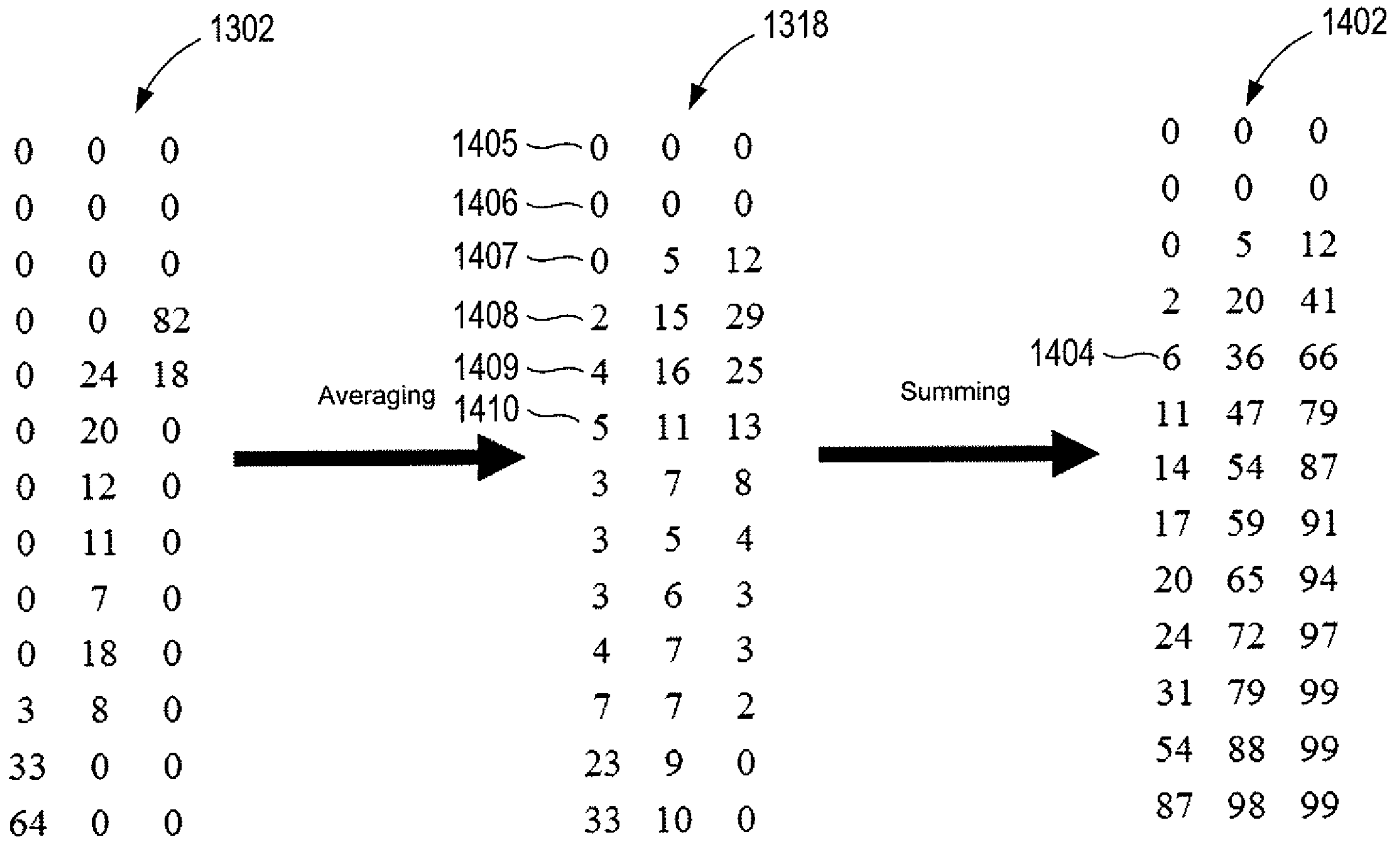

0	0	0
0	0	0
0	0	0
0	0	82
0	24	18
0	20	0
0	12	0
0	11	0
0	7	0
0	18	0
3	8	0
33	0	0
64	0	0

0	0	0
0	0	0
0	5	12
2	15	29
4	16	25
5	11	13
3	7	8
3	5	4
3	6	3
4	7	3
7	7	2
23	9	0
33	10	0

0	0	0
0	0	0
0	5	12
2	20	41
6	36	66
11	47	79
14	54	87
17	59	91
20	65	94
24	72	97
31	79	99
54	88	99
87	98	99

FIG. 14

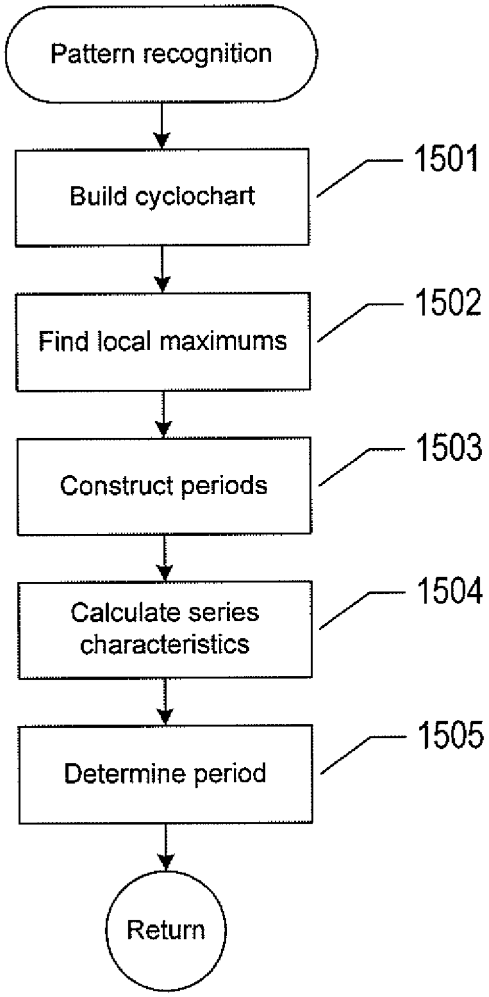
Pattern recognition
Build cyclochart
1501
Find local maximums
1502
Construct periods
1503
Calculate series characteristics
1504
Determine period
1505
Return

FIG. 15

A	B	C	D	E	F	G	H	I	J	K	L	M	N	O	P
0	0	0	0	1	0	0	1	1	0	0	1	1	1	0	1
T-cycle				T-cycle				T-cycle				T-cycle			

FIG. 16

A, E, I, M	B, F, J, M	C, G, K, O	D, H, L, P
1	0	0	1
← T-cycle →			

FIG. 17

$$\begin{Vmatrix} 1-time\_unit \\ 2-time\_unit \\ 3-time\_unit \\ 4-time\_unit \\ \vdots \\ 11-time\_unit \\ 12-time\_unit \end{Vmatrix} = \begin{Vmatrix} 0\% \\ 8\% \\ 8\% \\ 6\% \\ \vdots \\ 7\% \\ 17\% \end{Vmatrix}$$

FIG. 18

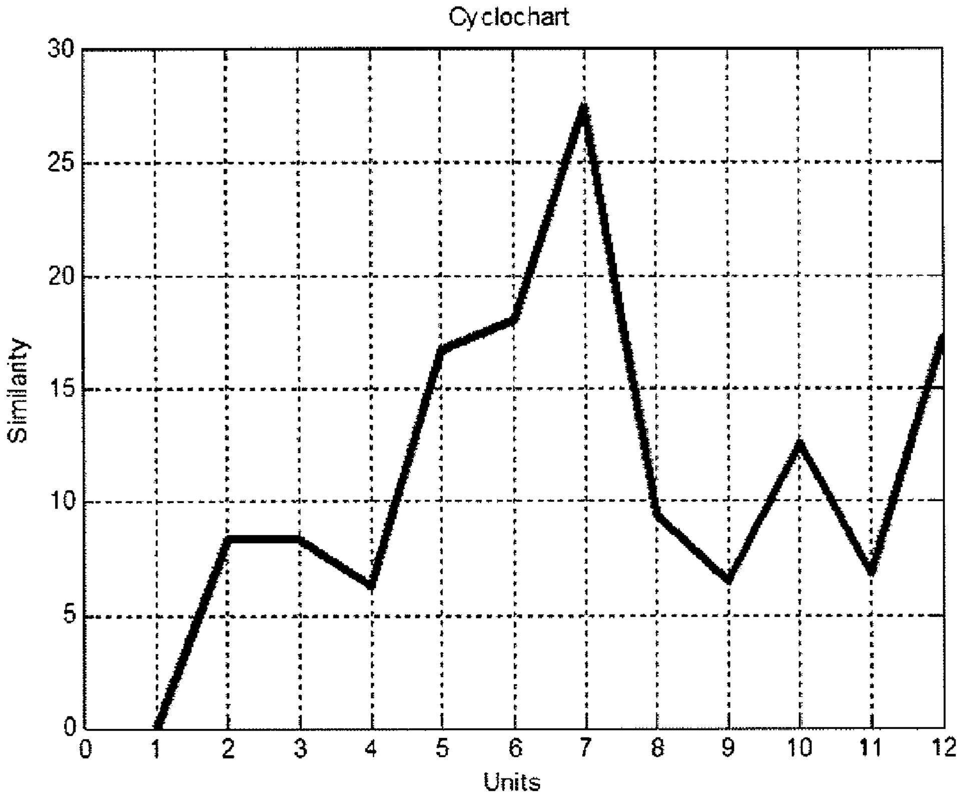
Cyclochart
30
25
20
15
10
5
0
Similarity
0
1
2
3
4
5
6
7
8
9
10
11
12
Units

FIG. 19

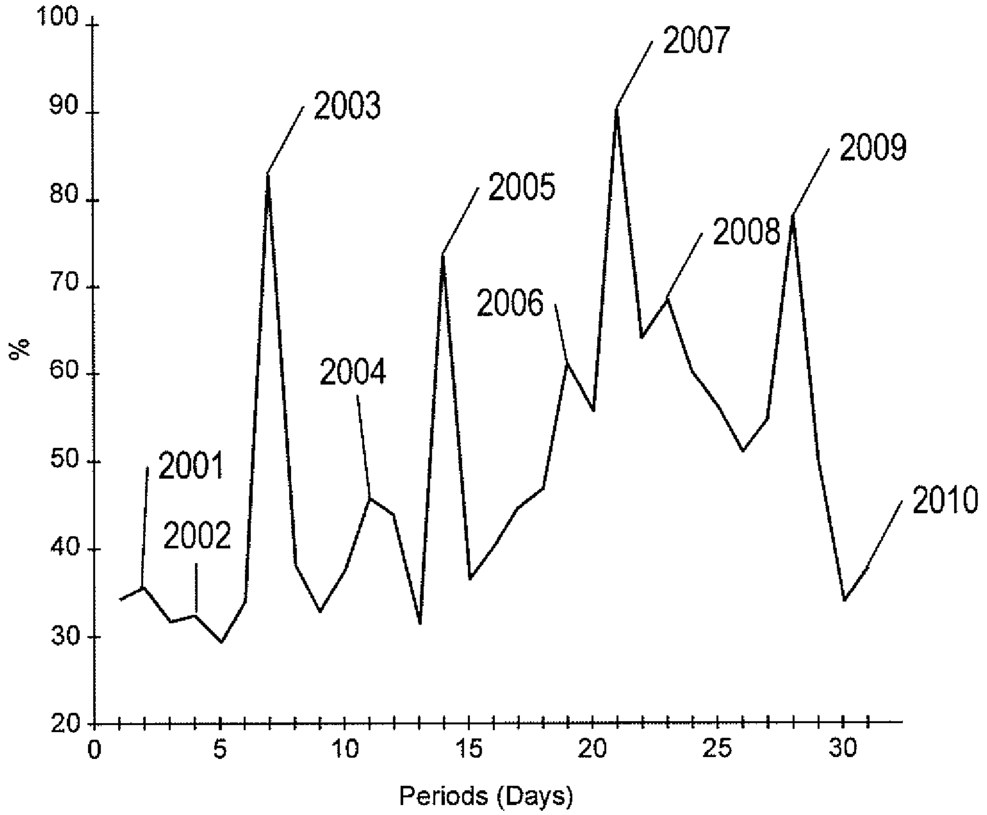
100
90
80
70
60
50
40
30
20
%
0
5
10
15
20
25
30
Periods (Days)
2001
2002
2003
2004
2005
2006
2007
2008
2009
2010

FIG. 20

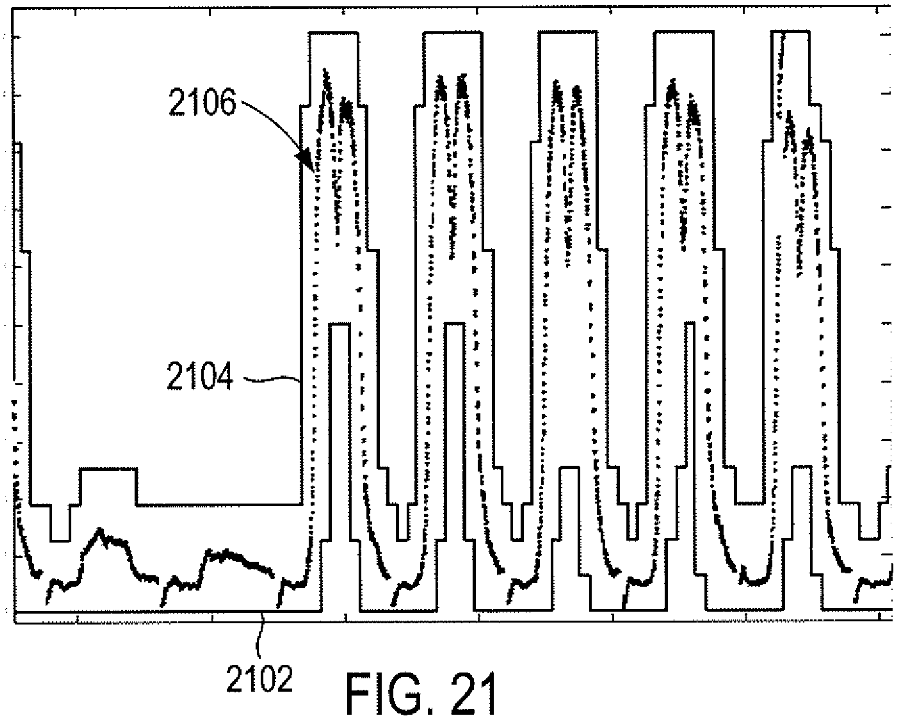
2106
2104
2102

FIG. 21

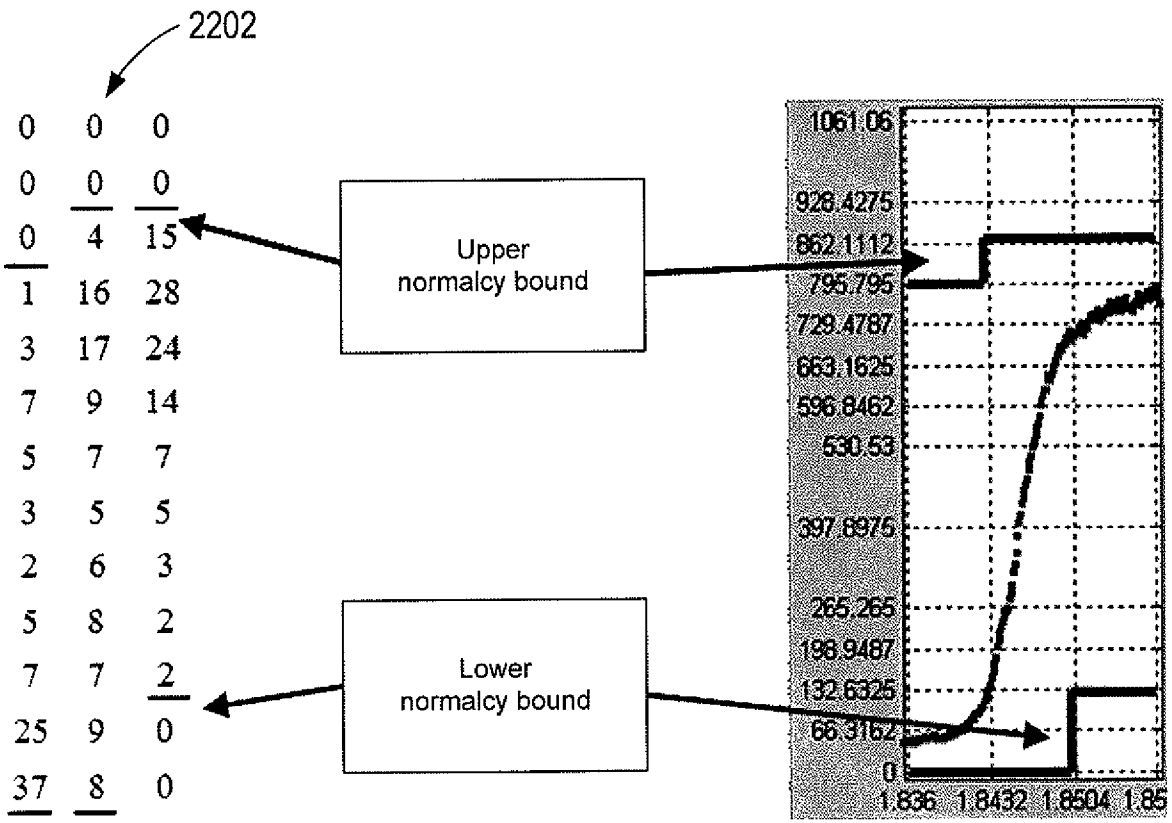
2202
0 0 0
0 0 0
0 4 15
1 16 28
3 17 24
7 9 14
5 7 7
3 5 5
2 6 3
5 8 2
7 7 2
25 9 0
37 8 0
Upper normalcy bound
Lower normalcy bound
1061.06
928.4275
862.1112
795.795
729.4787
663.1625
596.8462
530.53
397.8975
265.265
198.9487
132.6325
66.3162
0
1.836
1.8432
1.8504
1.85

FIG. 22

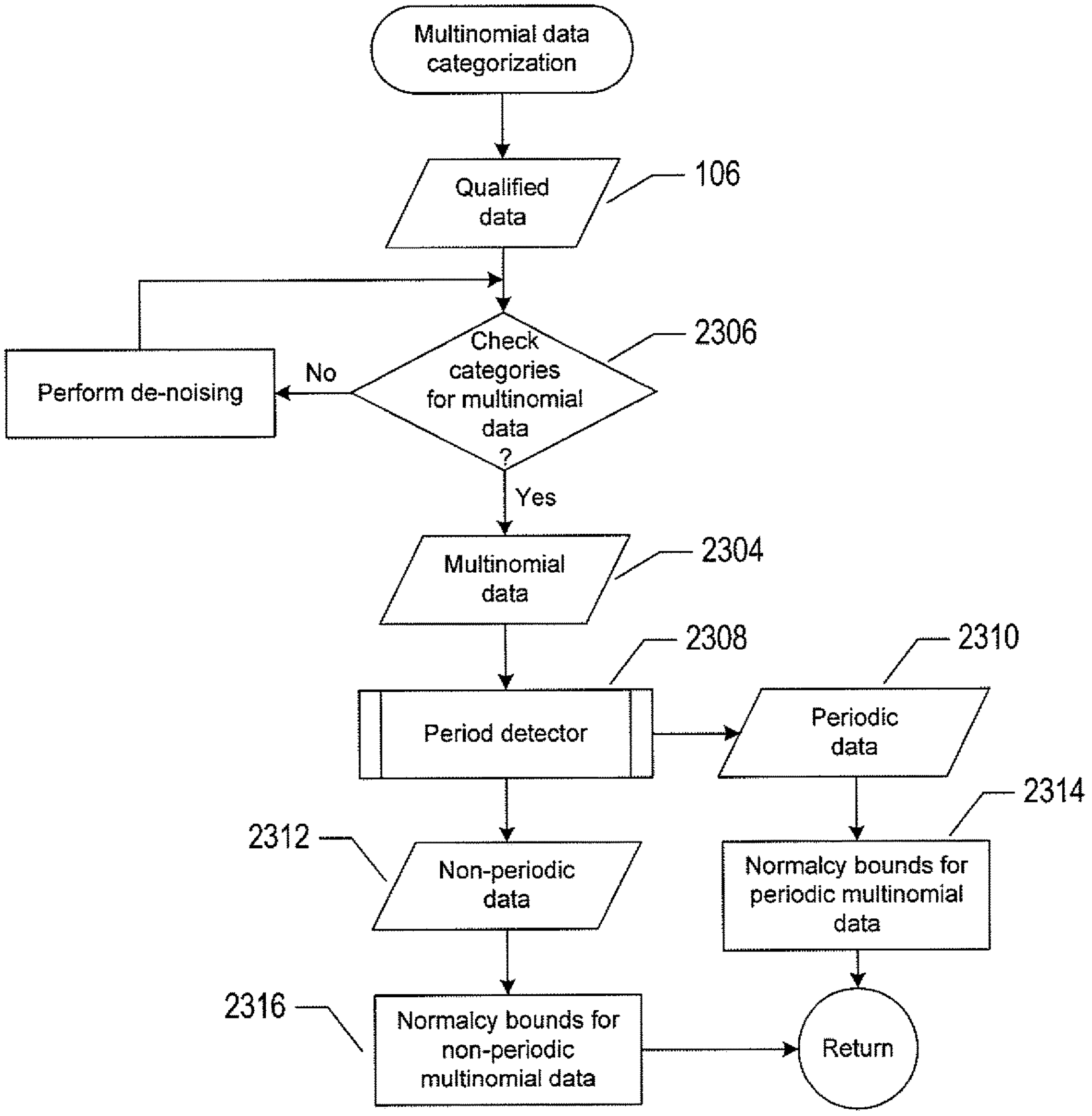
Multinomial data categorization
Qualified data
106
Check categories for multinomial data ?
2306
No
Perform de-noising
Yes
Multinomial data
2304
2308
2310
Period detector
Periodic data
2314
2312
Non-periodic data
Normalcy bounds for periodic multinomial data
2316
Normalcy bounds for non-periodic multinomial data
Return

FIG. 23

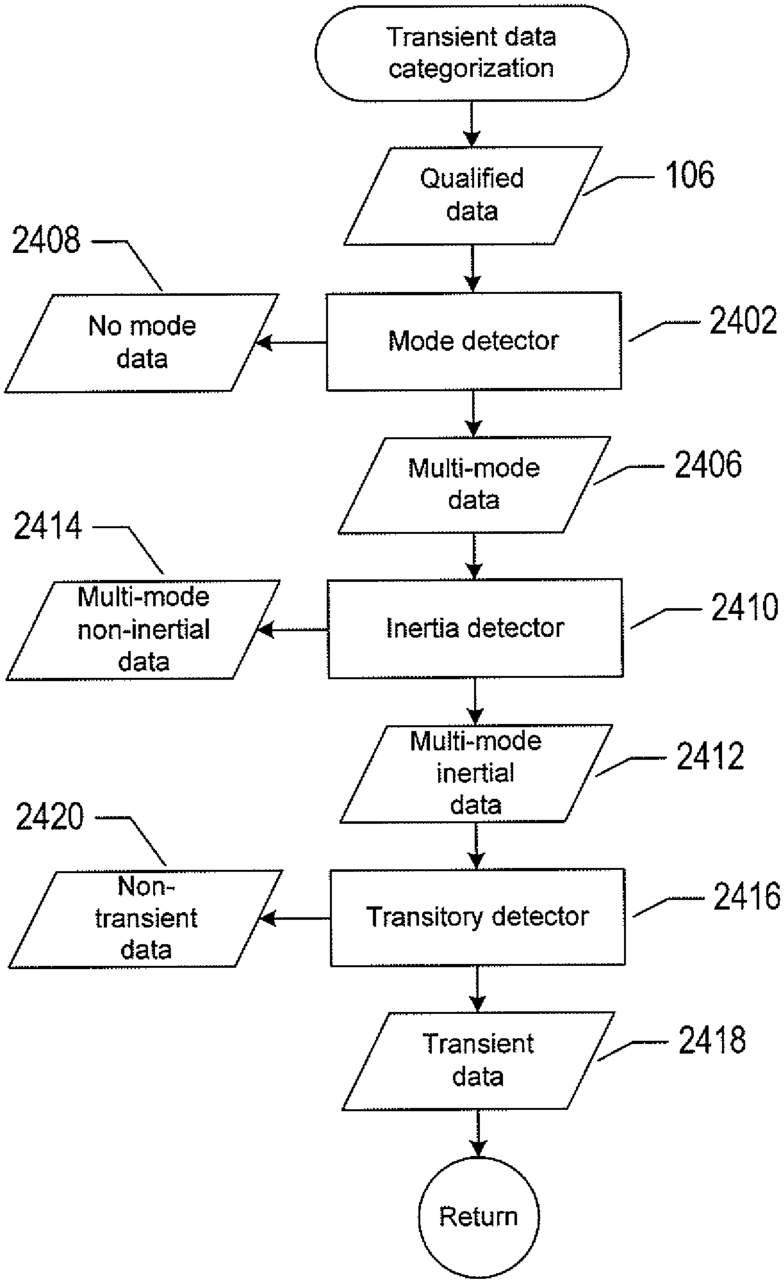
Transient data categorization
Qualified data
106
2408
No mode data
Mode detector
2402
Multi-mode data
2406
2414
Multi-mode non-inertial data
Inertia detector
2410
Multi-mode inertial data
2412
2420
Non-transient data
Transitory detector
2416
Transient data
2418
Return

FIG. 24

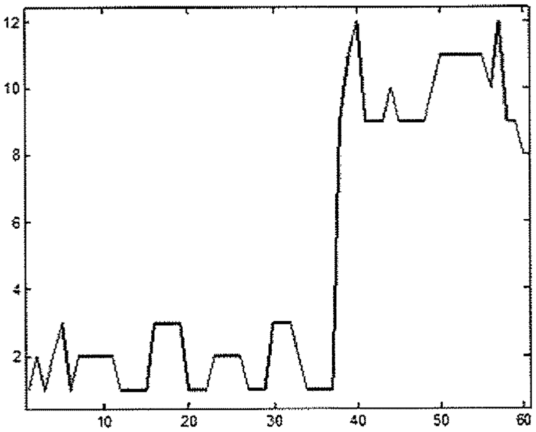

FIG. 25A

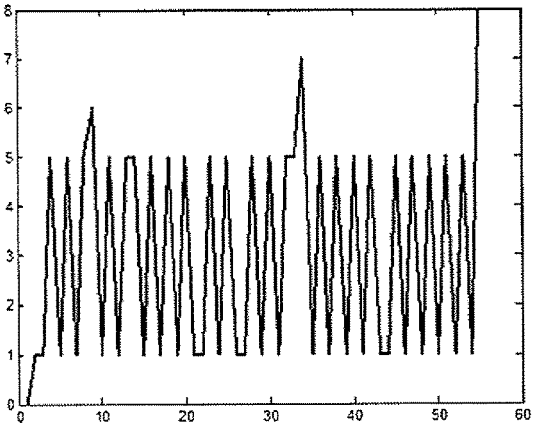

FIG. 25B

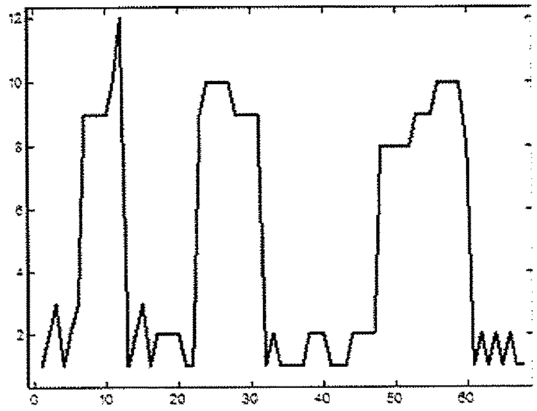

FIG. 25C

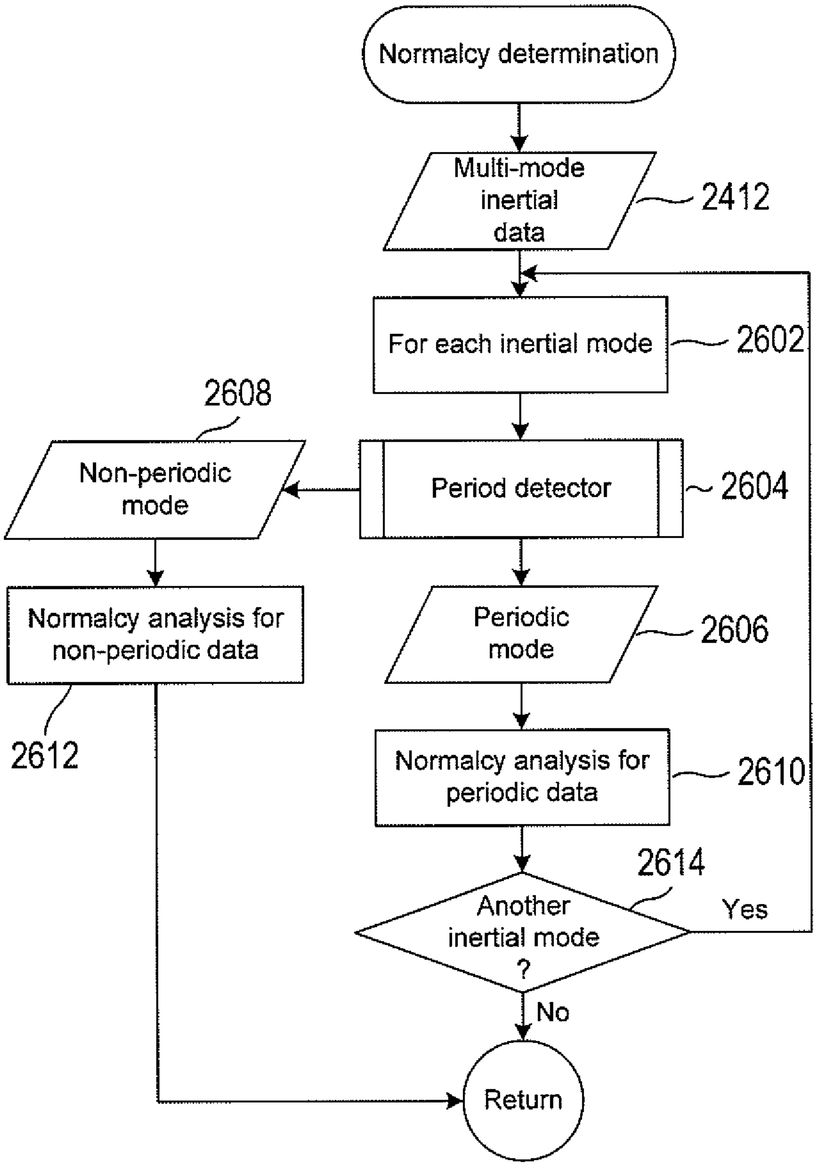
Normalcy determination
Multi-mode inertial data
2412
For each inertial mode
2602
2608
Non-periodic mode
Period detector
2604
Normalcy analysis for non-periodic data
Periodic mode
2606
2612
Normalcy analysis for periodic data
2610
2614
Another inertial mode ?
Yes
No
Return

FIG. 26

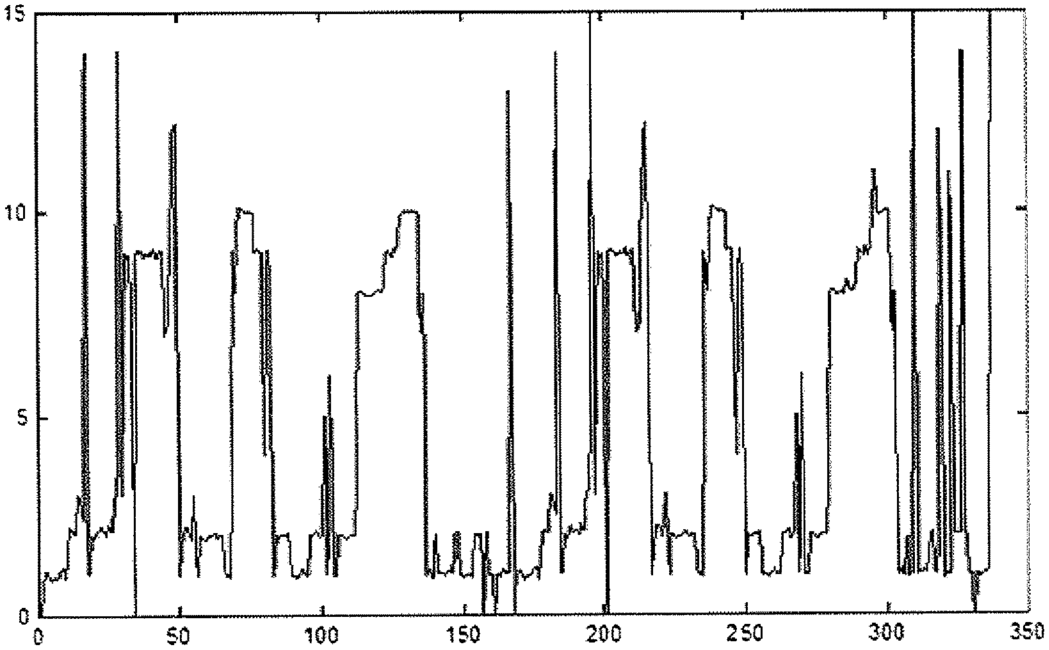

FIG. 27A

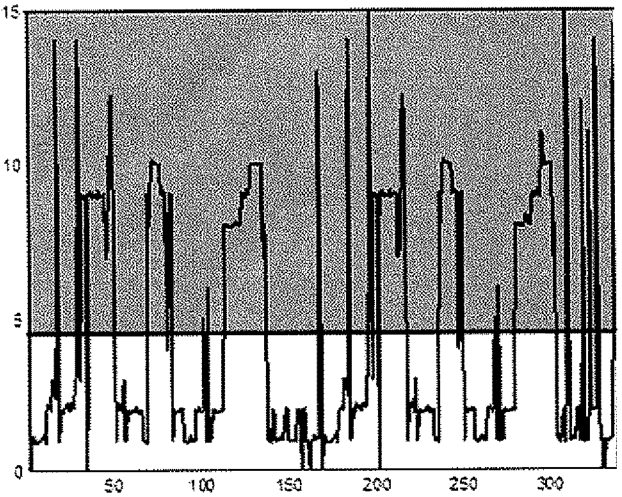

P_{CC}	0
P_{BB}	0.81967
P_{AA}	0.88732

FIG. 27B

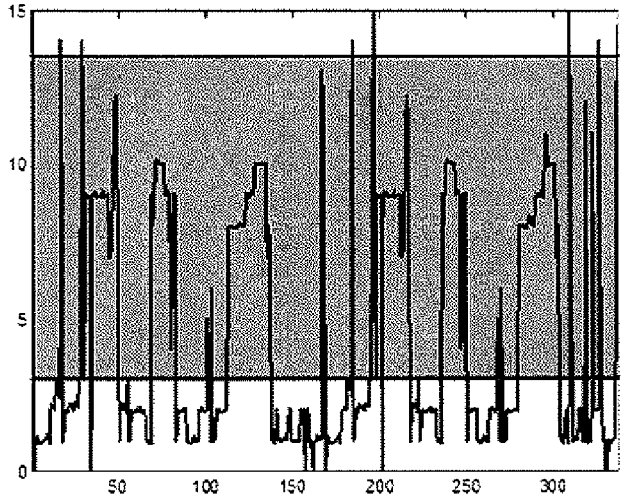

P_{CC}	0
P_{BB}	0.85484
P_{AA}	0.90338

FIG. 27C

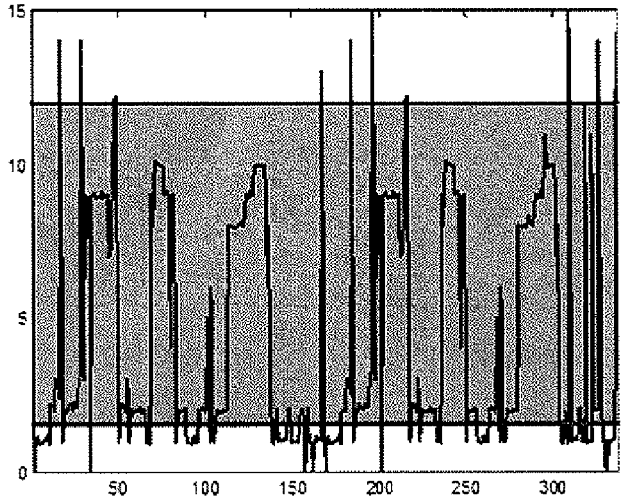

P_{CC}	0.21429
P_{BB}	0.86547
P_{AA}	0.69307

FIG. 27D

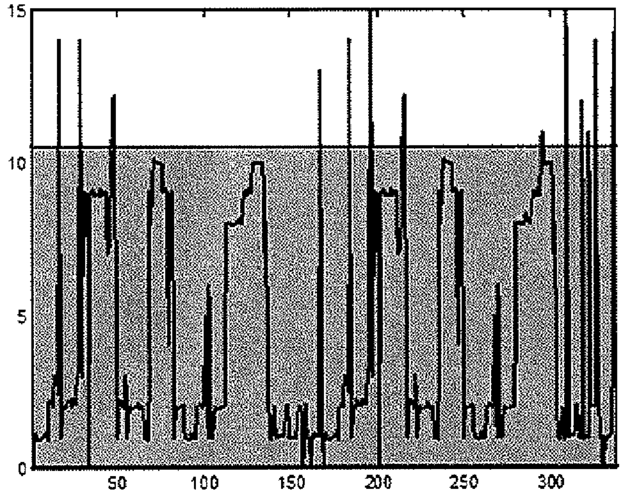

P_{CC}	0.1875
P_{BB}	0.9462
P_{AA}	0

FIG. 27E

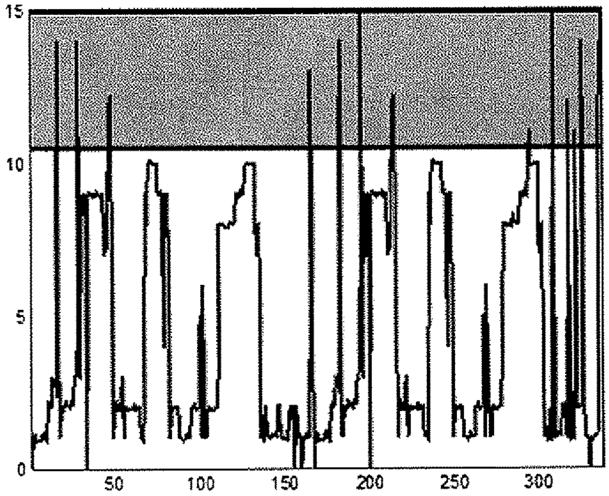

P_{CC}	0
P_{BB}	0.15385
P_{AA}	0.95963

FIG. 27F

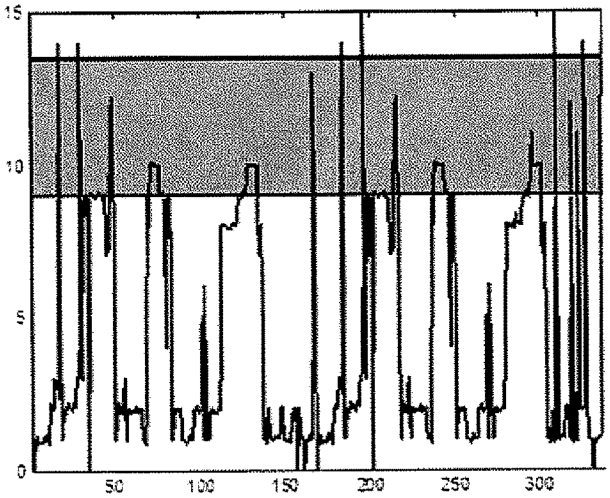

P_{CC}	0
P_{BB}	0.59091
P_{AA}	0.91638

FIG. 27G

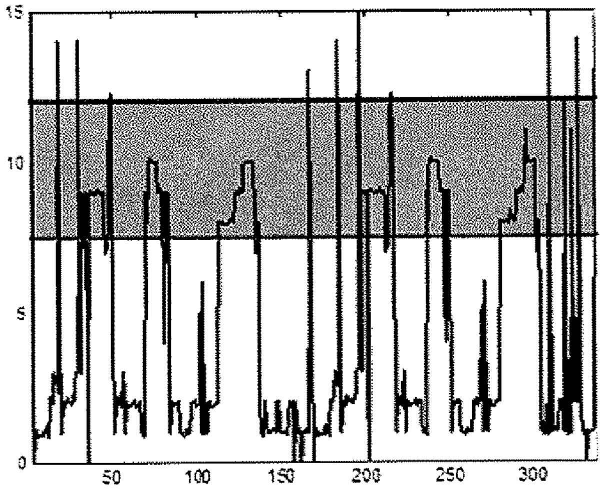

P_{CC}	0.21429
P_{BB}	0.85149
P_{AA}	0.89238

FIG. 27H

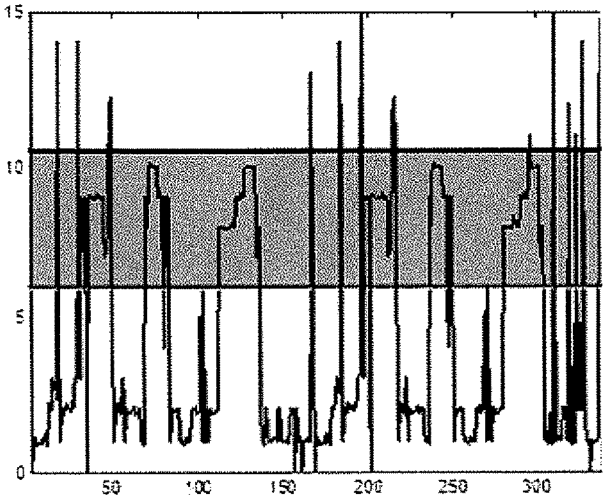

P_{CC}	0.1875
P_{BB}	0.89524
P_{AA}	0.90783

FIG. 27I

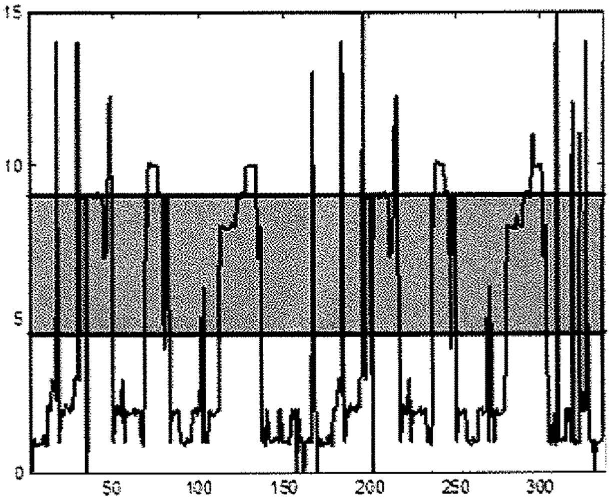

P_{CC}	0.58108
P_{BB}	0.54902
P_{AA}	0.88732

FIG. 27J

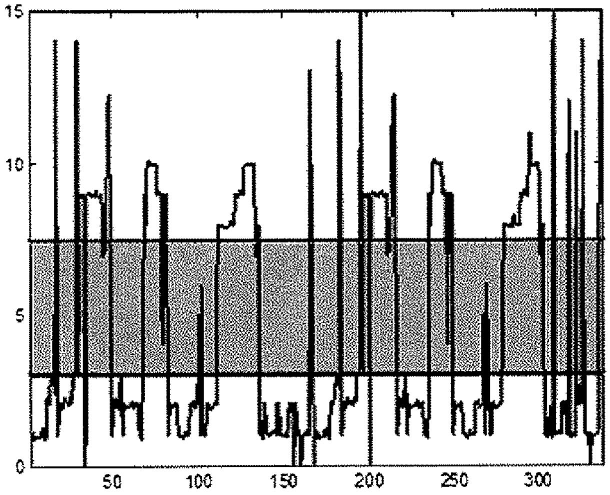

P_{CC}	0.7913
P_{BB}	0.125
P_{AA}	0.90338

FIG. 27K

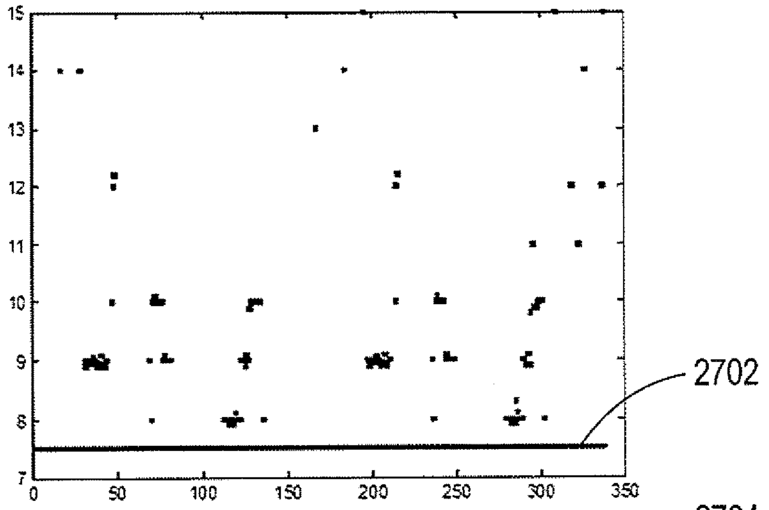

FIG. 27L

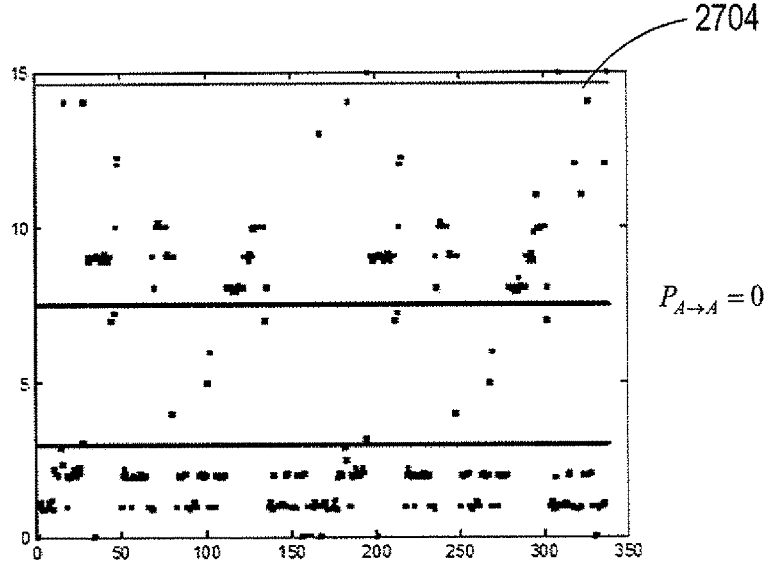

FIG. 27M

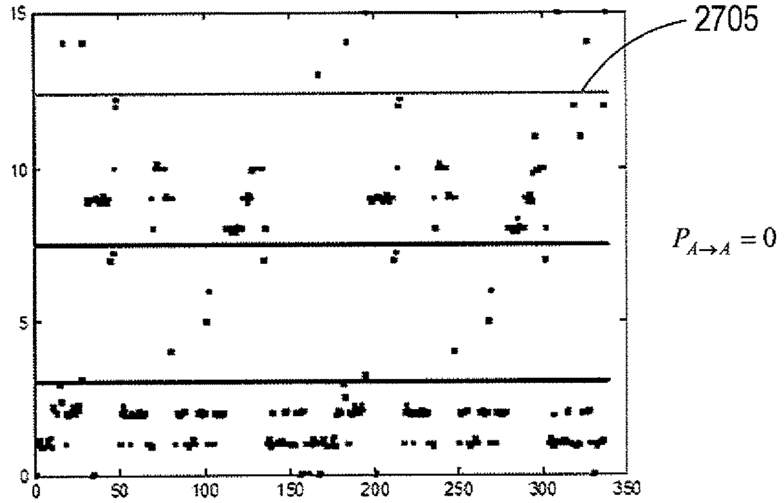

FIG. 27N

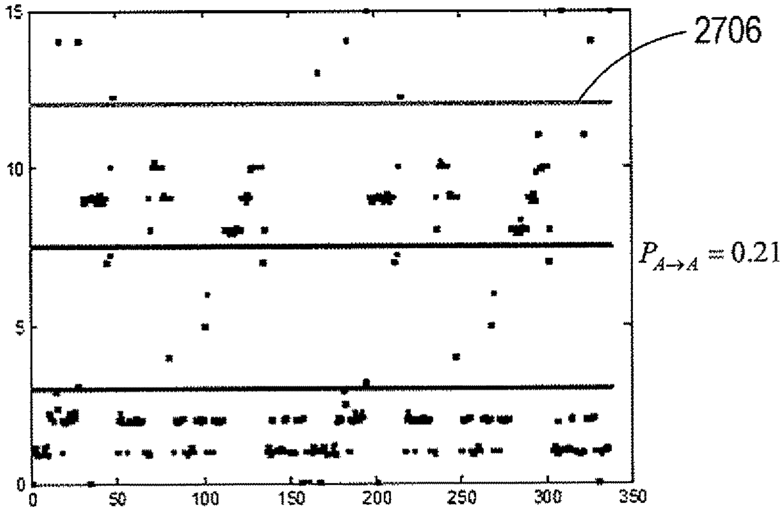

$P_{A \to A} = 0.21429$

FIG. 27O

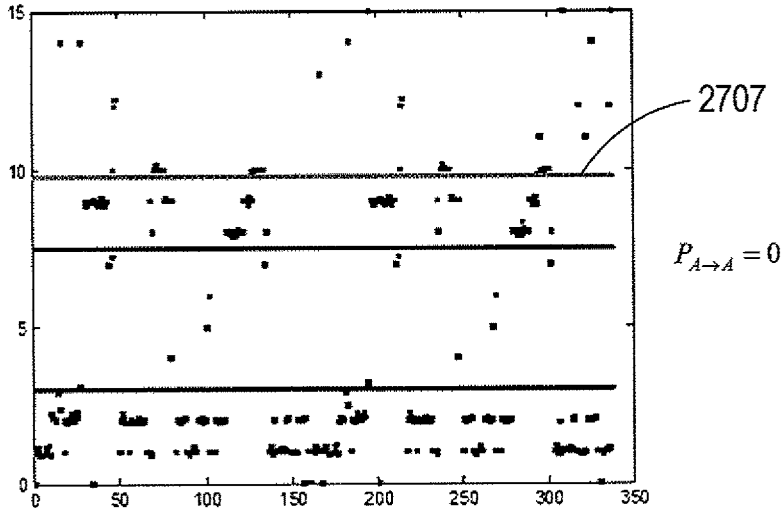

$P_{A \to A} = 0.62791$

FIG. 27P

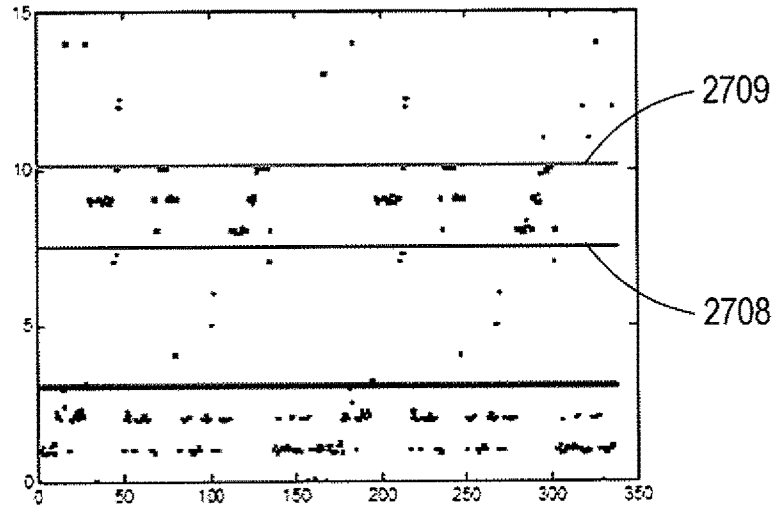

FIG. 27Q

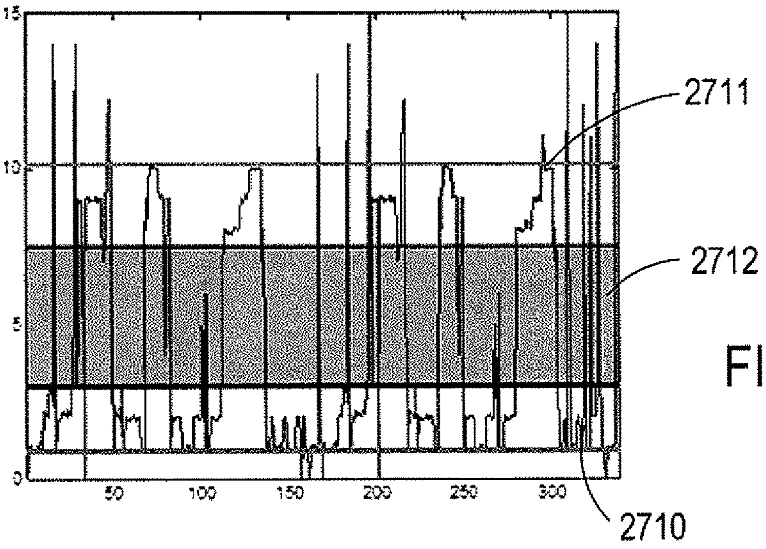

FIG. 27R

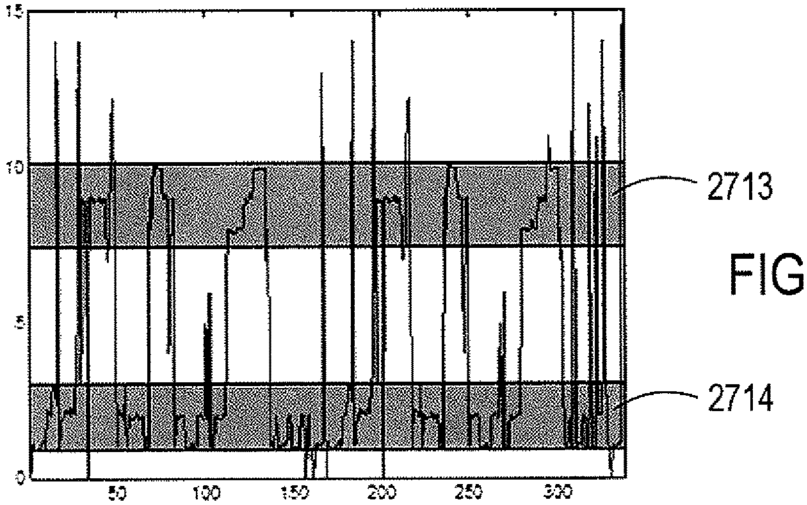

FIG. 27S

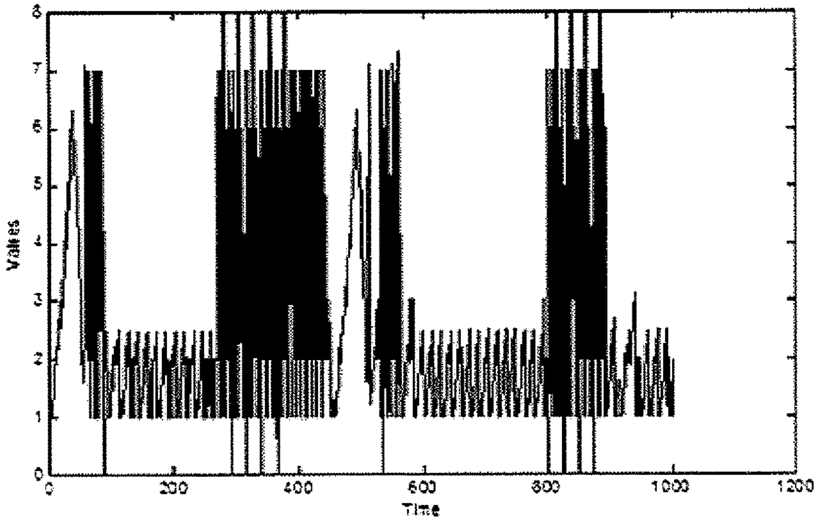

FIG. 27T

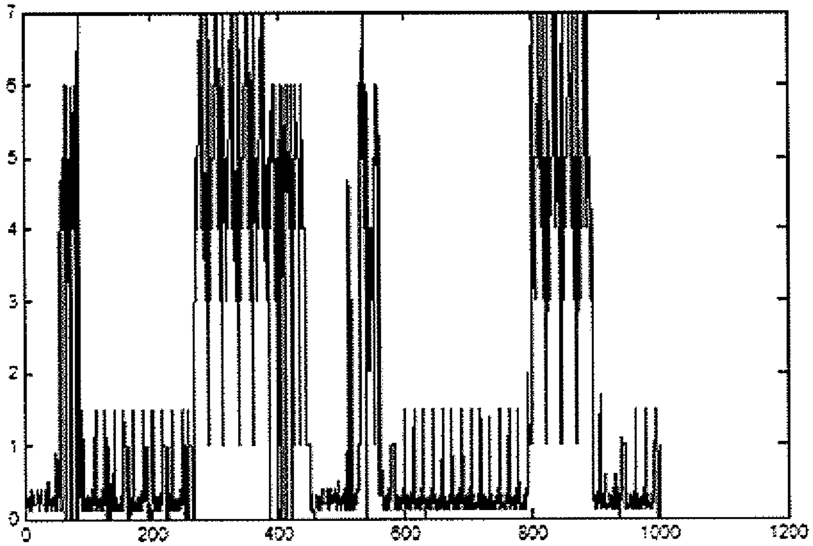

FIG. 27U

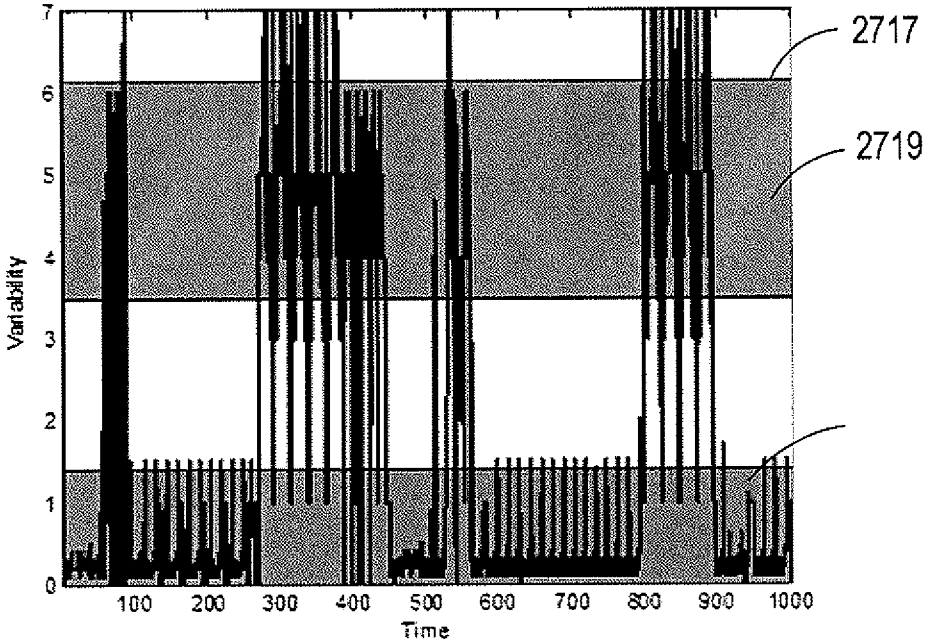

FIG. 27V

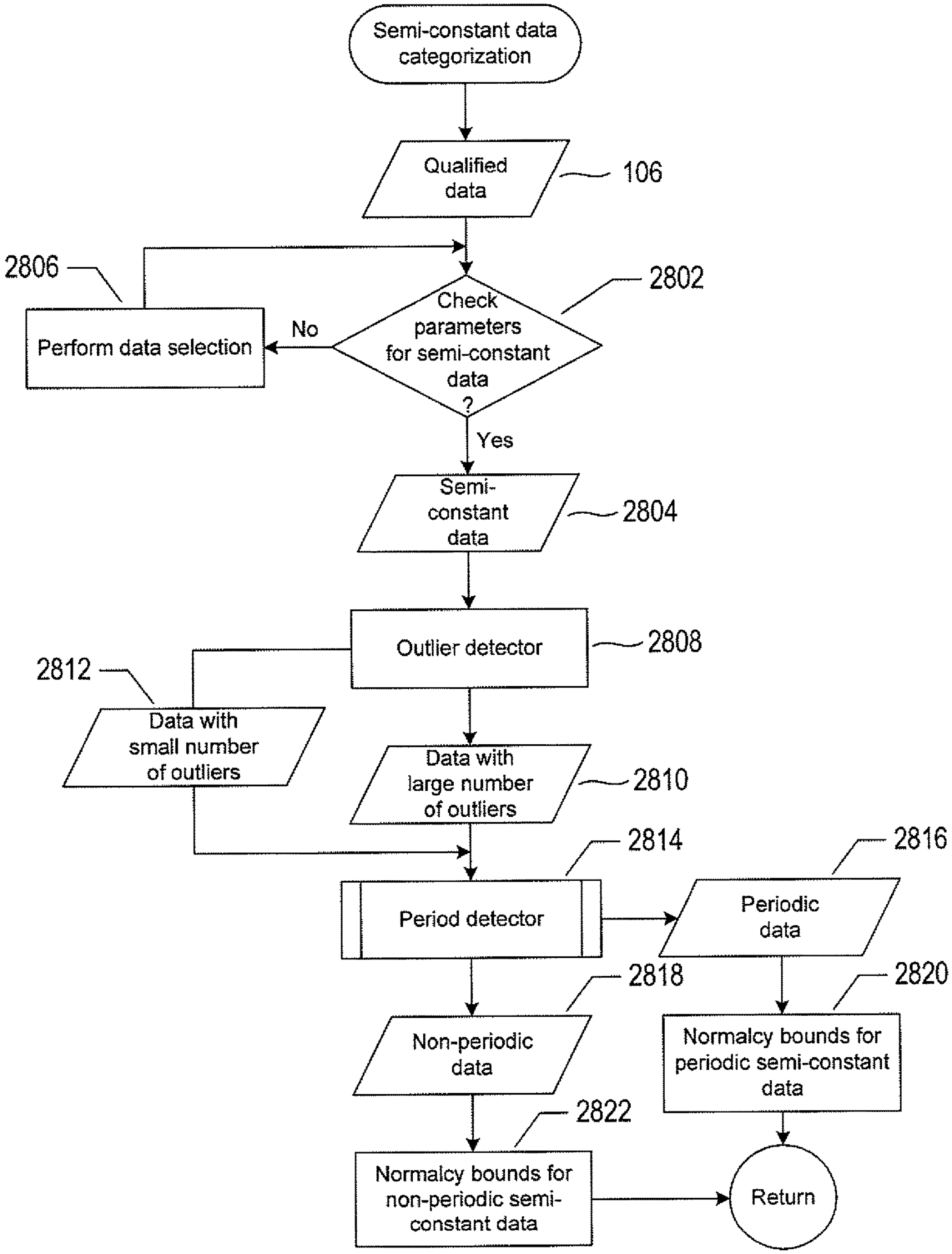
Semi-constant data categorization
Qualified data
106
2806
Perform data selection
No
2802
Check parameters for semi-constant data ?
Yes
Semi-constant data
2804
Outlier detector
2808
2812
Data with small number of outliers
Data with large number of outliers
2810
2814
Period detector
2816
Periodic data
2818
Non-periodic data
2820
Normalcy bounds for periodic semi-constant data
2822
Normalcy bounds for non-periodic semi-constant data
Return

FIG. 28

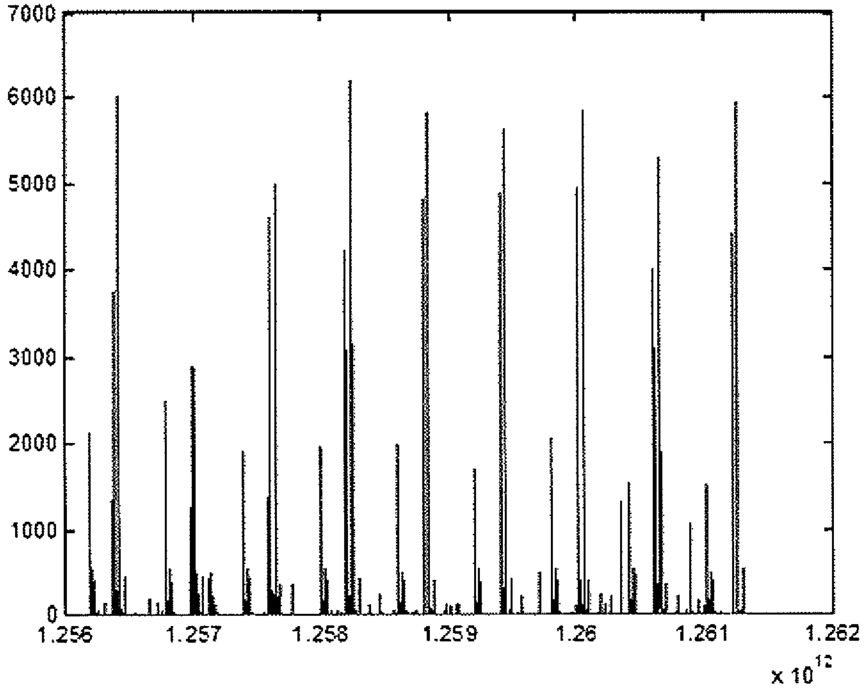

FIG. 29A

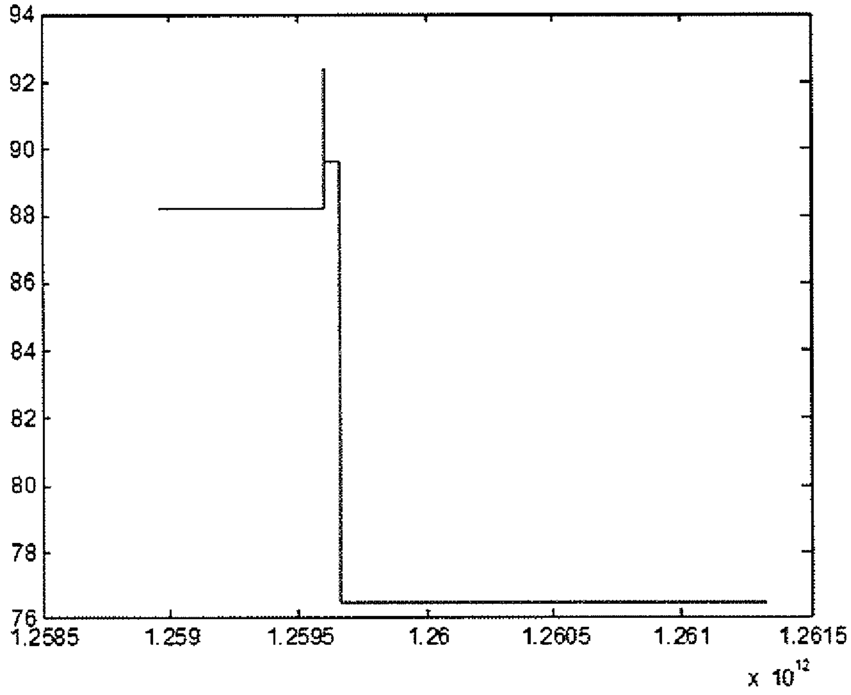

FIG. 29B

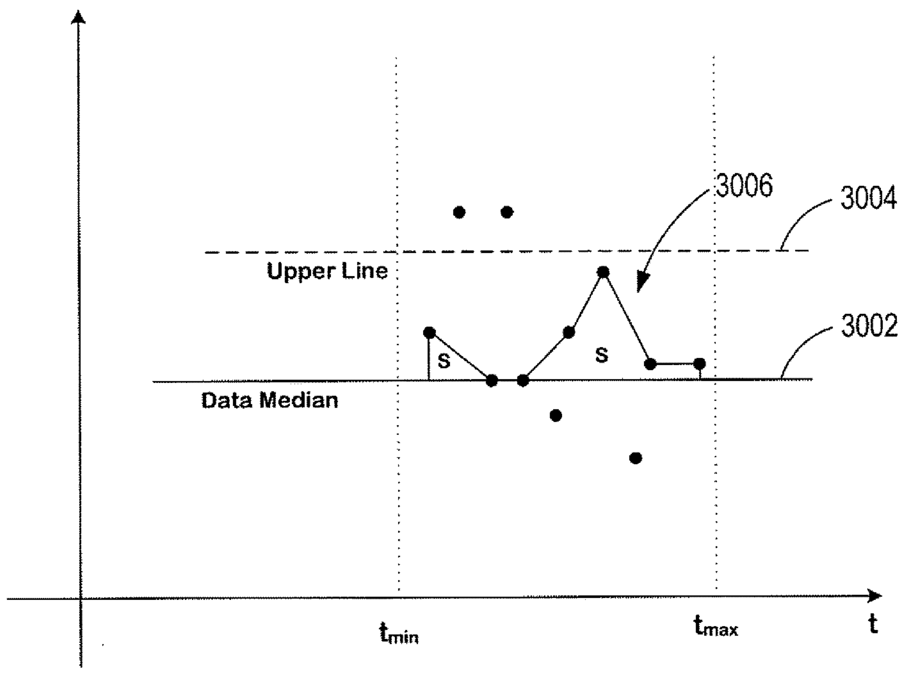

FIG. 30

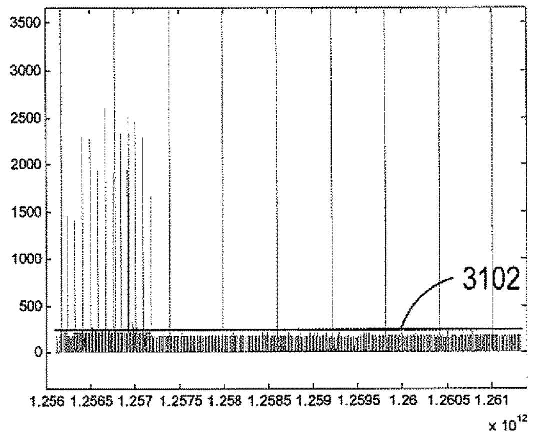

FIG. 31A

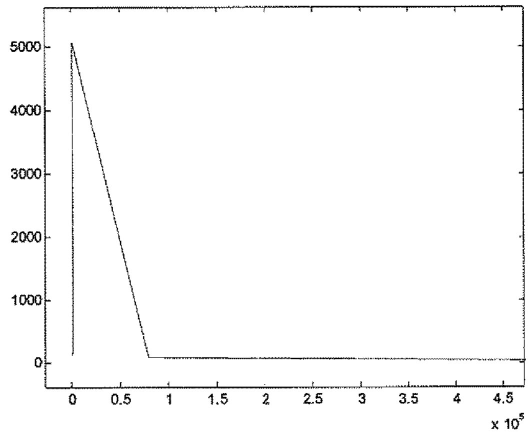

FIG. 31B

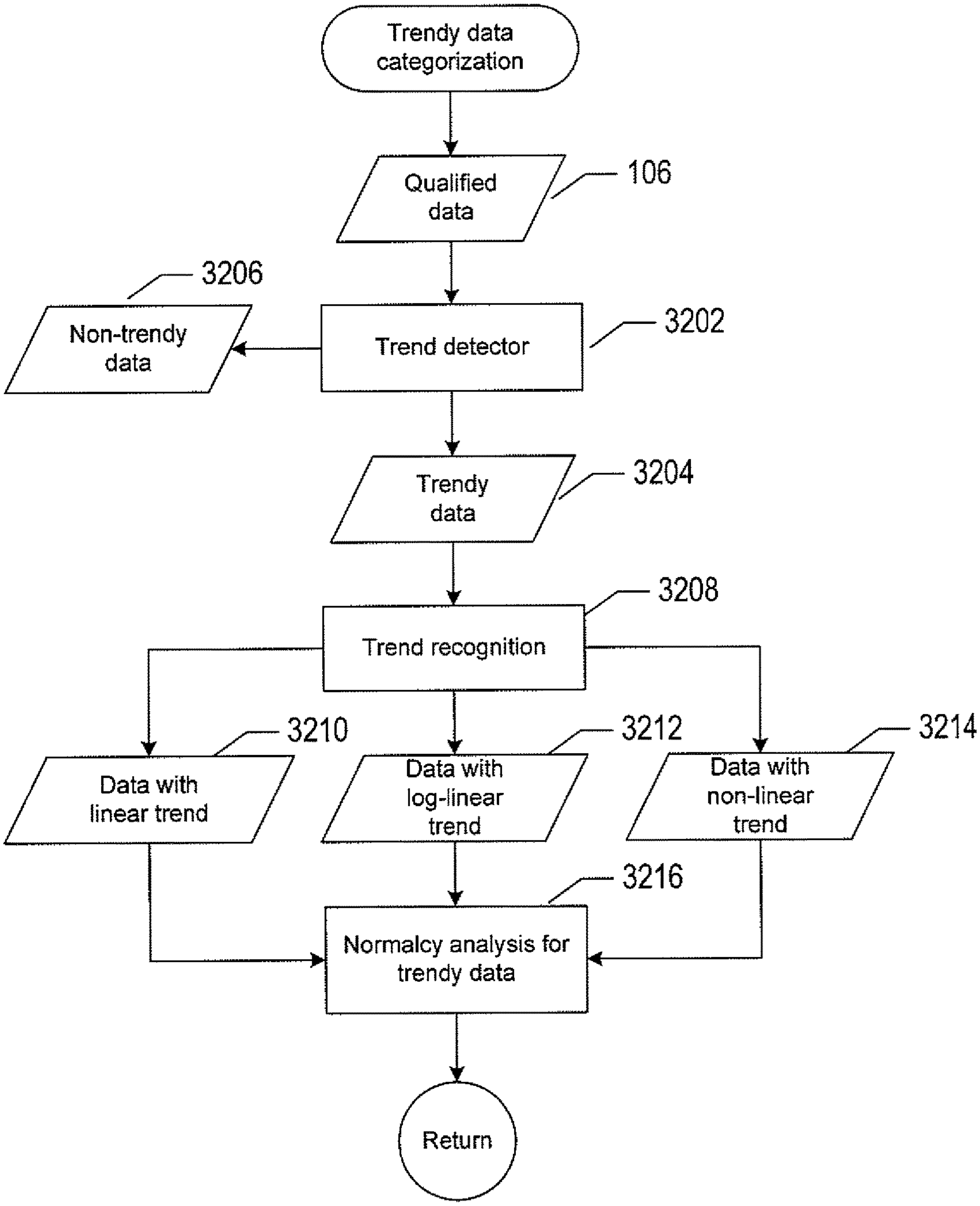
Trendy data categorization
Qualified data
106
3206
Non-trendy data
Trend detector
3202
Trendy data
3204
3208
Trend recognition
3210
Data with linear trend
3212
Data with log-linear trend
3214
Data with non-linear trend
3216
Normalcy analysis for trendy data
Return

FIG. 32

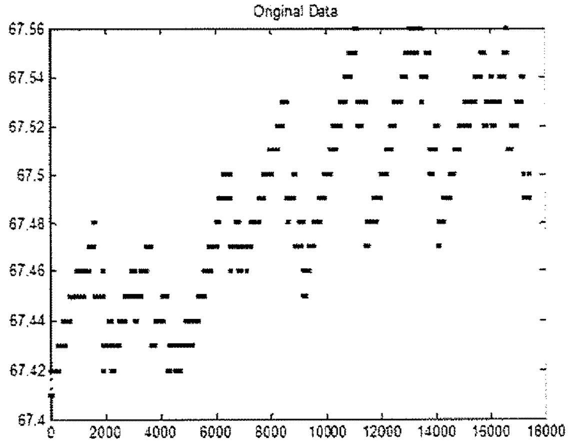

FIG. 33A

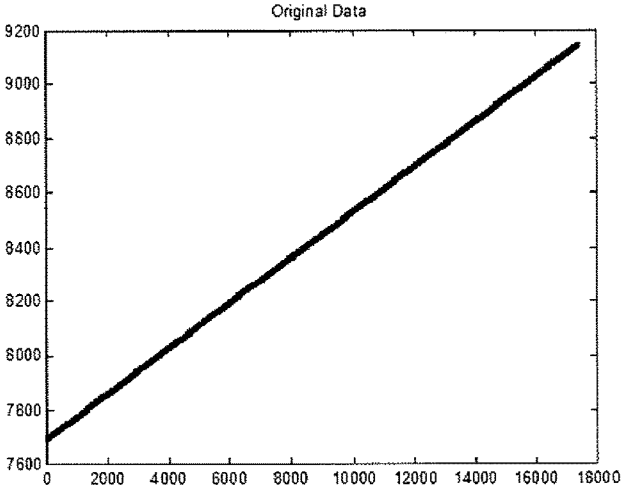

FIG. 33B

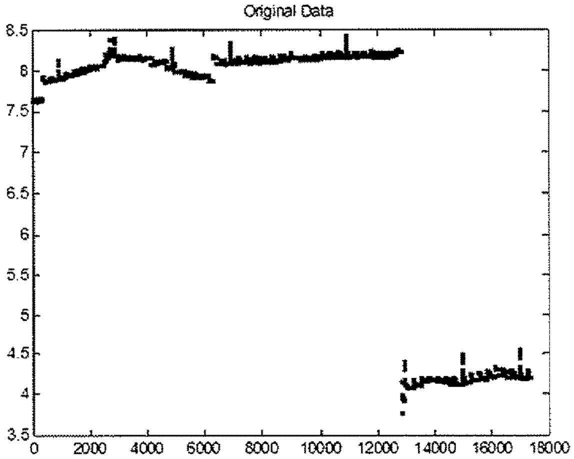

FIG. 33C

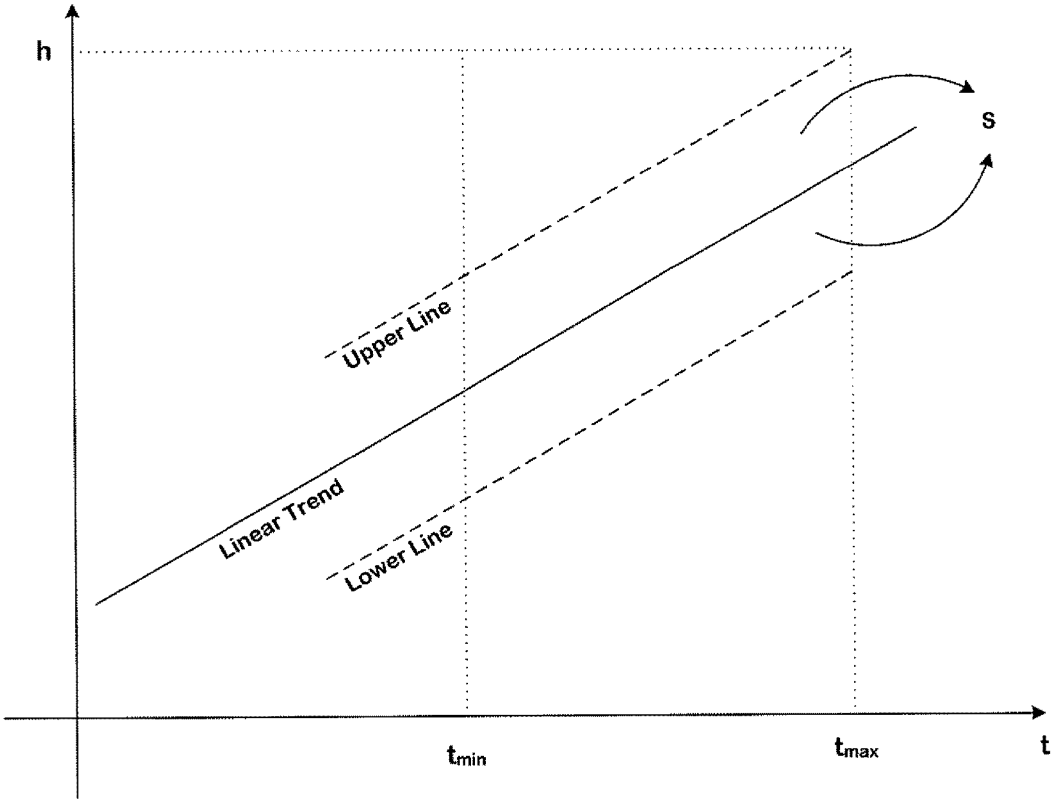

FIG. 34

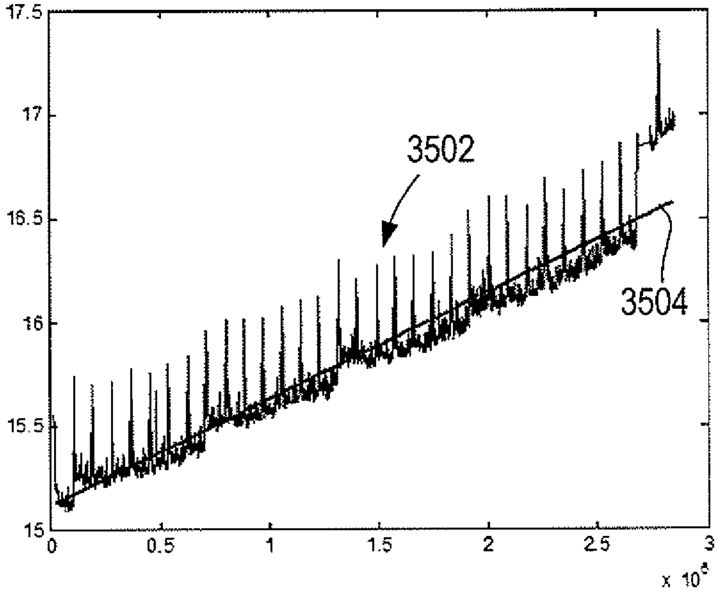

FIG. 35A

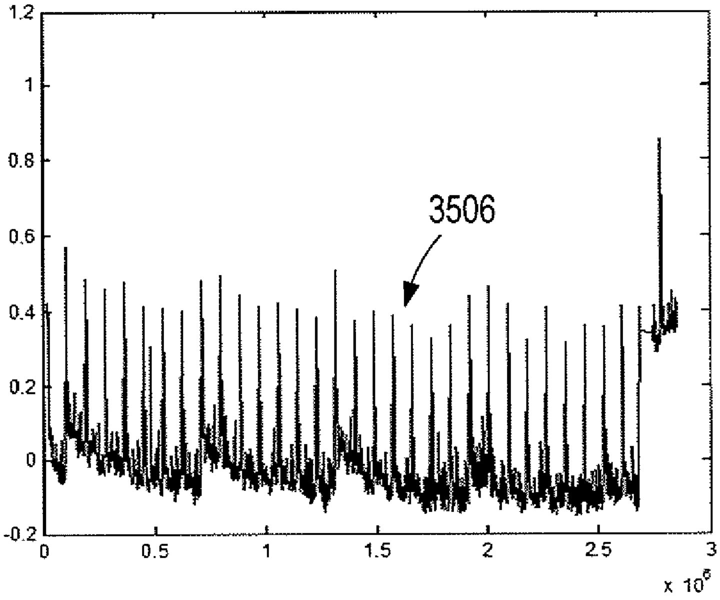

FIG. 35B

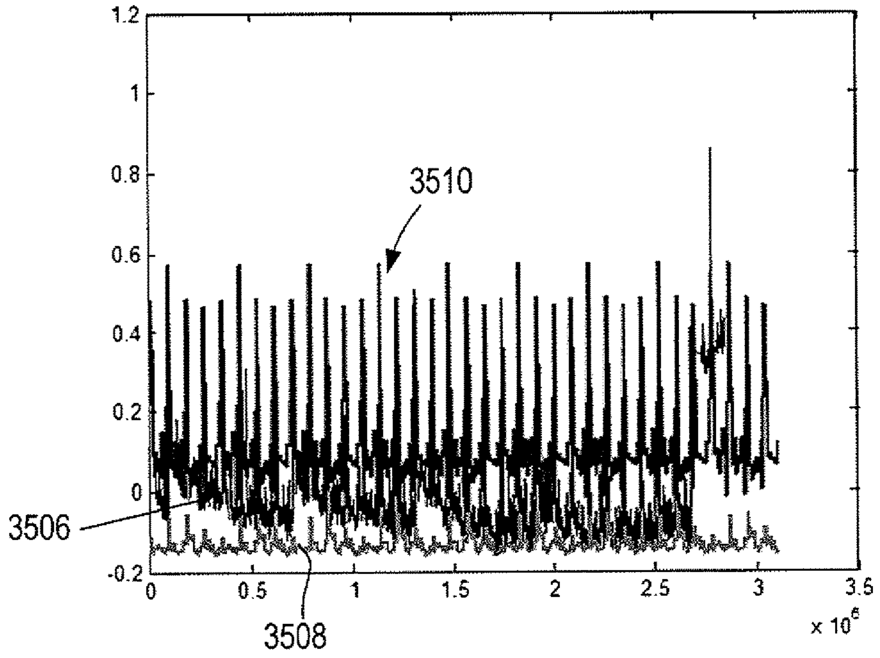

FIG. 35C

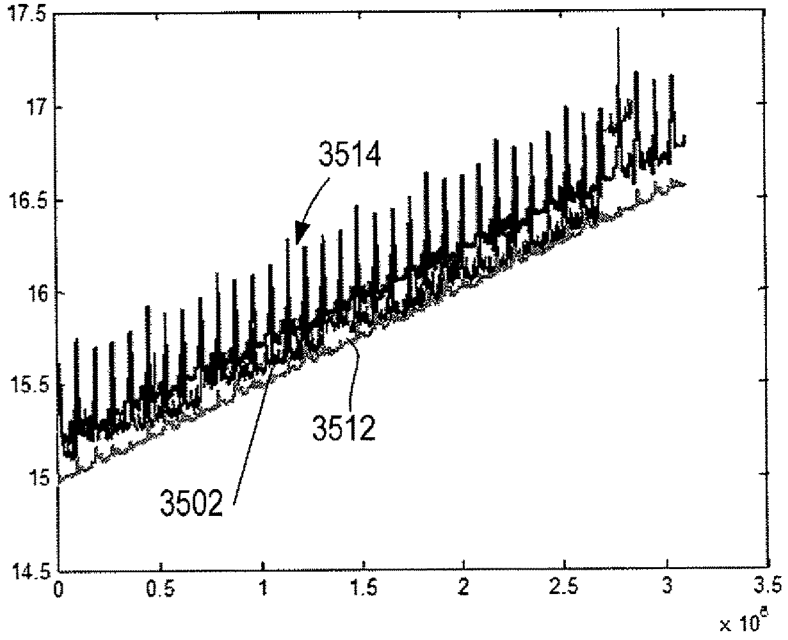

FIG. 35D

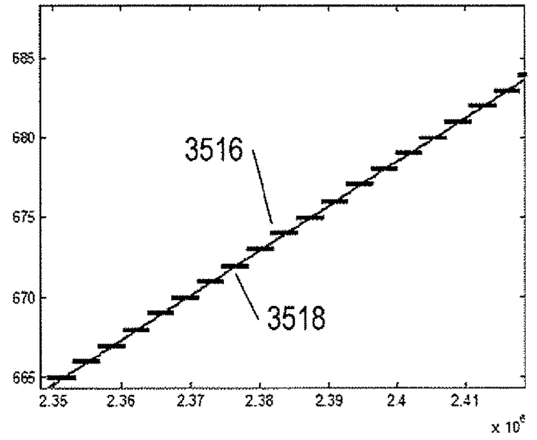

FIG. 35E

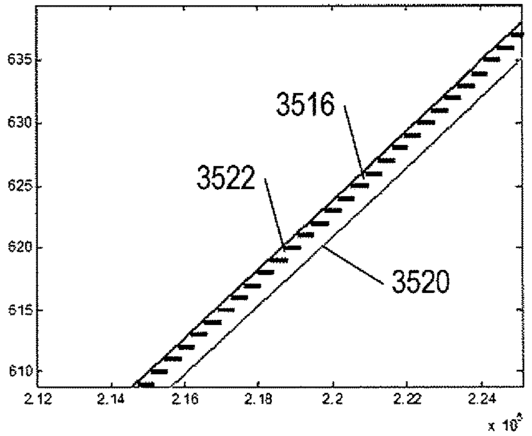

FIG. 35F

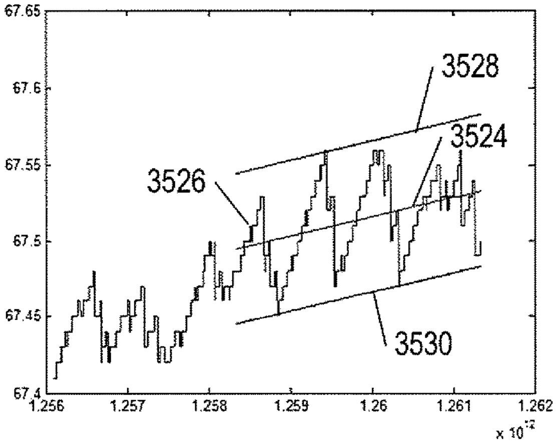

FIG. 35G

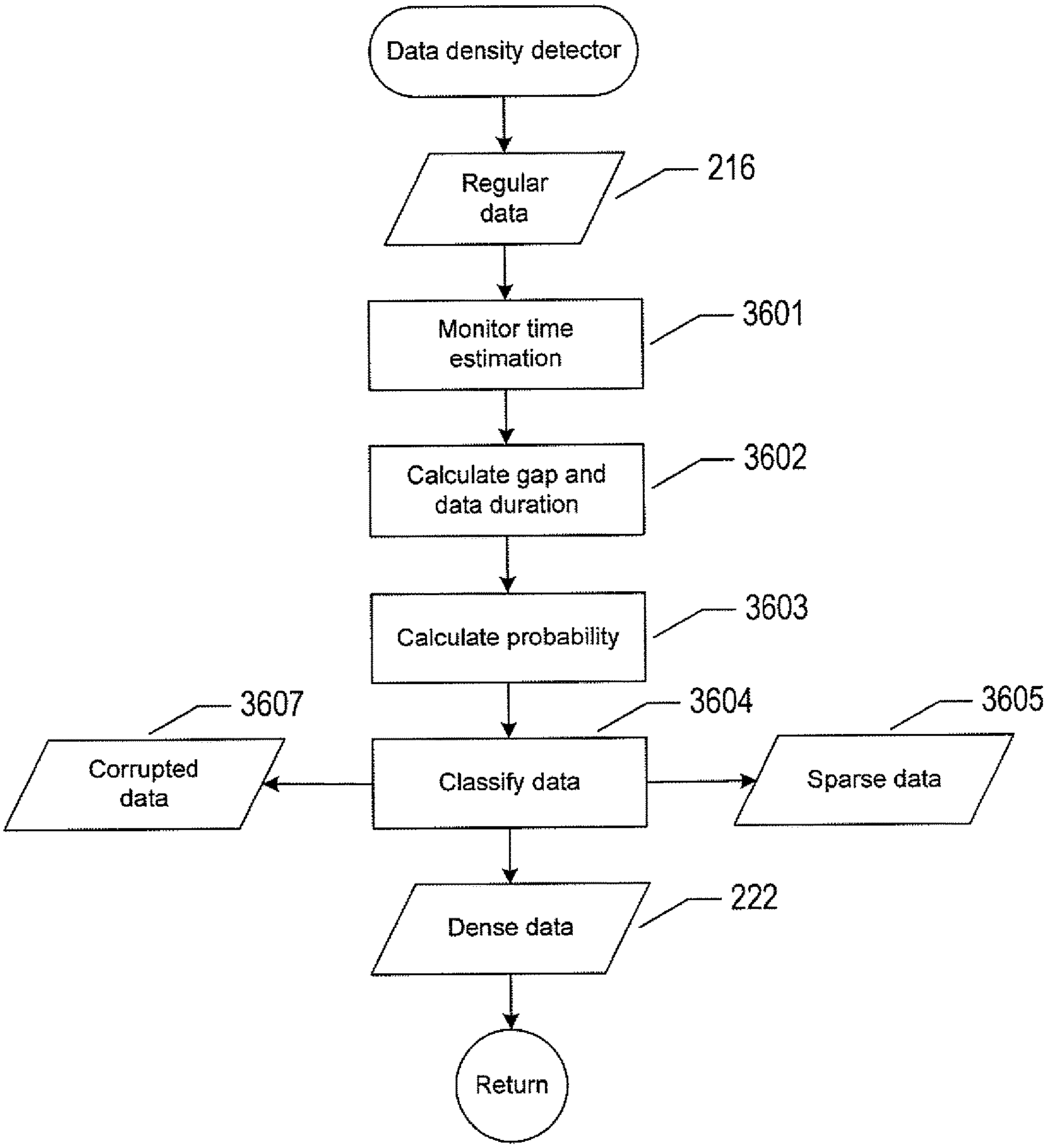
Data density detector
Regular data
216
Monitor time estimation
3601
Calculate gap and data duration
3602
Calculate probability
3603
3607
Corrupted data
Classify data
3604
Sparse data
3605
Dense data
222
Return

FIG. 36

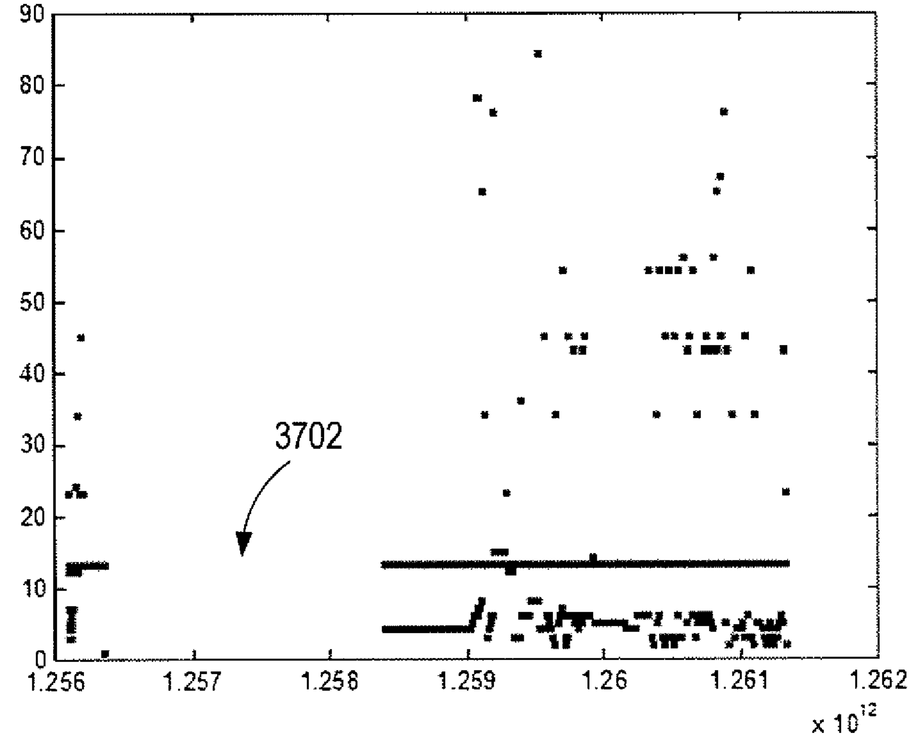

FIG. 37A

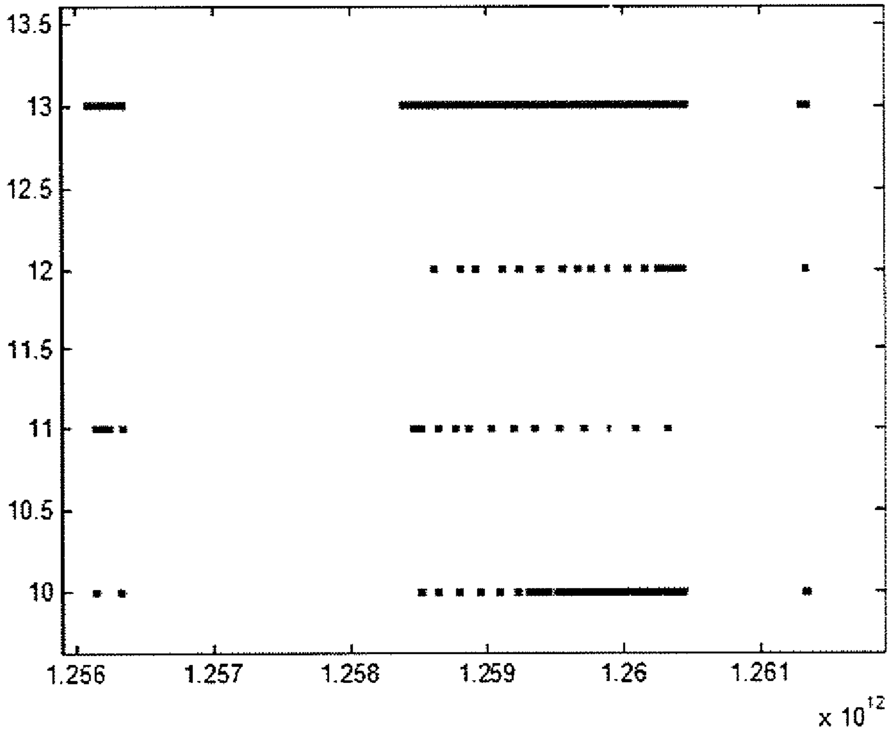

FIG. 37B

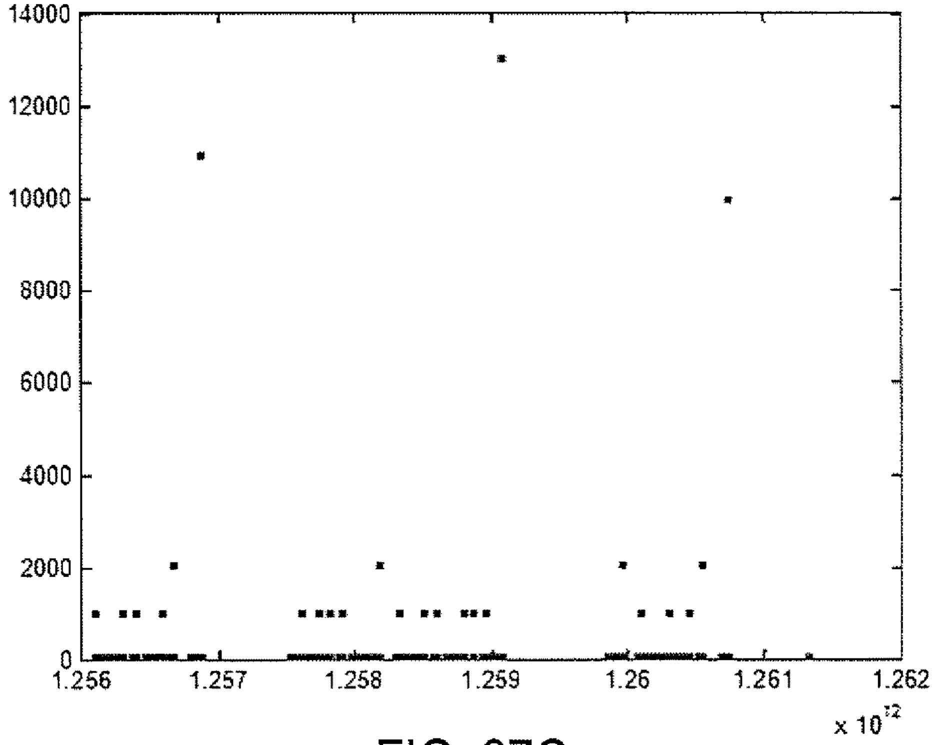

FIG. 37C

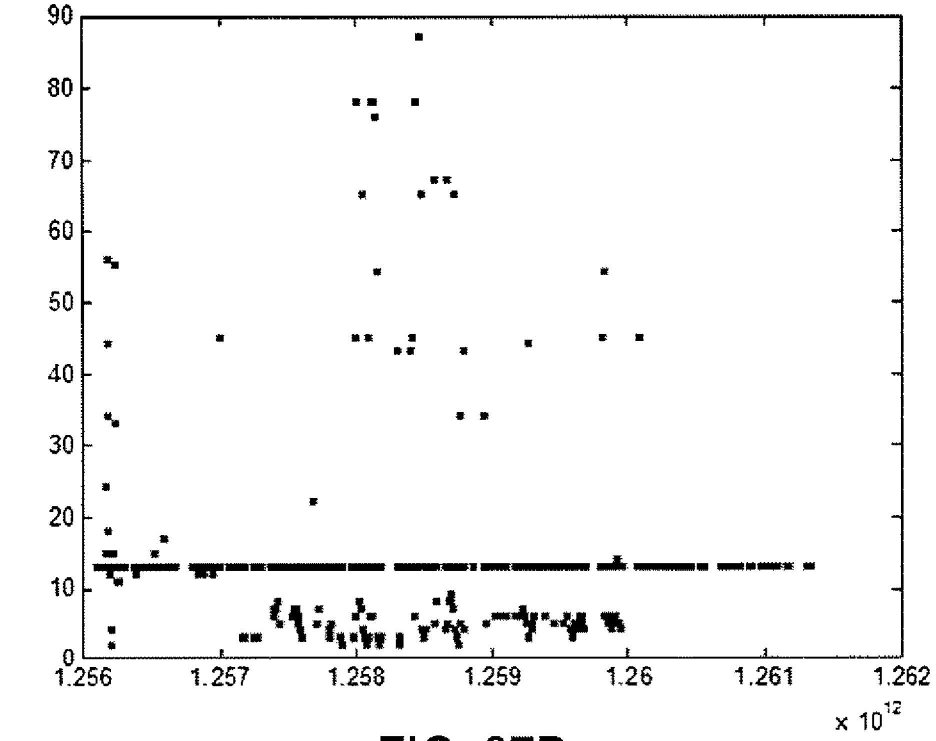

FIG. 37D

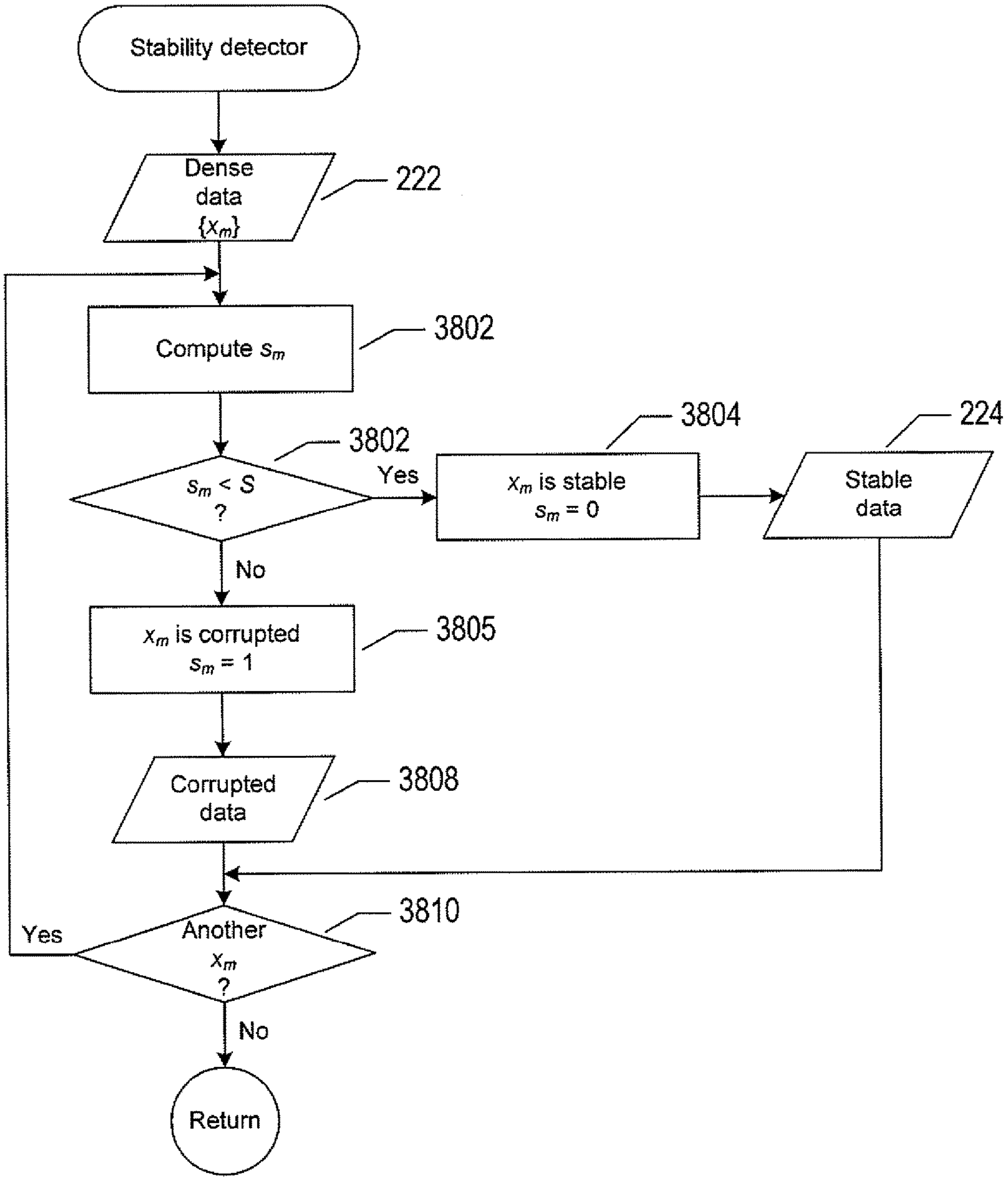
Stability detector
Dense data $\{x_m\}$
222
Compute s_m
3802
$s_m < S$?
3802
Yes
x_m is stable $s_m = 0$
3804
Stable data
224
No
x_m is corrupted $s_m = 1$
3805
Corrupted data
3808
Another x_m ?
3810
Yes
No
Return

FIG. 38

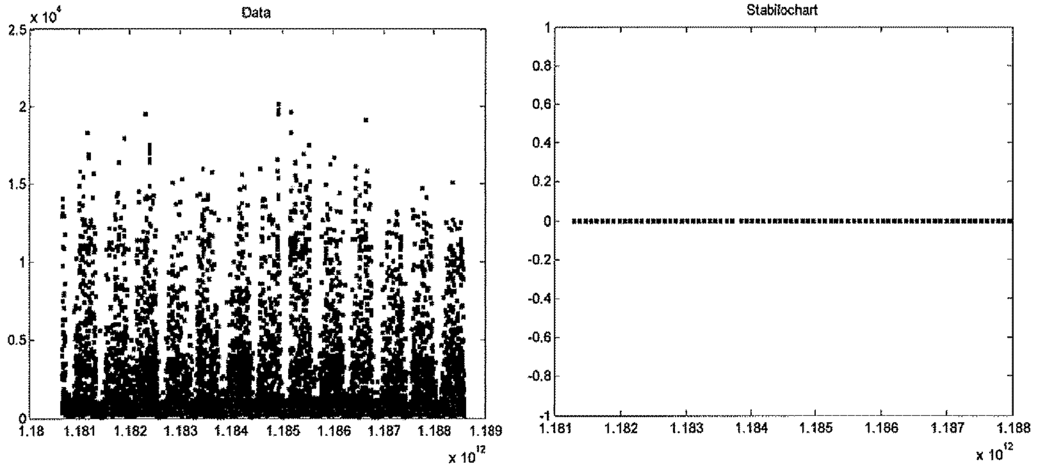

FIG. 39A

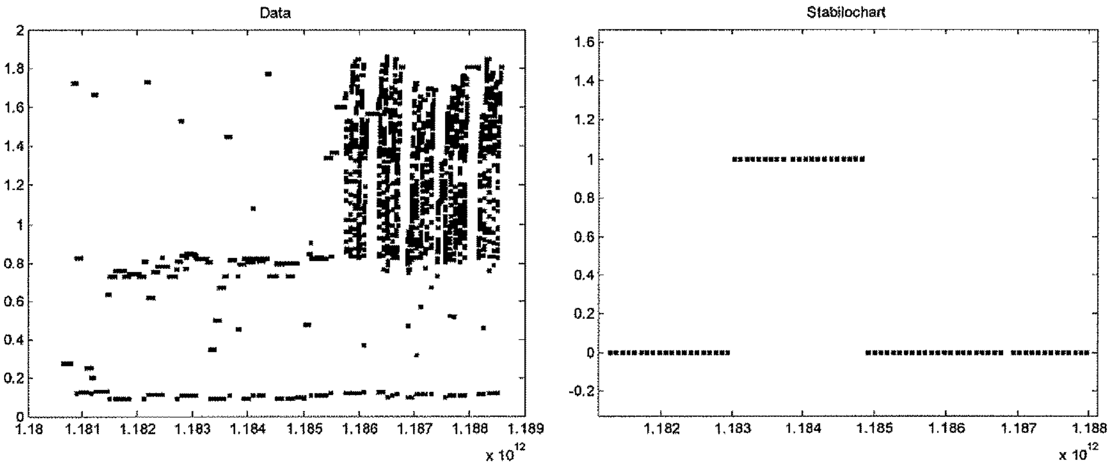

FIG. 39B

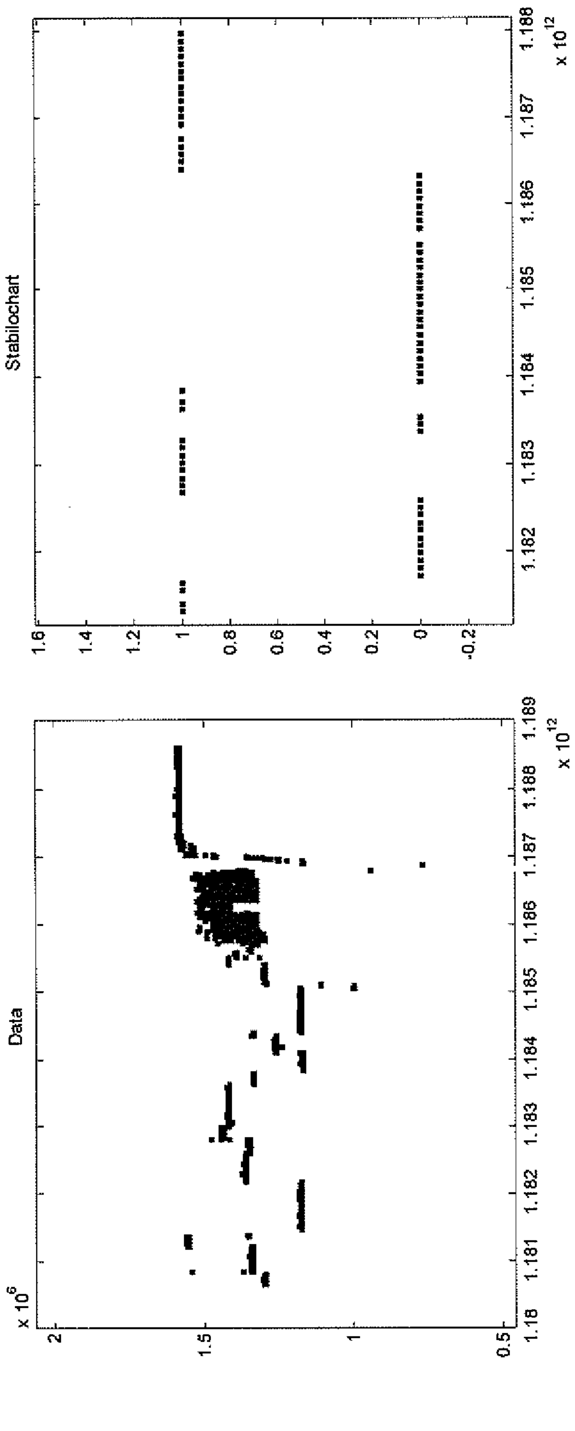
Data
x 10^6
2
1.5
1
0.5
1.18
1.181
1.182
1.183
1.184
1.185
1.186
1.187
1.188
1.189
x 10^12
Stabilochart
1.6
1.4
1.2
1
0.8
0.6
0.4
0.2
0
-0.2
1.182
1.183
1.184
1.185
1.186
1.187
1.188
x 10^12

FIG. 39C

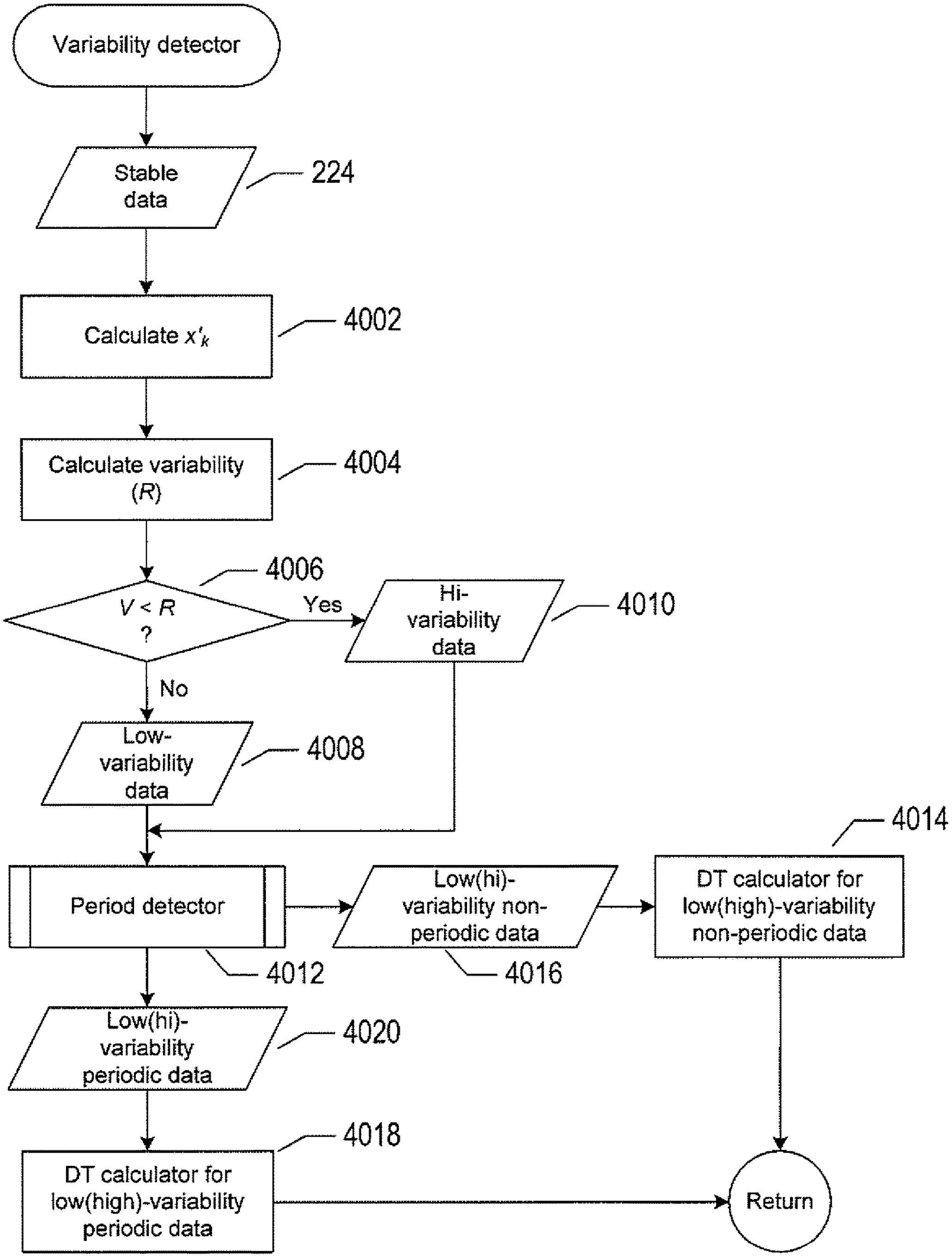
Variability detector
Stable data
224
Calculate x'_k
4002
Calculate variability (R)
4004
4006
$V < R$?
Yes
Hi-variability data
4010
No
Low-variability data
4008
4014
Period detector
Low(hi)-variability non-periodic data
DT calculator for low(high)-variability non-periodic data
4012
4016
Low(hi)-variability periodic data
4020
4018
DT calculator for low(high)-variability periodic data
Return

FIG. 40

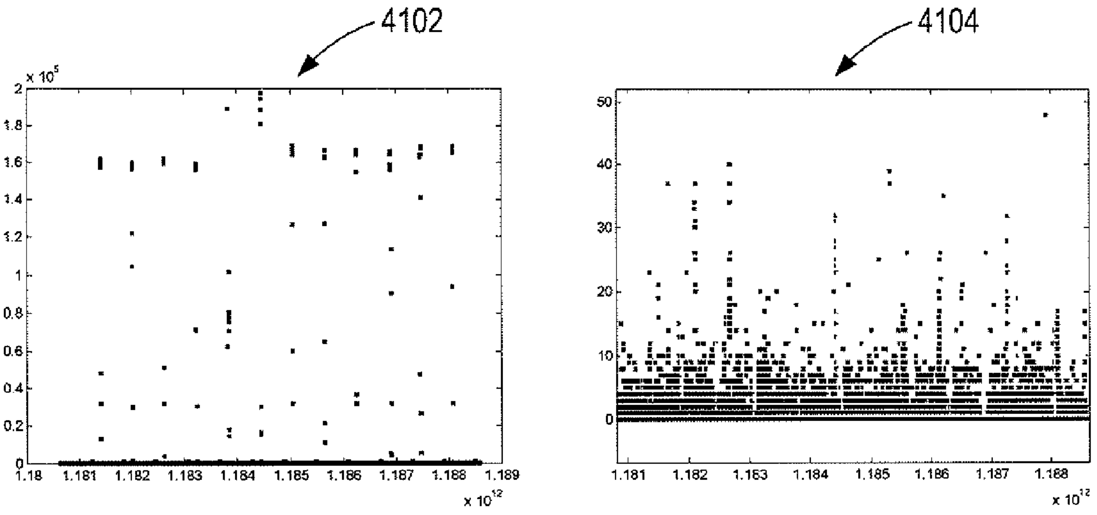

FIG. 41A

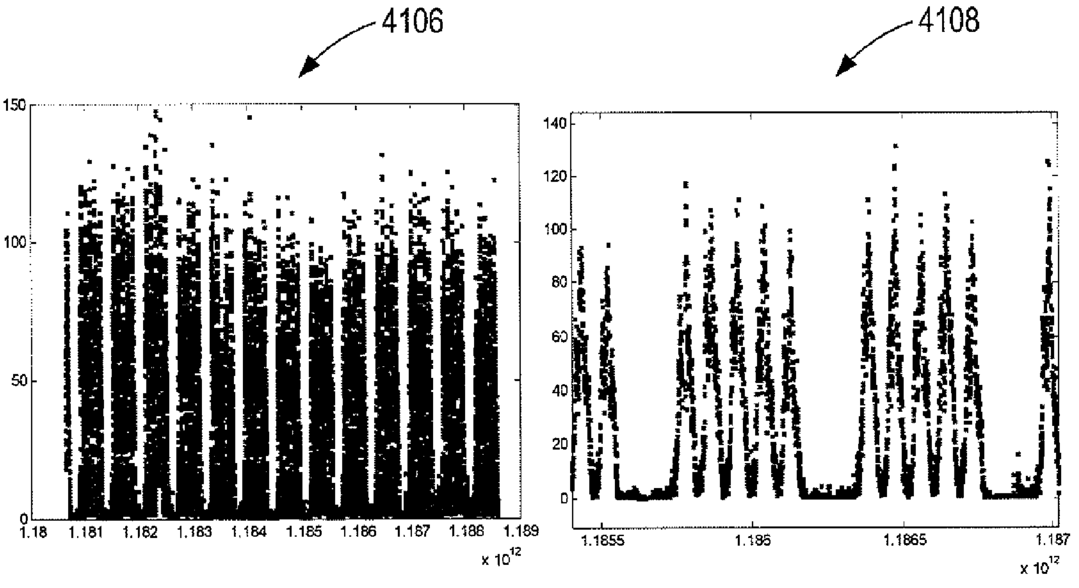

FIG. 41B

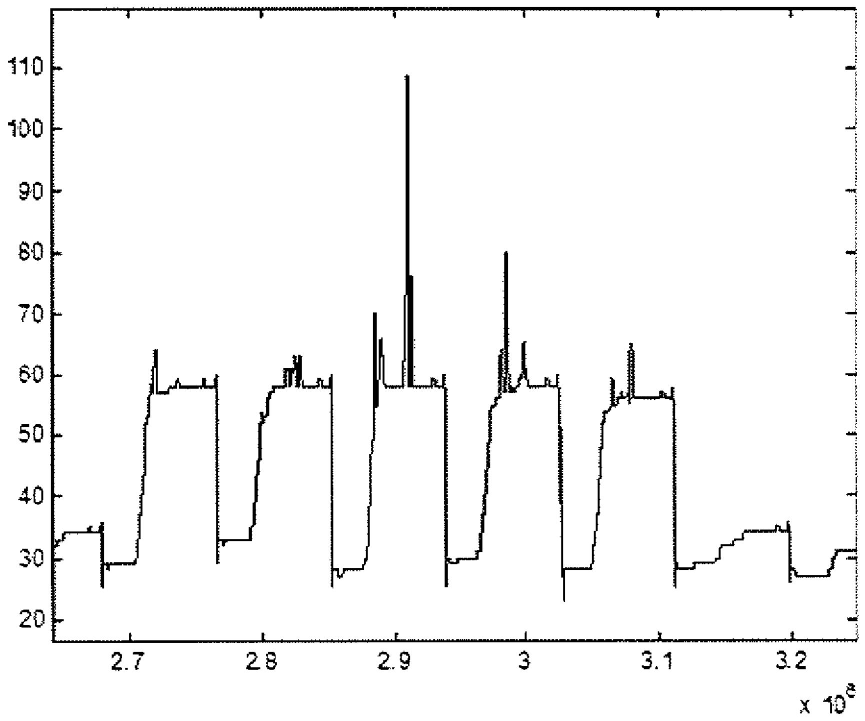

FIG. 42A

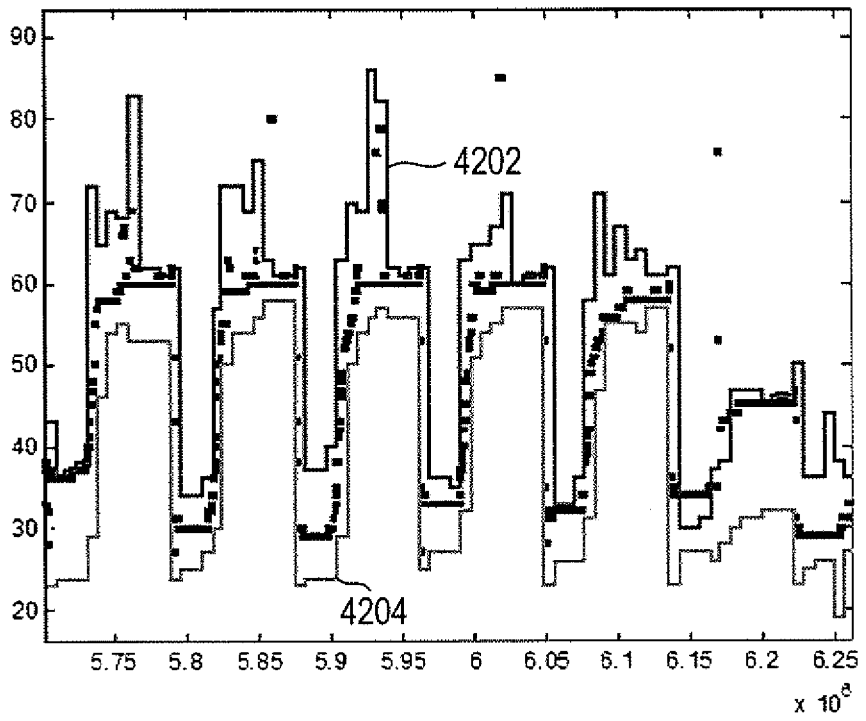

FIG. 42B

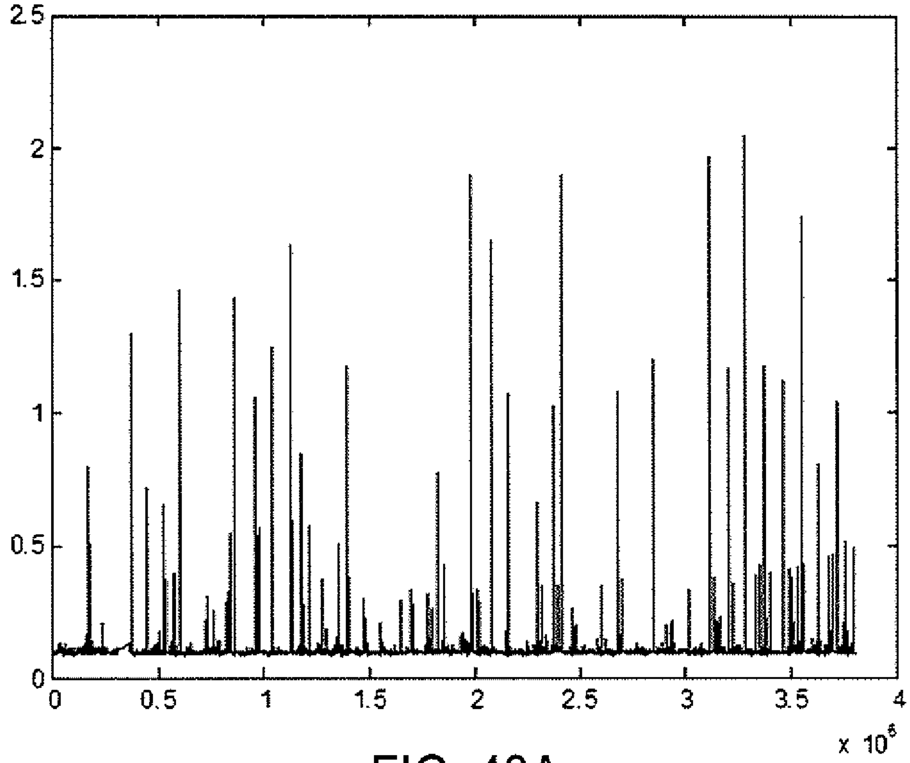

FIG. 43A

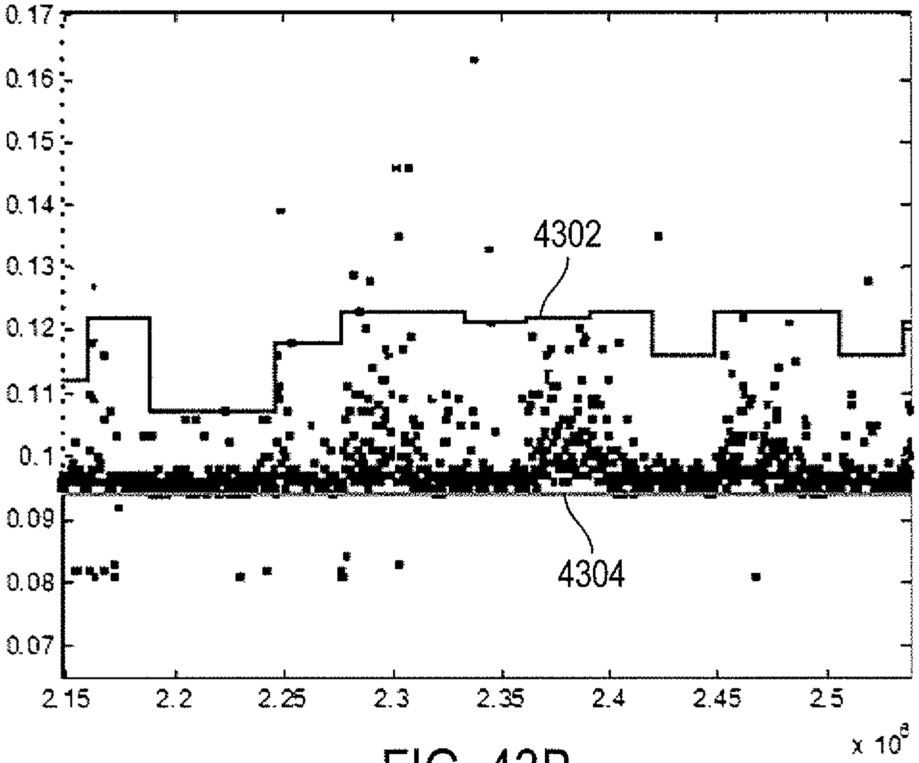

FIG. 43B

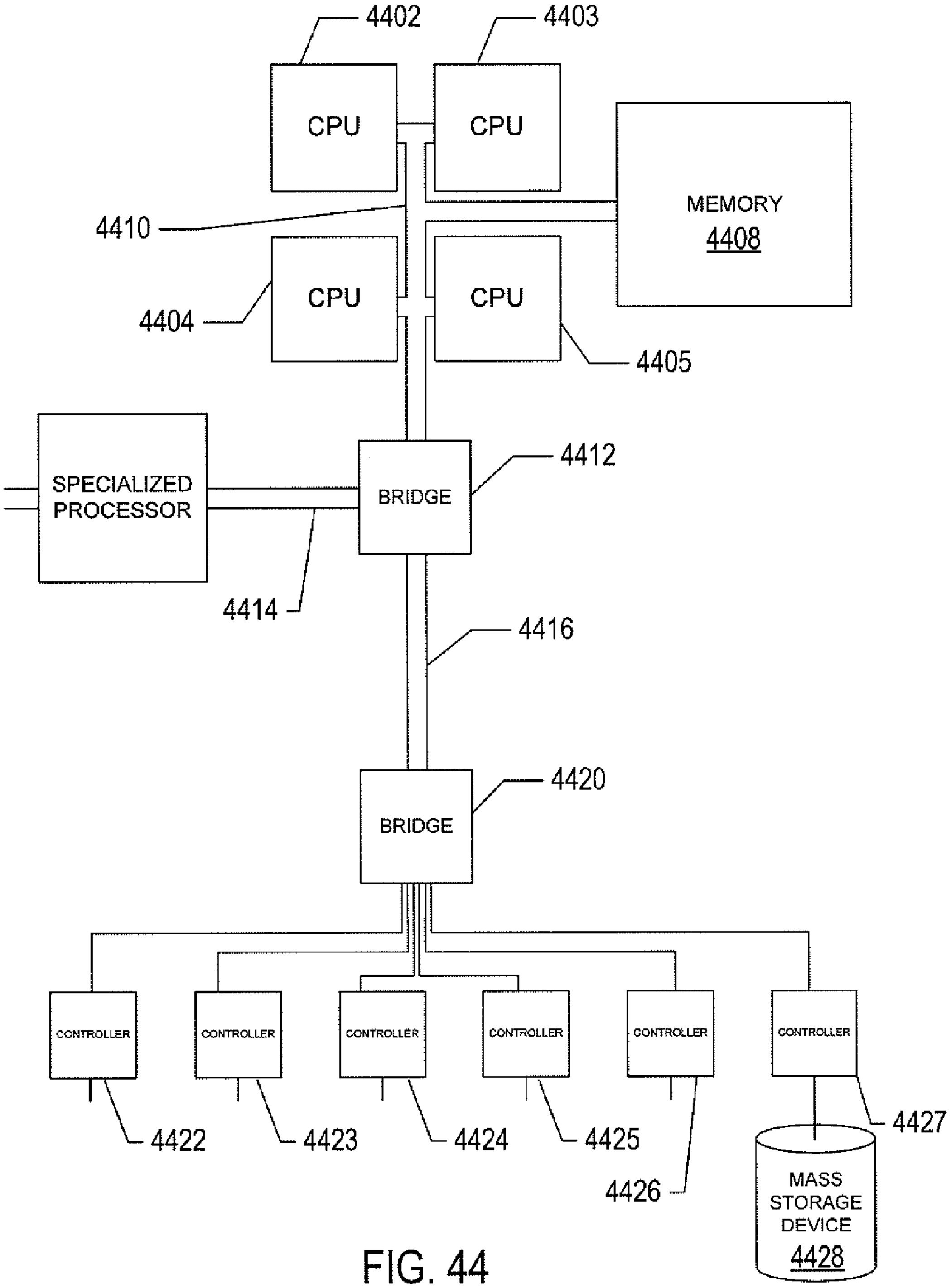
4402
4403
CPU
CPU
MEMORY
4408
4410
CPU
CPU
4404
4405
SPECIALIZED PROCESSOR
BRIDGE
4412
4414
4416
BRIDGE
4420
CONTROLLER
CONTROLLER
CONTROLLER
CONTROLLER
CONTROLLER
CONTROLLER
4422
4423
4424
4425
4426
4427
MASS STORAGE DEVICE
4428

FIG. 44

DATA-AGNOSTIC ANOMALY DETECTION

TECHNICAL FIELD

The present disclosure is directed to electronic data analyzing systems and, in particular, to computational methods and systems for detection of anomalies in data produced by any complex system.

BACKGROUND

With the advent of increased computing power and data storage, the development of computational tools to study ever increasingly complex systems in detail has increased. Examples of complex systems include weather systems, ecosystems, biological systems, and information technology systems. These computational tools enable vast amounts of information regarding a complex system to be collected, analyzed and presented for human understanding. Of particular importance to those who study these complex systems is the ability to identify variations, such as abnormalities, that occur within the complex system. For instance, in the case of an information technology infrastructure, variations from normal or expected operation could lead to failures, slowdown, threshold violations, and other problems. These types of problems are often triggered by unobserved variations or abnormalities in the operation of one or more nodes that cascade into larger problems.

In recent years, computational techniques have been developed to detect patterns in data produced by a complex system that do not conform to an established normal behavior for the complex system. These anomalies may translate into critical and actionable information in several application domains. However, many anomalies in complex systems do not adhere to common statistical definitions of an outlier. As a result, many anomaly detection techniques cannot be applied to a wide variety of different types of data generated by different complex systems. For instance, typical techniques for anomalous detection of time-series data rely heavily on parametric analysis. These techniques assume a known set of distributions for the metrics and perform simple calculations to detect percent out of normal. On the other hand, non-parametric techniques make no assumption about the data distribution and, as a result, can be applied to any data set but at the cost of complexity and more resource intensive algorithms. Those working in the computing industry continue to seek tools that can be used to detect anomalies in a given data set regardless of the type of data.

SUMMARY

This disclosure presents computational systems and methods for detecting anomalies in data output from any type of monitoring tool. The data is aggregated and sent to an alerting system for abnormality detection via comparison with normalcy bounds. The anomaly detection methods are performed by construction of normalcy bounds of the data based on the past behavior of the data output from the monitoring tool. The methods use data quality assurance and data categorization processes that allow choosing a correct procedure for determination of the normalcy bounds. The methods are completely data agnostic, and as a result, can also be used to detect abnormalities in time series data associated with any complex system. The methods described herein are comprehensive for addressing both accuracy and scalability and determination of the types of metrics that should not be analyzed due to a lack of proper information. In other words, the methods avoid false positive alerts.

DESCRIPTION OF THE DRAWINGS

FIG. **1** shows a flow-control diagram that provides an overview of data normalcy analysis.

FIG. **2** shows a flow-control diagram of a method for normalcy analysis.

FIGS. **3**A-**3**D show example plots of data from four different data categories with corresponding normalcy bounds.

FIG. **4** shows an example flow-control diagram of the routine "parametric category detector" called in block **202** of FIG. **2**.

FIG. **5** shows a flow-control diagram of a method for determining whether or not data is periodic data or non-periodic data.

FIG. **6** shows an example plot of elimination of outlier data.

FIGS. **7**A-**7**C shows three example plots of filtering using a moving average filter and a median filter.

FIG. **8** shows a flow diagram of the routine "data quantization" called in block **502** of FIG. **5**.

FIG. **9** shows an example of a frame with grid lines.

FIG. **10** shows calculation of the percentages of data in the grid cells arranged in a column.

FIGS. **11**A-**11**B show an example of smoothing a grid cell.

FIG. **12** shows an example of a cumulative summation of a sequence of values arranged in a column.

FIG. **13** shows an example of a 3×3 grid-cell window of grid-cell values.

FIG. **14** shows an example of cumulative summation of a weighted average of grid cells.

FIG. **15** shows a flow diagram of a method for pattern recognition called in block **503** of FIG. **5**.

FIG. **16** shows an example of a T-cycle checking procedure.

FIG. **17** shows periodic columns of a two-dimensional footprint matrix.

FIG. **18** shows a cyclochart in a tabular format.

FIG. **19** shows an example cyclochart.

FIG. **20** shows an example cyclochart.

FIG. **21** shows a plot of lower and upper normalcy bounds for periodic data.

FIG. **22** shows normalcy bounds constructed of an example footprint matrix.

FIG. **23** shows a flow-control diagram of a method for multinomial data categorization called in block **401** of FIG. **4**.

FIG. **24** shows a flow-control diagram of a method for transient data categorization called in block **402** of FIG. **4**.

FIGS. **25**A-**25**C show example plots of bimodal data.

FIG. **26** shows a flow-control diagram of a method for normalcy analysis.

FIGS. **27**A-**27**V show plots of experimental results for an example set of bimodal data.

FIG. **28** shows a flow-control diagram of a method for semi-constant data categorization called in block **403** of FIG. **4**.

FIG. **29**A shows an example plot of semi-constant data.

FIG. **29**B shows an example plot of piecewise semi-constant data.

FIG. **30** shows an example plot of a number of data points between a median line and an upper line.

FIG. **31**A shows an example plot of qualified data.

FIG. **31**B shows an example plot of the objective function calculated for the data shown in FIG. **31**A.

FIG. **32** shows a flow-control diagram of a method for trendy data categorization called in block **404** of FIG. **4**.

FIGS. **33**A-**33**C show plots of trendy data and non-trendy data.

FIG. **34** shows lower and upper lines associated with a linear trend.

FIGS. **35**A-**35**D show example plots of periodic data with linear trends.

FIGS. **35**E-**35**G show example plots of data with a non-periodic base and linear trends.

FIG. **36** shows a flow-control diagram of the data density detector called in block **203** of FIG. **2**.

FIGS. **37**A-**37**D show example plots of non-uniform data with and without gaps.

FIG. **38** shows a flow-control diagram of a stability detector method called in block **204** of FIG. **2**.

FIGS. **39**A-**39**C shows example stabilocharts of data.

FIG. **40** shows a flow-control diagram of a variability detector method called in block **205** of FIG. **2**.

FIGS. **41**A-**41**B show plots of low- and high-variability categories of data.

FIGS. **42**A-**42**B show example plots of low-variability data with upper and lower normalcy bounds.

FIGS. **43**A-**43**B show example plots of high-variability data with with upper and lower normalcy bounds.

FIG. **44** shows an example of a generalized computer system that executes efficient methods for anomaly detection.

DETAILED DESCRIPTION

This disclosure presents computational systems and methods for fully data-agnostic anomaly detection using time-series data based on normalcy analysis. FIG. **1** shows a flow-control diagram that provides an overview of data normalcy analysis. In block **102**, data quality assurance ("DQA") receives input data **104** supplied by any one of various different types of monitoring tools. For example, the monitoring tools can be sensors, such as biosensors, and network monitoring tools, such as HTTP, SMTP, or status requests, network traffic measurements, and network tomography. The DQA operation identifies the input data **104** as qualified data **106** or corrupted data **108** by checking the input data **104** against different statistical characteristics defined for data qualification. Corrupted data **108** is useless for further analysis and may be discarded. In block **110**, data categorization ("DC") is used to identify and sort the qualified data **106** into categorized data **112**. In other words, for each time series, the DC operation performs category checking and identification with hierarchical/priority ordering on the qualified data **106**. For example, the qualified data **106** can be interpreted as being composed of subsets, where each subset belongs to a different data category:

$$\text{Data Set}=C_1 \cup C_2 \cup \ldots \cup C_n \tag{1}$$

where C_i stands for the ith statistical data category. The DC operation performed in block **110** produces statistically categorized data **112**. When the categorized data **112** belongs to a statistical category C_j determined in block **110**, no further categorization is performed, and in block **114**, category specific normalcy analysis is performed on the specified data **112** to end the process. It should be noted that the type of specific normalcy analysis applied to the categorized data **112** depends on the statistical category to which the categorized data **112** belongs. The categorized data **112** may be input to an alerting engine for abnormality detection via comparison with normalcy states for the data.

It should be noted at the onset that the input data **104**, categorized data **112**, any intermediately generated data, and normalcy bounds are not, in any sense, abstract or intangible. Instead, the input data is necessarily digitally encoded and stored in a physical data-storage computer-readable medium, such as an electronic memory, mass-storage device, or other physical, tangible, data-storage device and medium. It should also be noted that the currently described data-processing and data-storage methods cannot be carried out annually by a human analyst, because of the complexity and vast numbers of intermediate results generated for processing and analysis of even quite modest amounts of data. Instead, the currently described methods are necessarily carried out by electronic computing systems on electronically stored data, with the results of the data processing and data analysis digitally encoded and stored in one or more tangible, physical, data-storage devices and media.

FIG. **2** shows a flow-control diagram of a method for normalcy analysis that provides an expansion of the processes of blocks **102** and **110** introduced in FIG. **1**. The method includes calls to three routines **201**, **203**, and **204** that comprise the DQA described above with reference to block **102** of FIG. **1** and calls to two routines **202** and **205** that comprise the DC operation described above with reference to block **110** of FIG. **1**. The method receives the input data **104** generated by a monitoring tool, and the routines **202**-**205** indentify the input data **104** as belonging to one of the data categories: parametric data **207**, sparse data **208**, high-variability data **209**, and low-variability data **210**, respectively. In block **201**, a data quality detector receives the input data **104** and performs a check of sufficient statistics. Sufficient statistics can be certain user defined parameters about the data. For example, sufficient statistics can be a minimum number of available data points and a minimum data-time duration. Block **201** identifies the input data **104** as qualified data **106** when available data points and length of data are sufficient for further analysis or identifies the input data **104** as corrupted data **108** that may be discarded. In block **202**, a routine "parametric category detector" is called to perform data categorization by verifying qualified data **106** against selected statistical parametric models. When parametric data categorization is possible, the qualified data **106** is identified as parametric data **207**, otherwise, the qualified data **106** is identified as regular data **216**. The parametric category detector **202** further categorizes the parametric data **207** as multinomial data, transient data, semi-constant data, and trendy data, as described below with reference to a flow-control diagram in FIG. **4**. In block **203**, a routine "data density detector" is called to assess gaps in the regular data **216**. When the regular data **216** has a high percentage of gaps the data is considered corrupted data **220** that may be discarded; otherwise, the regular data **216** has a lower percentage of gaps and is identified as dense data **222**. The data density detector **203** also categorizes regular data **216** with a high percentage of gaps that are uniformly distributed in time as sparse data **208** and regular data **216** with a high percentage of gaps that are localization in time is further processed in block **203** with a gap filter that outputs dense data **222** or corrupted data **220**. In block **204**, a routine "stability detector" is called to analyze the dense data **222** in terms of statistical stability. When the dense data **222** is piecewise stable and the latest stable region is enough for further processing the block **204** categorizes the data as stable data **224**, otherwise, the data **222** is categorized as corrupted data **226** that may be discarded. In block **205**, a routine "variability detector" is called to receive the stable data **224** and categorizes the data as high-variability data **209** or low-variability data **210**. For each of the data categories identified in blocks **202-205**, normalcy analysis is performed in blocks **212-215**, which is different for each data category. The categorized data with normalcy bounds output from the blocks **212-215** may be input to an alerting engine for abnormality detection.

FIGS. **3**A-**3**D show example plots of data that belongs to four different data categories with corresponding normalcy bounds. In FIGS. **3**A-**3**D, horizontal axes represent time and vertical axes represent data values. FIG. **3**A shows an example plot of linear periodic data **301** located between an upper linear-periodic normalcy bound **302** and a lower linear-periodic normalcy bound **303**. FIG. **3**B shows an example plot of normalcy bounds **305** and **306** for high-variability periodic data **307**. FIG. **3**C shows normalcy bounds **309** and **310** for low-variability periodic data **311**. FIG. **3**D shows normalcy bounds **313** and **314** for semi-constant non-periodic data **315**.

FIG. **4** shows an example flow-control diagram of the routine "parametric category detector" called in block **202** of FIG. **2**. In this example, blocks **401-404** represent routines called in the flow-control diagram of FIG. **2**. The routines **401-404** are used to categorize the qualified data **106** as belonging to the parametric data categories identified as multinomial data **406**, transient data **407**, semi-constant data **408**, and trendy data **409**, respectively. Qualified data **106** that is not categorized as belonging to one of the four parametric categories is categorized as regular data **216**. The parametric data output from each of the routines **401-404** undergoes normalcy analysis, which is as represented by a single block **410**, is different for each of the parametric categories. The normalcy analysis applied to each of the different parametric data categories includes the operation of determining whether or not the particular category of parametric data is periodic or non-periodic data.

FIG. **5** shows a flow-control diagram of a period detector method for determining whether or not data is periodic data or non-periodic data. The data can fit any of the data categories discuss above. In block **501**, data preprocessing performs data smoothing and outlier removal. Examples of two techniques for data preprocessing are whisker's method and moving median filtering or whisker's method and moving average filtering. After data smoothing by whisker's method, the moving median filter or moving average filter removes small fluctuations from the data. When the number of outliers removed by whisker's method is large (e.g., more than 5%) one of the moving filters is applied. Whisker's method is carried out to remove abnormally high-value data points. Whisker's method calculates two different quantiles of historical data q_a and q_b, where $0 \leq a < b \leq 1$. Every data point that lies outside the interval:

$$(q_a - c(q_b - q_a), q_b + c(q_b - q_a)) \tag{2}$$

where c is a positive parameter, is an abnormal outlier to be removed. For example, letting c equal 1.5, data points greater than an upper whisker given by:

$$q_{0.75} + 1.5iqr \tag{3a}$$

and less than a lower whisker given by:

$$q_a = q_{0.25} - 1.5iqr \tag{3b}$$

are removed, were iqr represents the interquartile range given by:

$$iqr = q_{0.75} - q_{0.25} \tag{3c}$$

FIG. **6** shows an example plot of elimination of outliers **601** by whisker's method. After whisker's method, the moving median or average filter smooths the data by replacing each data point with a median or average of the neighboring data points. The moving average filter is given by:

$$y_s(i) = \frac{1}{2N+1} \sum_{k=-N}^{N} y(i+k) \tag{4a}$$

where

$y_s(i)$ is the smoothed value for the ith data point $y(i)$;

N is the number of neighboring data points of $y(i)$; and

2N+1 is the span.

A moving average filter can be implemented by recursion. Moving average filter are trend following indicators that can be used to reduce random noise. The moving median filter also smooths the data by replacing each data point with a median of the neighboring data points and is given by:

$$y_s(i) = \text{median}\{y(i+k)\}_{k=-N}^{N} \tag{4b}$$

where

$y_s(i)$ is the smoothed value for the ith data point $y(i)$;

N is the number of neighboring data points of $y(i)$; and

2N+1 is the span.

FIGS. **7**A-**7**C shows three example plots of filtering using a moving average filter and a median filter. In FIG. **7**A, a moving average is applied to the highly oscillatory data represented by light curve **701** to obtain smoothed data represented by heavy curve **702**. In FIG. **7**B, a moving median is applied to data represented by light curve **703** to obtain smoothed data represented by heavy curve **704**. In FIG. **7**C, a moving average filter is applied to data represented by an oscillatory curve **705** of small fluctuations and a spike **706** to obtain smoothed data represented by curve **707**.

Returning to FIG. **5**, in block **502** a routine "data quantization" is called to construct a footprint of historical data. FIG. **8** shows a flow diagram of the routine "data quantization" called in block **502** of FIG. **5**. In block **802**, the range of the data is divided into intervals by the q_k quantiles with $k=k_1, \ldots, k_m$ and $0 \leq k_1 < \ldots < k_m \leq 100$, where the parameter m and the values for k_j are user-defined. The data may be divided into non-uniform intervals identified by grid lines. The grid lines are close where the data is dense and the grid lines are spread out where the data is sparse. For division of data into parts by time, two user defined parameters "time_unit" and "time_unit_parts" are used. "Time_unit" is a parameter that defines a minimal length of possible cycles that can be found and any cycle can be a factor only of the length of the "time_unit". The parameter "time_unit_parts" represents the number of subintervals the "time_unit" is divided by and is the measure of resolution. The larger the value of "time_unit_parts", the more sensitive or higher resolution of the footprint of historical data.

FIG. **9** shows an example of a frame with grid lines. Vertical grid lines, such as grid line **901**, are regularly spaced along the horizontal or time axis and vertical grid lines, such as grid line **903**, are non-uniformly spaced along the range axis. The region between any two neighboring horizontal grid lines that intersect any two neighboring vertical grid lines is called a grid cell. For example, a grid cell **905** is the region between vertical grid lines **901** and **902** and horizontal grid lines **903** and **904**. One possibility is parameters q_k, "time_unit" and "time_unit_parts" with an estimated monitoring time Δt that allows sufficient statistics for normal statistical analysis. For example, the monitoring time Δt can be given by:

$$\Delta t = \text{median}(\Delta t_k) \tag{5}$$

where $\Delta t_k = t_{k+1} - t_k$.

Examples of possible settings for "time_unit" are

$$\begin{cases} \Delta t > 1 \text{ day} & \text{"time\_unit"} = 1 \text{ week} \\ \Delta t \leq 1 \text{ day} & \text{"time\_unit"} = 1 \text{ day} \end{cases}$$

and an example of the following settings for q_k and "time_unit_parts" are:

$$\begin{cases} \Delta t \leq 20 \text{ minutes} & \text{"time\_unit\_parts"} = 12 & q_k = 5\% \\ 20 \text{ minutes} < \Delta t \leq 1 \text{ hour} & \text{"time\_unit\_parts"} = 6 & q_k = 5\% \\ 1 \text{ hour} < \Delta t \leq 2 \text{ hours} & \text{"time\_unit\_parts"} = 4 & q_k = 10\% \\ 2 \text{ hour} < \Delta t \leq 4 \text{ hours} & \text{"time\_unit\_parts"} = 3 & q_k = 10\% \\ 4 \text{ hour} < \Delta t \leq 12 \text{ hours} & \text{"time\_unit\_parts"} = 1 & q_k = 20\% \\ 12 \text{ hour} < \Delta t \leq 24 \text{ hours} & \text{"time\_unit\_parts"} = 1 & q_k = 25\% \\ \Delta t > 1 \text{ day} & \text{"time\_unit\_parts"} = 7 & q_k = 25\% \end{cases}$$

Returning to FIG. **8**, in block **802**, percentages are calculated for each column of grid cells. Each column corresponds to a time interval. For a given framework the percentage of the data in each grid-cell of a column of grid cells associated with a given time interval are calculated. FIG. **10** shows calculation of the percentages of data in the grid cells comprising the column of grid cells **1001-1009** arranged in a column of percentages **1010**. For example, grid cells **1001**, **1002**, and **1009** are empty, which correspond to 0% elements in the column **1010**. Grid cells **1003-1008** have data which corresponds to the percentages in the column **1010**. The percentages in the column **1010** correspond to the data in the column of grid cells **906** in FIG. **9**. Collecting all columns percentages produces a matrix of percentages for that particular framework. The final matrix is a two-dimensional ("2D") histogram of historical data.

Returning to FIG. **8**, in block **803**, the 2D histogram of historical data is smoothed. Smoothing can be a weighted averaging based of the percentages associated with the neighbors. For example, FIGS. **11A-11B** show an example of smoothing a grid cell **1101** based on a weighted average of the percentage of the grid cell **1101** and the percentages of eight surrounding grid cells. Suppose that grid cell **1101** has P % of data and the eight neighboring grid cells have the percentages A %, B %, C %, D %, E %, F %, G %, H % as represented by the nine grid cells shown in FIG. **11A**. FIG. **11B** shows an example of a 3×3 grid-cell window of weights assigned to each of the corresponding grid cells shown in FIG. **11A**. The resulting smoothed percentage or weighted average of the grid cell **1101** can be calculated as follows:

$$P_{new} = \frac{4P + A + 2B + C + 2D + F + 2E + H + 2G}{1 + 1 + 1 + 1 + 2 + 2 + 2 + 2 + 4} \tag{6}$$

Applying Equation (6) to all of the grid cell percentages comprising a 2D matrix gives a smoothed matrix that is less sensitive to time and value shifts. For grid cells located in end columns of the matrix, virtual columns of neighboring cells with zeros may be added to the matrix in order to apply Equation (6) to grid cells located in the end columns. Embodiments are not limited to 3×3 grid-cell windows and the weights presented in Equation (6) and FIG. **11B**. In other embodiments, 4×4 and 5×5, or even larger, grid-cell windows can be used with any desired weights. After the weighted averages have been obtained, cumulative sums are calculated for each column of the 2D matrix. A cumulative sum is a sequence of partial sums applied to a column of smoothed grid cell values. FIG. **12** shows an example of a cumulative summation of a sequence of values arranged in a column **1202**. Column **1204** represents the resulting cumulative sum of the values in the column **1202**.

FIGS. **13** and **14** show the procedure of weighted averaging and cumulative summing, respectively, applied to an example 2D matrix of grid-cell percentage values acquired as described above with reference to FIGS. **9** and **10**. FIG. **13** shows an example of a 3×3 grid-cell window **1304** of grid-cell values surrounding the grid cell **1300**. Matrix **1306** represents the grid-cell values in the window **1304** and matrix **1308** represents the weights shown in FIG. **11B**. Matrix **1310** is a product matrix produced by element-wise multiplication **1312** of the matrix **1306** by the weights in the matrix **1308**. Equation **1314** represents the mathematical operation of Equation (6), which gives a weighted average percentage **1316** for the grid cell **1300**. Applying the weighted average to each of the grid-cell values in the matrix **1302** in the same manner gives a 2D weighted-average grid-cell matrix **1318**.

FIG. **14** shows an example of cumulative summation of the weighted average grid cells **1306** in the matrix **1318**. 2D matrix **1402** represents grid-cell values generated by a cumulative summation of the grid-cell values in each column of the matrix **1318**. For example, the grid cell **1404** has the value "11" which is a cumulative sum of the grid-cell values **1405-1410** in the matrix **1318**. Each element in the matrix **1402** is an approximate cumulative distribution function of the data in that column. The resulting 2D matrix **1402** is an example of a "footprint" matrix of historical data.

Returning to FIG. **5**, in block **503**, a routine "pattern recognition" is is called. FIG. **15** shows a flow diagram of a method for pattern recognition called in block **503** of FIG. **5**. In block **1501**, a cyclochart of the 2D footprint matrix output from data quantization **502** in FIG. **5** is constructed. Suppose T=N×time_unit cycle checking procedure, where N is a positive integer. The columns of the footprint matrix are collected into subgroups where L=N×time_unit×time_unit_parts is the number of columns in every subgroup. The total number of subgroups is M=length(footprint)/L. The footprint matrix can be extended by adding columns of zeros. The distance between any two columns is checked using a relative L_2-norm given by:

$$d(A, B) = \frac{\left(\sum_{k=1}^{n} (a_k - b_k)^2\right)^{1/2}}{\max(\|a\|, \|b\|)} \tag{7}$$

where

$$A = \begin{pmatrix} a_1 \\ a_2 \\ \vdots \\ a_n \end{pmatrix}, B = \begin{pmatrix} b \\ b_2 \\ \vdots \\ a_n \end{pmatrix}$$

are any two columns in the footprint matrix. When

$$d(A,B) \leq \text{closeness} \tag{8}$$

for some user-defined parameter called "closeness," it is assumed that the two columns A and B are similar. For example, suppose a user defines a closeness parameter equal to 0.2 and a similarity parameter called "similarity" equal to 75%. FIG. **16** shows an example of a T-cycle checking procedure where columns of a footprint matrix are labeled A through P and are divided into T-cycles composed of four columns. Note that a number of the columns are identified as zero-data columns with the number "0" and columns with data are identified with the number "1." For this particular example, suppose

$$d(A,E)>\text{closeness},d(A,I)>\text{closeness},d(A,M)>\text{closeness}$$

In other words, column A is not similar to columns E, I, and M. Now suppose that for column E

$$d(E,I)\leq\text{closeness},d(E,M)\leq\text{closeness}$$

In other words, column E is similar to columns I and M. Because 3 out of 4 possible columns compose 75% or greater similarity, the first column of the T-cycle is assumed to be periodic. If during comparison only p % of the columns are similar where p %<similarity then the associated column is considered non-periodic. For example, FIG. **17** shows the periodic columns are marked by "1" and the non-periodic columns are marked by "0." Repeating this procedure for all possible T-cycles produces a Cyclochart of the footprint data. FIG. **18** shows a cyclochart in tabular format, and FIG. **19** shows a corresponding plot of the same cyclochart data. Next, the method of pattern recognition includes a period determination procedure of the cyclochart data, composed of the four operations represented by blocks **1502-1505**. The operations of blocks **1502-1505** are now described with reference to the data presented in an example cyclochart shown in FIG. **20**. In block **1502**, local maximums in the cyclochart are identified according to their corresponding similarities. For example, peaks **2001-2010** are local maximum similarities. Table 1 displays the local maximum time units and the corresponding local maximum similarities represented by the peaks **2001-2010** in the cyclochart of FIG. **20**.

TABLE 1

Local maximum time units (days)	Local maximum Similarities
2	34.7%
4	31.3%
7	82.5%
11	44.9%
14	73.28%
19	60.5%
21	90.3%
23	68.1%
28	78%
31	37%

Returning to FIG. **15**, in block **1503**, periods for each of the local maxima are constructed. For example, the data associated with each T-cycle has a kT cycle for every natural number k. So the local maximum with a 2-day period creates the following periodic series

2→2,4,6,8,10,12,14,16,18,20,22,24,26,28,30.

The local maximum with a 4-day period creates another periodic series

4→4,8,12,16,20,24,28.

Similarly, local maximums 7, 11, 14, 19, 21, 23, 28, and 31 day periods create periodic series given by:

7→7,14,21,28,

11→11,22,

14→14,28,

19→19,

21→21,

23→23,

28→28,

31→31.

In block **1504**, the series characteristics are calculated for each of the period series. The following series characteristics can be:

Positive factor of a period series is the number of peaks in the period series; and

Negative factor of a period series is the number of members in the period series that are not peaks; and

the strength of the time unit can be calculated using:

Strength=Positive factor−Negative factor

Table 2 shows positive factors, negative factors, and strengths for the data represented in Table 1.

TABLE 2

Local maximum	Positive factor	Negative factor	Strength	Similarity
2	4	11	−7	34.7%
4	2	5	−3	31.3%
7	4	0	4	82.5%
11	1	1	0	44.9%
14	2	0	2	73.28%
19	1	0	1	60.5%
21	1	0	1	90.3%
23	1	0	1	68.1%
28	1	0	1	78%
31	1	0	1	37%

In bock **1505**, a period is determined by selecting the periods with maximum strength. From that list the periods with minimum negative factor are selected. From that list, periods with maximum similarity are selected. Finally, the period with minimum length is selected. A user can define different limitations on the calculated period. For example, when the similarity of the determined period is small (e.g., less than 20%), the data may be considered non-periodic. This procedure applied to the cyclochart data shown in FIG. **20** leads to the 7-day period having the maximum Strength=4.

Returning to FIG. **5**, in general, the period detector classifies data as periodic data **504** and non-periodic data **505**. The general procedure of normalcy bounds determination is described below for each of the different data categories. Determination of normalcy bounds for both types of data takes into account the specific data categories. For non-periodic data **505**, one approach to determining normalcy bounds may be to apply whisker's method, and another approach may be to utilize an objective function based on data range or variability calculation. On the other hand, for periodic data **504**, normalcy bounds may be calculated column-wise for every "time_unit_parts" by the same procedure and then normalcy is extended into the future based on the cycle information. FIG. **21** shows a plot of lower and upper normalcy bounds **2102** and **2104** for periodic data **2106**. More specifically, consider the case of cyclical data and the following four columns of data from a footprint matrix, which are shifted one from another by the period of data

$$A=\begin{pmatrix}a_1\\a_2\\a_3\\a_4\end{pmatrix},\ B=\begin{pmatrix}b_1\\b_2\\b_3\\b_4\end{pmatrix},\ C=\begin{pmatrix}c_1\\c_2\\c_3\\c_4\end{pmatrix},\ D=\begin{pmatrix}d_1\\d_2\\d_3\\d_4\end{pmatrix}$$

If d(A,B)≤closeness, d(A,C)≤closeness, and d(A,D)→closeness, then the columns form a cyclical subgroup and the normalcy bounds, also called dynamic thresholds ("DTs"), are calculated based on the four data columns. On the other hand, if d(A,B)≤closeness, d(A,C)≤closeness but d(A,D)>closeness, then only the columns A, B, and C form a cyclical subgroup. If d(A,D)≤closeness and d(A,B)>closeness then column A is discarded. If less than 75% of the four columns A, B, C, and D are similar, then the columns A, B, C, and D for a non-cyclical subgroup. From each group of columns, DTs are calculated using whisker's method, or by taking min or max values of the data, or by maximization of the objective function described below with reference to Equation (34). FIG. **22** shows an example of upper and lower normalcy bounds constructed from an example footprint matrix **2202** by taking into account the information on cycles.

Returning to FIG. **4**, in block **401**, the routine "multinomial data categorization" is called. FIG. **23** shows a flow-control diagram of a method for multinomial data ("MD") categorization. In block **2302**, the routine receives the qualified data **106** and calculates statistical parameters that are compared with predefined statistical parameters that may be calculated as follows. The qualified data can take different values, such as a_1, a_2, a_3, etc. The number of times each data value occurs is given by n_j. For example, n_1 is the number times a_1 occurs and n_2 is the number of times a_2 occurs. Let p_j be the frequency of occurrences of the integer n_j:

$$p_j=\frac{n_j}{N}100 \tag{9}$$

where

j=1, . . . , m;

N is the total number of integer values; and

m is the number of different integer values.

In block **2302**, the qualified data **106** is multinomial data **2304** when it takes less than m different integer values and at least s of the integer values have frequencies greater than a user defined parameter H_1. Otherwise, in block **2306**, de-noising is performed on the qualified data **106** with sequential checking of predefined parameters. Block **2306** may be implemented using one or two different de-noising procedures:

1) The de-noising procedure is filtering against non-integer values that are smaller than an H_2 percentage ($H_2<H_1$), where H_2 is a user defined parameter. When the condition $H_2<H_1$ is satisfied, the non-integer numbers are discarded.

2) The de-noising procedure is filtering against integer values with a small cumulative percentage. Sorting the percentages p_j in descending order, the cumulative sum of percentages c_j is given by:

$$c_1=100,$$

$$c_j=p_j+\ .\ .\ .\ +p_m,$$

$$c_m=p_m \tag{9}$$

When $c_k<H_3$, $C_{k-1}\geq H_3$, the integer values n_k, n_{k+1}, . . . n_m can be discarded from further analysis, where H_3 is a user defined parameter. The user defined parameters, H_1, H_2, and H_3 can be assigned the values 2.5%, 0.5%, and 0.5%, respectively.

Blocks **2308**, **2314** and **2316** comprise normalcy analysis for the multinomial data **2304** represented by block **410** in FIG. **4**. In block **2308**, the routine "period detector" described above with reference to FIG. **5** is called to identify periodic multinomial data **2310** and non-periodic multinomial data **2312**, which are then subject to determination of normalcy bounds for the periodic multinomial data **2314** and determination of normalcy bounds for the non-periodic multinomial data **2316**, respectively. Note that while constructing the footprint matrix in block **2308**, instead of using the percentages of data in every grid cell as described above with reference to FIG. **5**, the cumulative sum of percentage values c_k, described in Equation (9), are used to construct the footprint matrix. In block **2314** and **2316**, when multinomial data is periodic, the normalcy set for similar columns are calculated as follows. Data points in similar columns are collected and new values for the numbers c_k are calculated. When $c_{k+1}<H$, $c_k\geq H$, the values n_1, n_2, . . . , n_k are the most probable set (i.e., normalcy set) of similar columns, where H is a user defined parameter, typically equal to about 20%. When data is determined to be non-periodic, the numbers c_k are calculated for all data points and the normalcy set is determined similarly.

Returning to FIG. **4**, in block **402**, the routine "transient data categorization" is called. FIG. **24** shows a flow-control diagram of a method for transient data categorization called in block **402** of FIG. **4**. Transient data can be described in terms of a transformation operator that converts the original qualified time series data into a different type of time series data for which the final categorization can be performed. Normalcy bounds of the transient data are determined for different data characteristics, such as range, variability, and distribution/structure. The concept of transiency is that a transformation operator, denoted by T, transforms original qualified time series data, denoted by Y(t), into different time series data, denoted by X(t), as follows:

$$T:Y(t)\rightarrow X(t) \tag{10}$$

The operator T can be the identity operator E (i.e., T≡E):

$$E:Y(t)\rightarrow Y(t) \tag{11}$$

which represents the case where no transformation is performed. Two different types of operators T can be used. The operator T can be a point-wise operator or a time-window operator. The identity operator actually is an example of a point-wise operator. The differentiation operator (or its discrete analogue which reveals the variability of data) is also an example of point-wise operator. Smoothing operators are examples of time-window operators. The time series data Y(t) is called transient in terms of operator T when the transformed data X(t) is transient. Transiency of X(t) can be confirmed by checking multimodality of the data, inertia of each mode of the data, and randomness of modes appearing along the time axis. Normalcy bounds for the transient data are determined separately for each mode as described in the flow-control diagram shown in FIG. **26**. In block **2402**, a mode detector checks the multimodality of the qualified data **106** and separates the qualified data **106** into multimode data **2406** and no mode data **2408** that may be discarded. Transient data has at least two modes. A mode that corresponds to lower data values is called low mode ("LM") data, and a mode that correspond to higher data values is called high mode ("HM") data. When the data is multimodal, the lowest of the data values is the LM data and the other modes correspond to HM data. In block **2410**, the multimode data is separated in multi-mode data with inertia **2412** and multi-mode data with no inertia **2414**. Inertia refers to data that maintains are range of values for a period of time before switching to a different range of values. In other words, inertia can be associated with the time duration that data points remain in the selected mode. For example, the data cannot oscillate from one mode to the other too quickly.

FIGS. **25**A-**25**C show example plots of three types of bimodal data. FIG. **25**A shows an example plot of bimodal data without a random distribution of modes along the time axis. FIG. **25**B shows an example plot of bimodal data without inertia of data points. FIG. **25**C shows an example plot of transient data. The data plotted in FIG. **25**B is an example of multimode data (i.e., modes 1 and 5) without mode inertia. Because the LM data and HM data oscillate between 1 and 5, neither the LM data nor the HM data exhibit inertia with respect to either of the modes. By contrast, FIGS. **25**A and **25** show examples of data with inertial modes. For example, in FIG. **25**A, the LM data are between 1 and 2 for a period of time ranging from 0 to about 38 and HM data is between 9 and 12 for time greater than about 38. FIGS. **25**B and **25**C show examples of data with modes that randomly interchange over time. On the other hand, the data in FIG. **25**A is piecewise-stable data with discoverable change points.

Returning to FIG. **24**, in block **2410**, the multi-mode data is searched for intervals of sparse data values and for data with some inertia concentrated in upper and lower regions of the intervals. Let numbers a, b satisfy the condition:

$$x_{min} \le a < b \le x_{max} \tag{12}$$

where x_{min}, x_{max} are minimum and maximum data values, respectively, in an interval of sparse data. The numbers a and b divide the interval $[x_{min},x_{max}]$ into three regions $A\overset{def}{=}[x_{min},a]$, $B\overset{def}{=}(a,b)$, and $C\overset{def}{=}[b,x_{max}]$. Transition probabilities are given by:

$$p_{A\to A} = \frac{N_{A\to A}}{N_A} \tag{13a}$$

$$p_{B\to B} = \frac{N_{B\to B}}{N_B} \tag{13b}$$

$$p_{C\to C} = \frac{N_{C\to C}}{N_C} \tag{13c}$$

where

N_A is the number of data points in $[x_{min}, a)$;

N_B is the number of data points in $[a,b]$;

N_C is the number of data points in $(b,x_{max}]$;

$N_{A\to A}$ is the number of points with the property $x(t_i)\varepsilon A$ and $x(t_{i+1})\varepsilon A$;

$N_{B\to B}$ is the number of points with the property $x(t_i)\varepsilon B$ and $x(t_{i+1})\varepsilon B$;

and

$N_{C\to C}$ is the number of points with the property $x(t_i)\varepsilon C$ and $x(t_{i+1})\varepsilon C$.

Starting from the highest possible position and shifting the region B to the lowest possible position, the three transition probabilities are calculated and the procedure is stopped when the following conditions are satisfied:

$$p_{A\to A}>H,\ p_{C\to C}>H,\ P_{B\to B}<h, \text{ and } N_A,N_C>>1 \tag{14}$$

where the numbers H and h are user, predefined parameters. For example, H=0.75 and h=0.25. If this process ends without finding the time interval, the region B is narrowed and the procedure is repeated. Alternatively, the interval $[x_{min},x_{max}]$ can be divided into N+1 equally spaced subintervals given by:

$$x_{min}<x_1<x_2< \ldots <x_N<x_{max} \tag{15}$$

and check sequentially each of the following subintervals according to Equations (13a)-(13b) with the conditions given in Equation (14):

$$(x_{min},x_N),(x_1,x_{max}),(x_{min},x_{N-1}),(x_1,x_N),(x_2,x_{max}), \ldots ,(x_{min},x_1),(x_1,x_2), \ldots ,(x_N,x_{max}) \tag{16}$$

When an interval that satisfied the conditions in Equation (14) is found the procedure stops. The procedure may also be repeated for the lowest (A) region and the highest (C) region for finding new inertial modes if data is supposed to be multi-modal. If the interval is not found then the data is without inertial modes in terms of the given resolution. Now suppose that M inertial modes are found for the regions given by:

$$A_1=[a_1,b_1], \ldots ,A_M=[a_M,b_M] \tag{17}$$

In block **2416**, for each inertial mode, the transiency is determined in order to separate the multi-mode data with inertia into transient data **2418** and non-transient data **2420**. Transient data have periods where the LM data and the HM data randomly interchange over time. One of the found inertial modes is selected, and other data points outside of this region are deleted. Data points in the mode are denoted by $x(t_k)$. Suppose that time intervals with $\Delta t_k \le c\Delta t$ are normal data intervals and time interval with $\Delta t_k > c\Delta t$ are gaps in the time interval, where Δt is the monitoring time described above in Equation (5) and the constant c is a predefined parameter for gap determination. It is assumed that for transient data the gaps are substantially uniformly distributed along the time axis, which can be checked by applying the transition probabilities given in Equations (13a)-(13c). Let T_k be the duration (in milliseconds, seconds, minutes, etc., but in the same measures as the monitoring time) of the kth gapless data portion. For data without gaps only one portion exists and $T_k=t_N-t_1$. The sum $T=\Sigma_{k=1}^{N_T}T_k$ is the duration of the gapless data, where N_T is the number of gapless data portions. Let G_k be the duration (in the same measures as T_k) of the kth gap. The sum $G=\Sigma_{k=1}^{N_G}G_k$ is the duration of gaps in the data, where N_G is the number of gap portions. As a result, $G+T=t_N-t_1$. The percentage of gaps in the data is given by:

$$\rho = \frac{G}{G+T}100\% \tag{19}$$

where p_{11}, p_{10}, p_{00}, p_{01} are the probabilities of data-to-data, data-to-gap, gap-to-gap and gap-to-data transitions, respectively, and are given by

$$p_{11} = 1 - \frac{N_T}{\frac{T}{\Delta T}},\ p_{10} = 1 - p_{11},\ p_{00} = 1 - \frac{N_G}{G/\Delta t}, \text{ and} \tag{20}$$

$$p_{01} = 1 - p_{00}$$

When at least two inertial modes satisfy the following conditions:

$$\rho > P,\ p_{10} > \varepsilon,\ p_{01} > \varepsilon \tag{21}$$

where P and ε are user defined parameters, the multi-mode inertial data **2412** is transitory data **2418**, otherwise, the multi-mode inertial data is non-transient data **2420**.

FIG. **26** shows a flow-control diagram of a method for normalcy analysis of multi-mode inertial data represented by block **410** in FIG. **4**. In block **2602**, for each inertial mode in the multi-mode inertial data **2412**, the operations associated with blocks **2604**, **2610**, and **2610** are repeated. Different inertial modes can have different normalcy bounds. In block **2604**, period detector described above with reference to FIG. **5** is used to check the existence of periodicity in a given mode. When the mode is periodic **2606**, normalcy analysis **2610** is used to determine normalcy bounds along the found cycles, as described above with reference to FIG. **5**. On the other hand, when the inertial mode is non-periodic different statistical measures are applied for normalcy analysis **2612**. The following description is directed to normalcy analysis of non-periodic, multi-mode inertial data **2608**. Normalcy bounds can be set in terms of different statistical measures, including data range, distribution, and duration. The statistical measures can be calculated and used simultaneously for abnormality detection and the information can be stored in a binary vector:

$$\alpha = (\alpha_1, \ldots, \alpha_s) \tag{22}$$

where α_j is either 0 or 1. When $\alpha_j=0$ the jth statistical measure for abnormality detection is not calculated. When $\alpha_j=1$ appropriate normalcy bounds for the jth statistical measure are calculated. Different modes may require different settings for the vector α. When no normalcy determination is wanted for a certain modes, all of the α_j's may be set to 0. The methods for process calculating normalcy bounds for statistical measures data range, distribution, and duration are now described. Normalcy bounds for the statistical measure data range are calculated as follows. Because each detected mode A_j can be characterized by the interval $[a_j,b_j]$, the interval can be interpreted as a normalcy region for the jth mode. The interval $[a_j,b_j]$ can be divided into N+1 equally spaced intervals represented by:

$$a_j < x_1 < x_2 < \ldots < x_N < b_j \tag{23}$$

and check sequentially the subintervals

$$[x_N, b_j], [x_{N-1}, b_j], [x_{N-2}, b_j], \ldots, [x_1, b_j] \tag{24}$$

by calculating transition probabilities $p_{A \to A}$, where A is the region corresponding to the given interval. Subintervals for which $p_{A \to A} < 0.1$ are discarded. Performing similar calculations and eliminations for intervals

$$[a_j, x_1], [a_j, x_2], [a_j, x_3], \ldots [\alpha_j, x_{N1}] \tag{25}$$

gives strict normalcy bounds $[a'_j, b'_j]$, where

$$a_j \le a' < b' \le b_j \tag{26}$$

Normalcy bounds for the duration statistical measure are calculated as follows. Let T_k be duration of the kth gapless data portion of the jth mode, then from whisker's method, the normalcy bounds for durations of the jth mode is given by:

$$[q_{0.25}(T_k) - 1.5iqr(T_k), q_{0.75}(T_k) + 1.5iqr(T_k)] \tag{27}$$

Normalcy bounds for the distribution statistical measure are calculated as follows. Let C_k^j be a distribution of a kth gapless data portion (provided this portion has enough statistics for distribution calculation) of the jth mode. Distances $E_k = d(C_{k_1}^j, C_{k_2}^j)$ are calculated according to Equation (7) between all distributions by some measure (e.g. by mean square distance). As a result, the normalcy bounds for the interval E_k can be calculated from whisker's method as follows:

$$[q_{0.25}(E_k) - 1.5iqr(E_k), q_{0.75}(E_k) + 1.5iqr(E_k)] \tag{28}$$

In on-line mode, when enough statistics are available for distribution calculation, the corresponding distances ε_k between historical distributions and current distribution can be calculated. On-line or run-time mode refers to anomaly detection when the decision on the system abnormality state is made for real-time data monitoring. The median of ε_k compared with normalcy bounds demonstrates the abnormality of the current process. Normalcy bounds for the variability statistical measure are calculated as follows. Let x_k be data points of the sth gapless portion of the jth mode. The variability of the sth portion is given by:

$$R_s = \frac{iqr(\{x'_k\}_{k=1}^{N-1})}{iqr(\{x_k\}_{k=1}^{N})} 100\% \tag{29}$$

where

$$iqr(\{X_k\}_{k=1}{}^{N}) \neq 0;$$

x_k' are the absolute jumps of data points; and

$$x_k' = |x_{k+1} - x_k|.$$

The normalcy bounds for the interval R_s can be calculated from whisker's method to give:

$$[q_{0.25}(R_s) - 1.5iqr(R_s), q_{0.75}(R_s) + 1.5iqr(R_s)] \tag{30}$$

for the jth mode. In block **2614**, when another inertial mode is available, the operations associated with blocks **2604**, **2610**, and **2612** are repeated.

FIGS. **27**A-**27**V show plots of experimental results for an example set of bimodal data displayed in FIG. **27**A. FIGS. **27**B-**27**E show different [a,b] data value intervals represented by shaded rectangles with tables of corresponding transition probabilities calculated according to Equations (13a)-(13c). No inertial modes are present with this resolution for the [a,b] intervals selected in FIGS. **27**B-**27**E. FIGS. **27**F-**27**K show different [a,b] intervals with tables of corresponding transition probabilities calculated according to Equations (13a)-(13c). The transition probabilities for the [a,b] intervals in FIGS. **27**F-**27**K are collected and displayed in Table 3.

TABLE 3

P_CC	0	0	0.21429	0.1875	0.58108	0.7913	x	x
P_BB	0.15385	0.59091	0.85149	0.89524	0.54902	0.125	x	x
P_AA	0.95963	0.91638	0.89238	0.90783	0.88732	0.90338	x	x
b	15	13.5	12	10.5	9	7.5	6	4.5
a	10.5	9	7.5	6	4.5	3	1.5	0

The seventh column of the data displayed in Table 3 reveals an interval[3,7.5] (see FIG. **27**K) with a small transition probability $P_{B\rightarrow B}$=0.125 while transition probabilities for upper and lower regions are $P_{C\rightarrow C}$=0.7913 and $P_{A\rightarrow A}$=0.90338, respectively, which are indicators of inertial modes.

For transiency checking according to block **2416** described above, calculations were performed for an estimated monitoring time of Δt=1 minute. As a result, every duration time of 5 minutes or more in an interval without data points is considered a gap. The percentage of gaps calculated according to Equation (19) is ρ=62.3% and the probabilities given by Equations (20) are

$$p_{11}=0.93,\ p_{10}=0.067,\ p_{00}=0.965,\ p_{01}=0.035$$

Therefore, the data is bimodal transient according to the given resolution.

FIGS. **27**M-**27**Q show plots of data used in the determination of normalcy bounds for upper and lower inertial modes. In FIG. **27**L, the upper region is the interval [7.5,15] identified by a line **2702** that corresponds to the value 7.5. In FIGS. **27**M-**27**P, lines **2704**-**2707** represent values for the constant c described above with reference to Equation (18). For data values greater than corresponding lines **2704**-**2707**, transition probabilities $p_{A\rightarrow A}$ are displayed for the intervals [c,15], 7.5≤c<15 in Table 4.

TABLE 4

$p_{A\rightarrow A}$	0	0	0	0	0	0	0
c	15	14.625	14.25	13.875	13.5	13.125	12.75
$p_{A\rightarrow A}$	0.21	0.21	0.21	0.19	0.19	0.19	0.63
c	12.375	12	11.625	11.25	10.875	10.5	10.125
$p_{A\rightarrow A}$	0.63	0.58	0.74	0.73	0.79	0.79	0.79
c	9.75	9.375	9	8.625	8.25	7.875	7.5

Eliminating all regions with probabilities $p_{A\rightarrow A}$≤0.25 gives the normalcy region [7.5,10.125] also identified in FIG. **27**Q by lines **2708** and **2709**. Similar calculations for the lower region lead to FIG. **27**R where lines **2710** and **2711** represent the normalcy bounds and shaded interval **2712** represents an intermediate region within the inertial modes. FIG. **27**S shows the normalcy regions **2713** and **2714** for the lowest and highest inertial modes. FIG. **27**T shows another example of bimodal data. Computational experiments show that the data represented in FIG. **27**T is not transient, because the upper mode is not inertial in terms of the identity operator, but it is transient in terms of the differentiator operator. FIG. **27**U shows a plot of X(t) after differentiation of the data represented in FIG. **27**T, which gives bimodal data. FIG. **27**V shows associated normalcy bounds represented by lines **2716** and **2717** and inertial modes with normalcy regions **2718** and **2719** for the data displayed in FIG. **27**U.

Returning to FIG. **4**, in block **403**, a routine "semi-constant categorization" is called. FIG. **28** shows a flow-control diagram of a method for semi-constant data categorization called in block **403** of FIG. **4**. In block **2802**, the qualified data **106** is considered semi-constant data **2804** when

$$iqr(\{x_k\}_{k=1}^{N})=0 \tag{31}$$

where

N corresponds to data length; and

iqr stands for interquartile range of the qualified data x_k=x(t_k).

Otherwise, control flows to block **2806** in which data selection is performed to search the qualified data **106** for the longest data portion of the data that is semi-constant. In

particular, block **2806** performs an iterative data selection process by cutting off the last portion of data and returning the data back to block **2802**. When this iterative process between blocks **2802** and **2806** fails to reveal semi-constant data, the qualified data **106** is considered non-semi-constant data. In other words, when after cutting the next portion of the remaining data has insufficient statistics or when the remaining data is shorter than some user defined smallest portion, control flows to block **2808**. Formally, in block **2802**, when

$$iqr(\{x_k\}_{k=1}^{N})\neq 0 \tag{32}$$

control flows to block **2806** where cut data $\{x_k\}_{k=m_0}^{N_0}$ is determined for 1<m≤N_0<N. In block **2802**, the interquartile range is calculated for

$$s_m=iqr(\{x_k\}_{k=m}^{N_0}) \tag{33}$$

When s_m=0 for m=m_0 the cut data $\{x_k\}_{k=m_0}^{N_0}$ is semi-constant data and this portion of the qualified data **106** flows to the process in block **2808**.

FIG. **29**A shows an example plot of semi-constant data. The operations associated with blocks **2802** and **2806** can also identify piecewise semi-constant data. FIG. **29**B shows an example plot of piecewise semi-constant data.

Returning to FIG. **28**, blocks **2808**, **2814**, **2820**, and **2822** are used to carry out normalcy analysis on the semi-constant data as described in block **410** of FIG. **4**. In block **2808**, outlier detection is used to check the percentage of outliers in the semi-constant data **2804**. For semi-constant data every data point greater than $q_{0.75}$ or less than $q_{0.25}$ is identified as an outlier. When the percentage of outliers is greater than a user defined percentage p % (e.g., p=15%), the semi-constant data is identified as semi-constant data with a large number of outliers **2810**; otherwise, the semi-constant data is identified as semi-constant data with a small number of outliers **2812**. The outlier data **2810** or **2812** is passed to block **2814** to identify periodic semi-constant data **2816**. When no periods are detected, the semi-constant data is declared non-periodic data **2818**. Periodicity analysis of outlier data **2810** in block **2814** is performed using the period detector described above with reference to FIG. **5**, excluding the data points equal to the median of the original qualified data **106**. In block **2820**, normalcy bounds are determined for periodic semi-constant data **2816**, and in block **2822**, normalcy bounds are determined for non-periodic semi-constant data **2818**. Normalcy bounds determination is performed separately for upper (for data points that are greater or equal to the median) and lower (for data points that are less than or equal to the median) parts of data. Because the computational operation for determining both upper and lower bounds are similar, for the sake of brevity, determination of the upper bound is now described. The process includes maximization of an objective function given by:

$$f(P,S)=e^{aP}\frac{S}{S_{max}} \tag{34}$$

where

a>0 is a sensitivity parameter; and

P is the percentage of data points between the median of data and an upper line higher than the median.

The sensitivity parameter may be user selected. For example, the sensitivity parameter can be a=0.9. FIG. **30** shows an example plot of a number of data points between a median line **3002** and an upper line **3004**. The denominator of equation (34) is given by:

$$S_{max}=(t_{max}-t_{min})(\text{Upper Line}-\text{Data Median}) \tag{35}$$

and the numerator S of Equation (34) is the square of the area within data points, such as data points **3006**, and the data median **3002**. In the data-range-based analysis, the range within the median line and maximum of the data is divided into m parts and for each level values g_k for k=1, 2, . . . m of the objective function are calculated. The level that corresponds to a maximum of g_k is the upper bound. The same procedure is valid for determination of the lower bound with the minimum of g_k corresponding to the lower bound. Instead of dividing the range into equal parts, the range can also be divided by corresponding quantiles that give unequal division according to the density of data points along the range. In the data-range-based approach, preliminary abnormality cleaning of data can also be performed. Data points with abnormal concentrations are removed in a given time window. Abnormal concentrations can be detected as follows. For a given time window (e.g., 10% of data length) the percentage of data points with values greater than the 0.75 quantile are calculated. As the window is moved along the data, corresponding percentages are calculated. Any percentage greater than the upper whisker indicates an abnormal concentration of data, which is discarded. The same abnormality cleaning procedure is repeated for data points lower than the 0.25 quantile.

FIG. **31**A shows an example plot of qualified data with iqr=0 and with an upper bound **3102**. FIG. **31**B shows an example plot of the objective function calculated for the data in FIG. **31**A using Equation (34). Abnormality cleaning was also performed for the data represented in FIG. **31**B.

In the data-variability-based approach for determining normalcy bounds, the variability of data points x_k against median of data μ is calculated according to

$$v=\left(\frac{1}{N-1}\sum_{k=1}^{N}(x_k-\mu)^2\right)^{1/2} \tag{36}$$

Consider the following set of upper lines

$$[\mu+z_j v]$$

where j is a positive integer. For each interval j, the corresponding values g_j of the objective function are calculated and the $\max(g_j)$ is taken as the appropriate normalcy upper bound. For example, experimental values for z_j were

$$z_1=1,\ z_2=1.5,\ z_3=2,\ z_4=3,\ z_5=4$$

Normalcy bounds are determined for semi-constant periodic data **2816** as follows. Period detection as described above with reference to FIG. **5** is a way to get the period of the data and similar columns. For normalcy bounds (i.e., dynamic thresholds) determination of similar columns, the discarded data points (recall that the periodicity procedure was performed only for outliers in block **2808**) are returned, the variability v_k is calculated for each column against the global data median μ and the normalcy bounds are determined for each column, as described above for the non-periodic case.

Returning to FIG. **4**, in block **404**, a routine "trendy data categorization" is called. FIG. **32** shows a flow-control diagram of a method for trendy data categorization called in block **404** of FIG. **4**. In block **3202**, a trend detector is used to separate the qualified data **106** into trendy data **3204** and non-trendy data **3206**. In block **3208**, trend recognition identifies the trendy data **3204** as linear data **3210**, log-linear data **3212**, or non-linear data **3214**. The operation in block **3208** is to decompose the original time series $f_0(t)$ of N data points into a sum of non-trendy time series, f(t), and trend component trend(t) as follows:

$$f_0(t)=f(t)+\text{trend}(t) \tag{37}$$

Equation (37) provides normalcy analysis based on f(t). In block **3216**, specific normalcy bounds are calculated for each of the categories **3210**, **3212**, and **3214**.

The trend detector in block **3202** performs a number of different trend detection tests. For example, the Mann-Kendall ("MK") test can be used to calculate an MK statistic given by:

$$S_0=\sum_{k=1}^{N-1}\sum_{j=k+1}^{N}\operatorname{sign}(x_j-x_k) \tag{38}$$

The trend detector **3202** performs the following three operations:

1. Data smoothing as described above with reference to block **501** in FIG. **5**.

2. Calculation of the MK statistic S_0 for the smoothed data. When $S_0>0$ a trend is identified as increasing, and when $S_0<0$ the trend is identified as decreasing.

3. A trend measure is calculated according to

$$p=\left|\frac{S_0}{S_{max}}\right|100\% \tag{39}$$

where

$$S_{max}=\sum_{k=1}^{N-1}\sum_{j=k+1}^{N}1$$

When the trend measure p is greater than a user defined threshold, for example p>40%, the data is trendy data **3204**.

Trend recognition in block **3208** reveals the nature (i.e., linear, log-linear or non-linear) of the trendy data **3204**. Linear and log-linear trends can be checked using linear regression analysis. Trend recognition includes determining a goodness of fit given by:

$$R=1-\frac{R_{regression}}{R_0} \tag{40}$$

where

$R_{regression}$ is the sum of squares of the vertical distances of the points from the regression line; and

R_0 is the sum of squares of the vertical distances of the points from the line with zero slop and passing through the mean of data (i.e., the null hypothesis).

When R is, for example, greater than a user defined parameter 0.6 it is assumed that the trend is linear, otherwise the log-linearity is checked by the same procedure for $f(e^{ct})$, where c is a constant. When the goodness of fit given by Equation (40) is greater than 0.6 the data is assumed to be log-linear. If the data is not linear or not log-linear, the data is assumed to be non-linear trendy data.

FIG. **33**A shows a plot of increasing trendy data with $S_0=48464$, $S_{max}=77421$, p=62.6%>40%. In this example, R=0.44<0.6. FIG. **33**B also shows a plot of increasing trendy data with S_0=77421, S_{max}=77421, p=100%>40%. The trend is linear because R=0.999>0.6. FIG. **33**C shows a plot of non-trendy data with S_0=−3504, S_{max}=77421, and p=4.5%<40%.

Block **3216** is the normalcy analysis represented by block **410** in FIG. **4** performed on the different categories of trendy data **3210**, **3212**, and **3214** to calculate the normalcy bounds for each category. When the data has a linear trend, the data $f_0(t)$ is decomposed into

$$f_0(t)=f(t)+\text{trend}(t) \tag{41}$$

where trend(t)=kt+b is a linear function with coefficients k and b determined by linear regression analysis. When f(t) is non-periodic, normalcy bounds of $f_0(t)$ are straight lines with upper and lower dynamic thresholds that are determined by maximizing the objective function given by:

$$g(P, S) = \frac{e^{aP}-1}{e^a-1}\frac{S}{S_{max}} \tag{42}$$

where

S is the square of the area limited by t_{min} and t_{max} and lower and upper lines as shown in the example of plot of FIG. **34**;

$S_{max}=h(t_{max}-t_{min})$; and

P is the fraction of data within the upper and lower lines and a is a user defined parameter.

Variability (i.e., standard deviation) of f(t) is calculated by:

$$\sigma=\text{std}(f(t)) \tag{43}$$

The upper and lower lines are given by:

$$[kt+b-z_j\sigma, kt+b+z_j\sigma] \tag{44}$$

where j is a positive integer. The corresponding value g_j of the objective function is calculated for each time. Lines that correspond to max(g_j) are appropriate normalcy bounds. Experimentally determined values for z_j are given by:

$$z_1=1,\ z_2=1.5,\ z_3=2,\ z_4=3,\ z_5=4$$

When f(t) is periodic, the variability σ_m of the mth is calculated for each set of similar columns and the normalcy bounds are given by

$$[kt+b-z_j\sigma_m, kt+b+z_j\sigma_m] \tag{45}$$

The maximum of the objective function gives the normalcy bounds of the mth set. When the data has a log-linear trend, the time series $f(e^{ct})$ is data with a linear trend using the same procedure in Equations (41)-(45). For data with a non-Linear trend, the last portion of data is selected and normalcy bounds are calculated according to the above described procedure for non-periodic case.

FIGS. **35**A-**35**D show example plots of periodic with linear trends. FIG. **35**A shows periodic data **3502** that follows and a linear regression line **3504**. For this example, the goodness of fit is R=0.7, which indicates a linear trend as shown. FIG. **35**B shows the periodic data **3506** after subtraction of the linear trend shown in FIG. **35**A. FIG. **35**C shows an example of dynamic thresholds **3508** and **3510** for periodic data **3506** shown in FIG. **35**B. FIG. **35**D shows normalcy bounds **3512** and **3514** for the original periodic data **3503** after reconstruction of the linear trend.

FIGS. **35**E-**35**G show example plots of data with a non-periodic base but also have linear trends. FIG. **35**E shows data **3516** with a linear trend represented by linear regression line **3518**. In this example, the goodness of fit is R=0.99, which indicates a linear trend. FIG. **35**F shows the data **3516** with final DTs represented by lines **3520** and **3522**. In this example, no periods were found and the DTs are straight lines. The lines **3520** and **3522** can be constructed by maximization of objective function. FIG. **35**G shows an example plots of data with a non-linear trend base. Line **3524** is a regression line for the last portion of the data **3526** and boundary lines **3528** and **3530** are upper and lower thresholds for the same portion.

Returning to FIG. **2**, in block **203**, a routine "data density detector" is called. FIG. **36** shows a flow-control diagram of the data density detector called in block **203** of FIG. **2**. The data density detector performs data density recognition based on probability calculations that reveal the distribution of gaps in the data. Gaps in the regular data **216** are determined relative to data monitoring time Δt, which is estimated statistically from data time stamps. For categorization purposes, the following measures characterize the nature of the gaps present in the data **216**: 1) percentage of gaps, 2) probabilities of gap-to-gap, data-to-data, gap-to-data and data-to-gap transitions. When the total percentage of gaps is acceptable, the data is categorized as dense data. When the total percentage of gaps is greater than a user defined limit and the percentage of gags have a non-uniform distribution in time then a gap clean-up procedure gives dense data. When gaps in data have a uniform distribution in time, the data belongs to a sparse data cluster. When gaps in the data occur with an extremely high percentage, further analysis is not typically possible, and the data is identified as corrupted data. In block **3601**, as described above, an estimate of the monitoring time Δt is calculated according Equation (18) as the median of $\Delta t_k=t_{k+1}-t_k$. In block **3602**, time intervals with $\Delta t_k \le c\Delta t$ are normal data intervals while $\Delta t_k > c\Delta t$ are gaps are calculated, where c is user predefined gap parameter. As also described above with reference to Equation (19), the percentage of gaps are represented by ρ. In block **3603**, the probabilities p_{11}, p_{10}, p_{00}, and p_{01} in Equations (20) are calculated for data-to-data, data-to-gap, gap-to-gap and gap-to-data transitions. In block **3604**, the percentage of gaps ρ, and the probabilities p_{11}, p_{10}, p_{00}, and p_{01} are used to classify the data. For example, dense data **222** with gaps non-uniformly distributed in time can be specified by the condition:

$$\begin{cases} \rho > H_1 \\ p_{10} < \varepsilon \\ p_{01} < \varepsilon \end{cases} \tag{46}$$

where H_1 and ε are user defined parameters, and E is a small parameter. For example, H_1=25% and ε=0.0005. The main reason for smallness of p_{10} and p_{01} is the smallness of the numbers N_T and N_G, while G and T are as large as ρ. The data of this category can be further processed via data selection procedure to eliminate concentration of gaps, which can be done as follows. The total percentage of gaps in the series of data $\{x_k\}_{k=i}^{j}$, j=j_1, j_2, . . . , j_s, i=i_1, i_2, . . . , i_r is calculated and the portion for which ρ≤H_i is selected. Sparse data **3606** has gaps that are uniformly distributed in time and are specified by the condition

$$\begin{cases} \rho > H_2 \ge H_1 \\ p_{10} \ge \varepsilon \\ p_{01} \ge \varepsilon \end{cases} \tag{47}$$

where H_2 is a user defined parameter. For example, H_2=60%. The second condition $p_{10} \geq \varepsilon$ and third condition $p_{01} \geq \varepsilon$ indicate that the gaps are uniform in time and cleanup is not possible. Corrupted data **3607** is identified when $\rho > H_3$, where H_3 is a user defined parameter, such as H_3=95%.

FIG. **37**A shows an example plot of data that is non-uniform in time and has a gap **3702**. The data is considered dense data with ρ=39%, p_{11}=0.99991, p_{10}=9.4e-05, p_{00}=0.99985, p_{01}=0.00015. FIG. **37**B shows a plot of example data that is non-uniform in time gaps. The data is also considered dense data ρ=55%, p_{11}=0.99974, p_{10}=0.00026, P_{00}=0.9998, p_{01}=0.00021. FIG. **37**C shows an example plot of sparse data with p=68%, p_{11}=0.9957, p_{10}=0.0043, p_{00}=0.9979, p_{01}=0.0020. FIG. **37**D shows an example of dense data with ρ=48%, p_{11}=0.9962, p_{10}=0.0038, P_{00}=0.9958, p_{01}=0.0042.

Period determination of normalcy bounds is performed using a standard described above with reference to FIG. **5**, where the parameter "time_unit_parts" is given by:

$$\text{"time\_unit\_parts"} = \left[\frac{\text{"time\_unit"}}{\text{median}(T_k) + \text{median}(G_k)}\right]$$

The data may be periodic or non-periodic. In both cases, the normalcy bounds are determined as described above with reference to FIG. **5** for classifying the data as periodic or non-periodic.

Returning to FIG. **2**, in block **204**, a routine "stability detector" is called to check the stability of the dense data **222** output from the routine "data density detector." FIG. **38** shows a flow-control diagram of a stability detector method called in block **204** of FIG. **2**. The stability detector performs statistical stability recognition of dense data **222**. When the dense data **222** is stable or a stable portion of the data can be identified, the data, or a selected portion, is categorized as stable data, otherwise the data is categorized as corrupted. Stability categorization may be accomplished by construction a "stabilochart" that represents stability intervals of time series and allows for selection of recent and sufficiently long data regions for further analysis. Blocks **3802**-**3805** are repeated for every m. In block **3802**, calculate the quantity

$$s_m = \frac{|iqr(\{x_k\}_{k=m-n}^{m}) - iqr(\{x_k\}_{k=m}^{m+n})|}{iqr(\{x_k\}_{k=1}^{N})} 100\% \tag{48}$$

where n is a user defined parameter. For example,

$$n = \left[\frac{T}{4}\right],$$

where T is the length of data. In block **3803**, when s_m<S, control flows to block **3805**, otherwise control flows to block **3805**. The parameter S can be set to 50%. In block **3804**, s_m is set to zero and the associated datum x_m is identified as stable data **3807**. In block **3805**, s_m is set to one and the associated datum x_m is identified as corrupted data **3808**. In block **3810**, when another datum x_m is available the operations of blocks **3802**-**3805** are repeated. The collection of data $\{s_m\}$ is the stabilochart of the set of data $\{x_m\}$.

FIGS. **39**A-**39**C shows example plots stabilocharts of data calculated for S=50%. FIG. **39**A shows an example of stable data. FIG. **39**B shows an example plot of data where the portion of data beyond about 1.186×10^{12} is considered stable. FIG. **39**C shows an example plot of unstable data.

In other embodiments, the method in FIG. **38** can be carried out for the data tail $\{x_k\}_{k=m}^{N}$ with a corresponding stabilochart denoted by S_m. The start time of the latest stable portion of the data is denoted by T_m. A series of stabilocharts $\{S_m\}_{m=1}^{n}$ are generated for each of the series of start times $\{T_m\}_{m=1}^{n}$ showing the start times of the latest stability portions of data tails. The minimum time min(T_m) indicates the start time of the longest stable portion. Note that the set $\{T_m\}_{m=1}^{n}$ can be empty, which indicates the data is corrupted.

Returning to FIG. **2**, in block **205**, a routine "variability detector" is called to assess the variability of the stable data **224** output from the stability detector **204**. FIG. **40** shows a flow-control diagram of a variability detector method called in block **205** of FIG. **2**. The variability detector performs variability recognition of input stable data **224**. In block **4002**, absolute jumps x_k' of data points are computed according to

$$x_k' = |x_{k+1} - x_k| \tag{49}$$

where x_k belongs to the set of data $\{x_k\}_{k=1}^{N}$. Low-variability and high-variability data categories are recognized based on the size of the jumps x_k'. In block **4004**, a measure R of variability is calculated according to

$$R = \frac{iqr(\{x_k'\}_{k=1}^{N-1})}{iqr(\{x_k\}_{k=1}^{N})} 100\% \tag{50}$$

where iqr($\{x_k\}_{k=1}^{N}$)≠0. In block **4006**, data clustering is determined by comparing the measure R with a user defined threshold parameter V. For example, the threshold parameter V can be 20%. When

$$R \leq V$$

the data is categorized as low-variability data **4008**, otherwise when

$$R > V$$

the data is categorized as high-variability data **4010**.

FIGS. **41**A-**41**B shows data from low- and high-variability categories for a threshold V=20%. In FIG. **41**A, R=200%. Because R≥20%, the data is from a high-variability cluster of data. Plot **4102** shows original data and plot **4104** shows a zoom in of the data values shown in plot **4102**, which reveals the high-variability of the data. In FIG. **41**B, R=12%. Because R<20%, the data is from a low-variability cluster. Plot **4106** shows the original data, and plot **4108** shows a zoom in of the data shown in plot **4108**. The data exhibits a regularly spaced pattern of 5 peaks, which represents low-variability of the data.

Returning to FIG. **40**, in block **4012**, the period detector **4012** described above with reference to FIG. **5** is used to assess the periodicity and non-periodicity of the low-variability data **4008** and the high-variability data **4010**. In block **4014**, a normalcy boundary calculation is performed for both low- and high-variability, non-periodic data **4016**. In block **4018**, a normalcy boundary calculation is performed for low- and high-variability periodic data **4018**. Different sets of parameters may be used in blocks **4014** and **4018** based on the variability.

FIG. **42**A shows an example plot of low-variability data with R=0%. FIG. **42**B shows an example plot of the low-variability data shown in FIG. **42**A with upper and lower normalcy bounds **4202** and **4204**, respectively. The low-variability data in FIG. **42**A is periodic with corresponding normalcy bounds determined using a parameter "time_unit_parts"=12, which divides a day into 12 parts and hence is used to calculate separate dynamic thresholds on 2-hour intervals as shown in FIG. **42**B.

FIG. **43**A shows an example plot of high-variability data with R=100%. FIG. **43**B shows an example plot of the high-variability data shown in FIG. **43**B with upper and lower normalcy bounds **4302** and **4304**, respectively. The high-variability data shown in FIG. **43**A is periodic with corresponding normalcy bounds determined using a parameter "time_unit_parts"=3, which divides a day into 3 parts and hence is used to calculate separate thresholds on 8-hour intervals as shown in FIG. **43**B.

FIG. **44** shows an example of a generalized computer system that executes efficient methods for anomaly detection and therefore represents a data-processing system. The internal components of many small, mid-sized, and large computer systems as well as specialized processor-based storage systems can be described with respect to this generalized architecture, although each particular system may feature many additional components, subsystems, and similar, parallel systems with architectures similar to this generalized architecture. The computer system contains one or multiple central processing units ("CPUs") **4402-4405**, one or more electronic memories **4408** interconnected with the CPUs by a CPU/memory-subsystem bus **4410** or multiple busses, a first bridge **4412** that interconnects the CPU/memory-subsystem bus **4410** with additional busses **4414** and **4416**, or other types of high-speed interconnection media, including multiple, high-speed serial interconnects. The busses or serial interconnections, in turn, connect the CPUs and memory with specialized processors, such as a graphics processor **4418**, and with one or more additional bridges **4420**, which are interconnected with high-speed serial links or with multiple controllers **4422-4427**, such as controller **4427**, that provide access to various different types of computer-readable media, such as computer-readable medium **4428**, electronic displays, input devices, and other such components, subcomponents, and computational resources. The electronic displays, including visual display screen, audio speakers, and other output interfaces, and the input devices, including mice, keyboards, touch screens, and other such input interfaces, together constitute input and output interfaces that allow the computer system to interact with human users. Computer-readable medium **4428** is a data-storage device, including electronic memory, optical or magnetic disk drive, USB drive, flash memory and other such data-storage device. The computer-readable medium **4428** can be used to store machine-readable instructions that encode the computational methods described above and can be used to store encoded data, during store operations, and from which encoded data can be retrieved, during read operations, by computer systems, data-storage systems, and peripheral devices.

Embodiments are not intended to be limited to the descriptions above. For example, any number of different computational-processing-method implementations that carry out the methods for identifying anomalies in data may be designed and developed using various different programming languages and computer platforms and by varying different implementation parameters, including control structures, variables, data structures, modular organization, and other such parameters. The systems and methods can be executed in near-real time. The term "near-real time" refers to a time delay due to data transmission and data processing that is short enough to allow timely use of the data generated by the methods and systems described above.

It is appreciated that the previous description of the disclosed embodiments is provided to enable any person skilled in the art to make or use the present disclosure. Various modifications to these embodiments will be readily apparent to those skilled in the art, and the generic principles defined herein may be applied to other embodiments without departing from the spirit or scope of the disclosure. Thus, the present disclosure is not intended to be limited to the embodiments shown herein but is to be accorded the widest scope consistent with the principles and novel features disclosed herein.

The invention claimed is:

1. A data-anomaly detection system comprising:
- one or more processors;
- one or more computer-readable media; and
- a routine that executes on the one or more processors to analyze digitally encoded data output from a system monitoring tool and stored in the computer-readable media by
  - identifying the output data as qualified data or corrupted data;
  - identifying and sorting the qualified data into categorized data;
  - calculating normalcy bounds for the categorized data;
  - discarding the corrupted data from the computer-readable media; and
  - inputting the categorized data and normalcy bounds to an alerting engine that generates an alert when the categorized data is outside the normalcy bounds.

2. The system of claim **1**, wherein identifying qualified data further comprises
- determining whether the input data is qualified data or corrupted data; and
- determining whether the qualified data is dense data or sparse data.

3. The system of claim **2**, wherein determining whether the qualified data is dense data or sparse data further comprises
- calculating a percentage of gaps in the qualified data, based on a user defined gap parameter;
- calculating data-to-data, data-to-gap, gap-to-gap, and gap-to-data transition probabilities; and
- based on the transitions probabilities and the percentage of gaps, classifying the qualified data as dense data, sparse data, or corrupted data.

4. The system of claim **1**, wherein identifying the qualified data further comprises
- determining whether the qualified data is stable data or corrupted data; and
- categorizing stable qualified data as high-variability data or low-variability data.

5. The system of claim **4**, wherein determining whether the qualified data is stable data or corrupted data further comprises
- generating a stabilochart for the qualified data; and
- for each stabilochart value,
  - when the stabilochart value is less than a user defined value, the qualified data is stable data, otherwise the qualified data is corrupted data.

6. The system of claim **4**, wherein categorizing stable data as high-variability data or low-variability data further comprises
- calculating jumps for the stable qualified data;
- calculating a measure of variability based on the jumps and the stable data; and

identifying the stable data as low-variability data when the measure of variability is less than a user defined threshold, otherwise the stable data is high-variability data.

7. The system of claim **1**, wherein identifying and sorting the qualified data into categorized data further comprises

determining whether the qualified data as parametric data or regular data; and

when the qualified data is parametric data, calculating normalcy bounds for the parametric data.

8. The system of claim **7**, wherein determining whether the qualified data is parametric data further comprises

checking the qualified data for categories of multinomial data;

when no categories of multinomial data are found, denoising the qualified data followed by rechecking the qualified data for categories of multinomial data;

determining whether the qualified data is periodic or non-periodic; and

calculating normalcy bounds for the qualified data based on the periodicity.

9. The system of claim **7**, wherein determining whether the qualified data is parametric data further comprises

searching for two or more modes in the qualified data;

checking each mode of qualified data for inertia;

checking each mode identified as having inertia for transiency;

for each inertial mode,

determining whether the mode is periodic or non-periodic; and

calculating normalcy bounds for the inertial mode based on the periodicity of the mode.

10. The system of claim **7**, wherein determining whether the qualified data is parametric data further comprises

checking parameters of the qualified data for semi-constant data;

when no semi-constant data is found, searching the qualified data for the longest data portion of the data that is semi-constant;

detecting the number of outliers in the semi-constant data;

determining whether the semi-constant data is periodic or non-periodic; and

calculating normalcy bounds for the semi-constant data based on the periodicity.

11. The system of claim **7**, wherein determining whether the qualified data is parametric data further comprises

searching the qualified data for a trend;

identifying the trend of the qualified data as linear, log-linear, or non-trendy; and

calculating normalcy bounds based on the identified trend for the qualified data.

12. The system of claim **1**, wherein calculating the normalcy bounds further comprises

removing abnormal outliers from the data;

smoothing the data;

generating a footprint matrix of the smooth data;

determining whether the data in the footprint matrix is periodic or non-periodic; and

calculating upper and lower normalcy bounds based on the footprint matrix.

13. A method carried out within a computer system having one or more processors and an electronic memory that analyzes digitally encoded data stored in one or more computer-readable media, the method comprising:

identifying data output from a system monitoring tool as qualified data or corrupted data;

identifying and sorting the qualified data into categorized data;

calculating normalcy bounds for the categorized data;

discarding the corrupted data from the computer-readable media; and

inputting the categorized data and normalcy bounds to an alerting engine that generates an alert when the categorized data is outside the normalcy bounds.

14. The method of claim **13**, wherein identifying qualified data further comprises

determining whether the input data is qualified data or corrupted data; and

determining whether the qualified data is dense data or sparse data.

15. The method of claim **14**, wherein determining whether the qualified data is dense data or sparse data further comprises

calculating a percentage of gaps in the qualified data, based on a user defined gap parameter;

calculating data-to-data, data-to-gap, gap-to-gap, and gap-to-data transition probabilities; and

based on the transitions probabilities and the percentage of gaps, classifying the qualified data as dense data, sparse data, or corrupted data.

16. The method of claim **13**, wherein identifying the qualified data further comprises

determining whether the qualified data is stable data or corrupted data; and

categorizing stable qualified data as high-variability data or low-variability data.

17. The method of claim **16**, wherein determining whether the qualified data is stable data or corrupted data further comprises

generating a stabilochart for the qualified data; and

for each stabilochart value,

when the stabilochart value is less than a user defined value, the qualified data is stable data, otherwise the qualified data is corrupted data.

18. The method of claim **16**, wherein categorizing stable data as high-variability data or low-variability data further comprises

calculating jumps for the stable qualified data;

calculating a measure of variability based on the jumps and the stable data; and

identifying the stable data as low-variability data when the measure of variability is less than a user defined threshold, otherwise the stable data is high-variability data.

19. The method of claim **13**, wherein identifying and sorting the qualified data into categorized data further comprises

determining whether the qualified data as parametric data or regular data; and

when the qualified data is parametric data, calculating normalcy bounds for the parametric data.

20. The method of claim **19**, wherein determining whether the qualified data is parametric data further comprises

checking the qualified data for categories of multinomial data;

when no categories of multinomial data are found, denoising the qualified data followed by rechecking the qualified data for categories of multinomial data;

determining whether the qualified data is periodic or non-periodic; and

calculating normalcy bounds for the qualified data based on the periodicity.

21. The method of claim **19**, wherein determining whether the qualified data is parametric data further comprises

searching for two or more modes in the qualified data;

checking each mode of qualified data for inertia;

checking each mode identified as having inertia for transiency;

for each inertial mode,

determining whether the mode is periodic or non-periodic; and

calculating normalcy bounds for the inertial mode based on the periodicity of the mode.

22. The method of claim **19**, wherein determining whether the qualified data is parametric data further comprises

checking parameters of the qualified data for semi-constant data;

when no semi-constant data is found, searching the qualified data for the longest data portion of the data that is semi-constant;

detecting the number of outliers in the semi-constant data;

determining whether the semi-constant data is periodic or non-periodic; and

calculating normalcy bounds for the semi-constant data based on the periodicity.

23. The method of claim **19**, wherein determining whether the qualified data is parametric data further comprises

searching the qualified data for a trend;

identifying the trend of the qualified data as linear, log-linear, or non-trendy; and

calculating normalcy bounds based on the identified trend for the qualified data.

24. The method of claim **13**, wherein calculating the normalcy bounds further comprises

removing abnormal outliers from the data;

smoothing the data;

generating a footprint matrix of the smooth data;

determining whether the data in the footprint matrix is periodic or non-periodic; and

calculating upper and lower normalcy bounds based on the footprint matrix.

25. A non-transitory computer-readable medium encoded with machine-readable instructions that implement a method carried out by one or more processors of a computer system to perform the operations of

identifying data output from a system monitoring tool as qualified data or corrupted data;

identifying and sorting the qualified data into categorized data;

calculating normalcy bounds for the categorized data;

discarding the corrupted data from the computer-readable media; and

inputting the categorized data and normalcy bounds to an alerting engine that generates an alert when the categorized data is outside the normalcy bounds.

26. The medium of claim **25**, wherein identifying qualified data further comprises

determining whether the input data is qualified data or corrupted data; and

determining whether the qualified data is dense data or sparse data.

27. The medium of claim **26**, wherein determining whether the qualified data is dense data or sparse data further comprises

calculating a percentage of gaps in the qualified data, based on a user defined gap parameter;

calculating data-to-data, data-to-gap, gap-to-gap, and gap-to-data transition probabilities; and

based on the transitions probabilities and the percentage of gaps, classifying the qualified data as dense data, sparse data, or corrupted data.

28. The medium of claim **25**, wherein identifying the qualified data further comprises

determining whether the qualified data is stable data or corrupted data; and

categorizing stable qualified data as high-variability data or low-variability data.

29. The medium of claim **28**, wherein determining whether the qualified data is stable data or corrupted data further comprises

generating a stabilochart for the qualified data; and

for each stabilochart value,

when the stabilochart value is less than a user defined value, the qualified data is stable data, otherwise the qualified data is corrupted data.

30. The medium of claim **28**, wherein categorizing stable data as high-variability data or low-variability data further comprises

calculating jumps for the stable qualified data;

calculating a measure of variability based on the jumps and the stable data; and

identifying the stable data as low-variability data when the measure of variability is less than a user defined threshold, otherwise the stable data is high-variability data.

31. The medium of claim **25**, wherein identifying and sorting the qualified data into categorized data further comprises

determining whether the qualified data as parametric data or regular data; and

when the qualified data is parametric data, calculating normalcy bounds for the parametric data.

32. The medium of claim **31**, wherein determining whether the qualified data is parametric data further comprises

checking the qualified data for categories of multinomial data;

when no categories of multinomial data are found, denoising the qualified data followed by rechecking the qualified data for categories of multinomial data;

determining whether the qualified data is periodic or non-periodic; and

calculating normalcy bounds for the qualified data based on the periodicity.

33. The medium of claim **31**, wherein determining whether the qualified data is parametric data further comprises

searching for two or more modes in the qualified data;

checking each mode of qualified data for inertia;

checking each mode identified as having inertia for transiency;

for each inertial mode,

determining whether the mode is periodic or non-periodic; and

calculating normalcy bounds for the inertial mode based on the periodicity of the mode.

34. The medium of claim **31**, wherein determining whether the qualified data is parametric data further comprises

checking parameters of the qualified data for semi-constant data;

when no semi-constant data is found, searching the qualified data for the longest data portion of the data that is semi-constant;

detecting the number of outliers in the semi-constant data;

determining whether the semi-constant data is periodic or non-periodic; and

calculating normalcy bounds for the semi-constant data based on the periodicity.

35. The medium of claim **31**, wherein determining whether the qualified data is parametric data further comprises

searching the qualified data for a trend;

identifying the trend of the qualified data as linear, log-linear, or non-trendy; and

calculating normalcy bounds based on the identified trend for the qualified data.

36. The medium of claim **25**, wherein calculating the normalcy bounds further comprises

removing abnormal outliers from the data;

smoothing the data;

generating a footprint matrix of the smooth data;

determining whether the data in the footprint matrix is periodic or non-periodic; and

calculating upper and lower normalcy bounds based on the footprint matrix.

* * * * *